JAERI-M
85-099

HYDROGEN RE-EMISSION DATA ANALYSIS IN AUSTENITIC STAINLESS STEEL

July 1985

Kimichika FUKUSHIMA*, Kunio OZAWA,
Katsuyuki EBISAWA** and Mititaka TERASAWA***

日本原子力研究所
Japan Atomic Energy Research Institute

JAERI-M レポートは，日本原子力研究所が不定期に公刊している研究報告書です。
入手の問合わせは，日本原子力研究所技術情報部情報資料課（〒319—11 茨城県那珂郡東海村）あて，お申しこしください。なお，このほかに財団法人原子力弘済会資料センター（〒319-11 茨城県那珂郡東海村日本原子力研究所内）で複写による実費頒布をおこなっております。

JAERI-M reports are issued irregularly.
Inquiries about availability of the reports should be addressed to Information Division, Department of Technical Information, Japan Atomic Energy Research Institute, Tokai-mura, Naka-gun, Ibaraki-ken 319-11, Japan.

編集兼発行　日本原子力研究所
印　　刷　山洋軽印刷所

JAERI-M 85-099

Hydrogen Re-emission Data Analysis in Austenitic Stainless Steel

Kimichika Fukushima*, Kunio Ozawa,
Katsuyuki Ebisawa** and Mititaka Terasawa***

Department of Physics,
Tokai Research Establishment, JAERI

(Received June 21, 1985)

A diffusion analysis computer code HRF-1 was developed and the re-emission rate was computed for various diffusion constants. The computed re-emission rate was fitted to the experimental data and the effective diffusion constant was obtained neglecting the trapping and recombination process. The effective diffusion constant in high temperature was smaller than the diffusion constant obtained in the other experiments suggesting the hydrogen transport in stainless steel in high temperature is recombination limited. On the other hand, the effective diffusion constant in low temperature was larger than the diffusion constant extrapolated from the high temperature result, suggesting that a tunneling effect in low temperature is a major hydrogen transport process. In addition to the above analysis, the recombination constant in high temperature was computed as a function of the material temperature.

Keywords: Plasma-Surface Interactions, Recycling, Re-emission, Hydrogen Isotope Transport, Diffusion Constant, Recombination Constant, Stainless Steel, Radiation Effects, Analysis, Data Base

---

This report was prepared as an account of work supported partly by a research contract of JAERI with Toshiba Corporation in fiscal year 1984.

* Research and Development Center, Kawasaki, Toshiba Corporation.
** Nuclear Engineering Group, Mita, Tokyo, Toshiba Corporation.
*** Nuclear Engineering Laboratory, Kawasaki, Toshiba Corporation.

ステンレス鋼の水素リサイクリング過程に対する照射効果の解析と評価

日本原子力研究所東海研究所物理部
福島　公親*・小沢　国夫・海老沢克之**・寺澤　倫孝***

（1985年6月21日受理）

核融合炉のプラズマ・壁間で水素同位体が交換される水素リサイクリング過程は，燃料リサイクリングや冷却系へのトリチウム透過を考慮するうえで重要である。このため，第一壁候補材料にイオン注入した水素同位体の材料中での挙動を調べる実験が行われている。

本報告では，拡散計算コードＨＲＦ－１を用い，オーステナイト系ステンレス鋼中にイオン注入された水素同位体の再放出量に関する実験データから，実効拡散定数，再結合定数を求めた。実効拡散定数は，拡散過程のみを考慮した計算結果を実験データにフィットさせることにより求めた。再結合定数の解析では，拡散過程と表面における再結合過程を考慮し，拡散定数に実験値を用いた計算結果を実験データにフィットさせることにより再結合定数を求めた。また，求まった実効拡散定数の温度依存性を調べ，反応速度論から得られる式でまとめた。

本報告書は東芝㈱との共同研究の成果の一部をまとめたものである。

*）株式会社　東芝　総合研究所
**）株式会社　東芝　原子力事業本部
***）株式会社　東芝　原子力事業本部　原子力技術研究所

Contents

目　　次

1. Introduction

In nuclear fusion reactors, hydrogen isotopes such as deuterium and tritium are implanted into the first wall and the other wall structures such as diverter and limiter. Most of isotopes are diffused to the front surface and released to plasma. Some fractions of hydrogen isotopes implanted into material are trapped by the defects in material. Some of the isotopes pass through the wall material into coolant. Hydrogen recycling process between plasma and the first wall is an important one from the view point of the fuel recycling. In addition, if the excess tritium permeates into coolant, it causes problems for nuclear safety. Many works have been carried out on the hydrogen isotope behavior in the first wall candidate materials. In the previous report, the experimental data on the hydrogen recycling were collected [1]. The purpose of this work is to obtain the physical parameters such as a diffusion constant and a recombination constant from the analysis of the previously collected experimental data on the hydrogen isotope re-emission in stainless steel.

A diffusion analysis computer code HRF-1 (Hydrogen Recycling Analysis Code-1 for Fusion Reactor materials) was developed by one of the authors (K.F.) [2]. It is known that the transport of hydrogen isotopes is diffusion limited or recombination limited depending on the material temperature [3]. To clarify which is the dominant process in austenitic stainless steel, the re- emission rate was computed. The computed re-emission rate was fitted to the experimental data and the effective diffusion constant was obtained neglecting the trapping and recombination process. The effective diffusion constant was compared to the diffusion constant obtained in the other experiments. It can be seen that the hydrogen transport is recombination limited when the computed effective diffusion constant is larger than the experimentally obtained diffusion constant and if not so, the hydrogen transport is diffusion limited. Based on the result that the hydrogen transport is recombination limited in high temperature, the recombination constant in high temperature was computed as a function of the material temperature.

The computational method is given in Chap. 2 and the computed results are shown in Chap. 3.

2. Computational Method

The experimental data was analyzed by the use of the diffusion analysis computer code HRF-1. The diffusion equation is denoted as

$$\frac{\partial c}{\partial t} = G + D\frac{\partial^2 c}{\partial x^2} - R_T + R_D,$$

$$\frac{\partial m}{\partial t} = R_T - R_D, \qquad (2.1)$$

where

D : diffusion constant ($cm^2\ s^{-1}$),

c : concentration of hydrogen isotope (atom cm^{-3}),

m : concentration of hydrogen isotope trapped in defects (atom cm^{-3}),

G : depth profile of the hydrogen isotope implantation rate (atom $cm^{-3}\ s^{-1}$),

R_T : trappint rate (atom $cm^{-3}\ s^{-1}$),

R_D : detrapping rate (atom $cm^{-3}\ s^{-1}$).

The re-emission rate from the front surface depends on the transport process of hydrogen isotopes. In the diffusion-limited case, the re-emission rate is given by

$$j = -D\frac{\partial c_b}{\partial x}, \qquad (2.2)$$

where

j : re-emission rate (atom $cm^{-2}\ s^{-1}$),

c_b : surface concentration of hydrogen isotope (atom cm^{-3}).

In the re-combination limited case

$$j = Kc_b^2 . \qquad (2.3)$$

Here,

K : recombination constant ($cm^4\ s^{-1}$).

The depth profile of the hydrogen isotope implantation rate G was computed by TRIM code [4]. The diffusion equation was solved numerically by the Crank-Nicolson's method [5] given in Appendix.

3. Results and discussion

3.1 Experimental Data

The experimental data analyzed were the hydrogen isotope re-emission data in stainless steel reported in the literatures with the index numbers RE01 [6], RE02 [7], RE06 [8], RE07 [9], RE09 [10] in the previous report [1]. The implanted ions were hydrogen in RE01, RE09 experiments and deuterium in RE02, RE06, RE07 experiments. The target temperature were 330K, 198K, 180K in RE01 experiment, 77K in RE02 experiment, 373K, 323K, 308K in RE06 experiment, 338K 368K, 308K in RE07 experiment, and 100K, 160K, 220K, 275K, 285K, 605K in RE09 experiment.

3.2 Effective Diffusion Constant : D

In the computation of the effective diffusion constant, the surface recombination process was neglected and only the diffusion transport was analyzed. The results are shown in Figs. 1-3 for RE01, in Figs. 4-7 for RE02, in Figs. 8-10 for RE06, in Figs. 11-15 for RE07, and in Figs. 16-21 for RE09. In the figures are shown the re-emission curves for the following four cases with the symbols from 1 to 4:

1 : experimental data,
2 : computed re-emission rate for the diffusion constant larger than that in the case "3",
3 : computed re-emission rate which coincides with that obtained experimentally at the time when the re-emission rate equals half to the incident flux,
4 : computed re-emission rate for the diffusion constant smaller than those in the case "3".

3.3 Re-emission Rate Computed with the Experimentally Obtained Diffusion Constant : j

It is known that there are two type hydrogen isotope transport mechanisms. One is the diffusion-limited transport and the other is the recombination-limited transport. It is important to determine which is the dominant process. In this section, the only diffusion-limited transport was analyzed using the diffusion constant obtained by Lauthan et al. [11], Braun et al.[12], and Tison et al.[13]. The results are shown in Figs. 22-24 for RE01, in Figs. 25-28 for RE02, in Figs. 29-31 for RE06, in Figs. 32-36 for RE07, and in Figs. 37-42 for RE09. As is seen in Fig. 23 and Figs. 37-39, the computed re-emission rate in low temperature becomes quite smaller than the experimental re-emission rate. In high temperature, the computed re-emission rate becomes larger than the experimental data. These results show that the re-emission is recombination limited in high temperature and diffusion limited in low temperature.

3.4 Recombination Constant : K

The recombination constant was computed in the high temperature recombination-limited case. The diffusion constants used are those obtained experimentally by Lauthan et al.[11], Braun et al.[12], and Tison et al.[13]. The recombination constant was obtained by fitting the computed results to the experimental data. The results are shown in Figs. 43-51 for RE06 and Figs. 52-66 for RE07.

3.5 Temperature Dependence of the Effective Diffusion Constant and Recombination Constant

In Fig. 67, the temperature dependence of the effective diffusion constant is shown. The adopted dada are those denoted as the symbol "3" in Sec. 3.2. The computed results were fitted to the Arrenius equation

$$D = D_o \exp(-\frac{E}{RT}), \qquad (3.1)$$

where

E : activation energy (kcal mol^{-1}),

R : gas constant (1.987×10^{-3} kcal mol^{-1} K).

In Fig. 67, the slope, which indicates the activation energy in low temperature, is smaller than that in the high temperature case. In high temperature, $D_o=2.7\times10^{-6}$ cm^{-2} s^{-1} and E=4.1 kcal mol^{-1}, while $D_o=4.4\times10^{-13}$ cm^{-2} s^{-1} and E=0.16 kcal mol^{-1}. The reduction of the activation energy in low temperature is probably due to the tunneling effect. That is, the hydrogen isotope penetrates the lattice potential barrier instead of the thermal activation over the potential barrier.

In Figs. 68-70, the temperature dependence of the recombination constnat is shown computed using the diffusion constant obtained by Lauthan et al., Braun et al., and Tison dt al., respectively. In Fig. 71 are shown all of the data. The temperature dependence was fitted to the equation

$$K = \frac{K_o}{T^{1/2}} \exp(-\frac{E}{RT}), \qquad (3.2)$$

which was derived from the reaction kinetics. The least square fit shows $K_o=4.4\times10^{-13}$, 6.5×10^{-15}, 2.5×10^{-10} (cm^4 s^{-1} $K^{1/2}$) and E=8.4, 7.3, 10.1 (kcal mol^{-1}) for the diffusion constants obtained experimentally by Lauthan et al., Braun et al., and Tison et al., respectively. The fitting of the all data to (3.2) yields $K_o=5.1\times10^{-14}$ (cm^4 s^{-1} $K^{1/2}$) and E=7.9 kcal mol^{-1}.

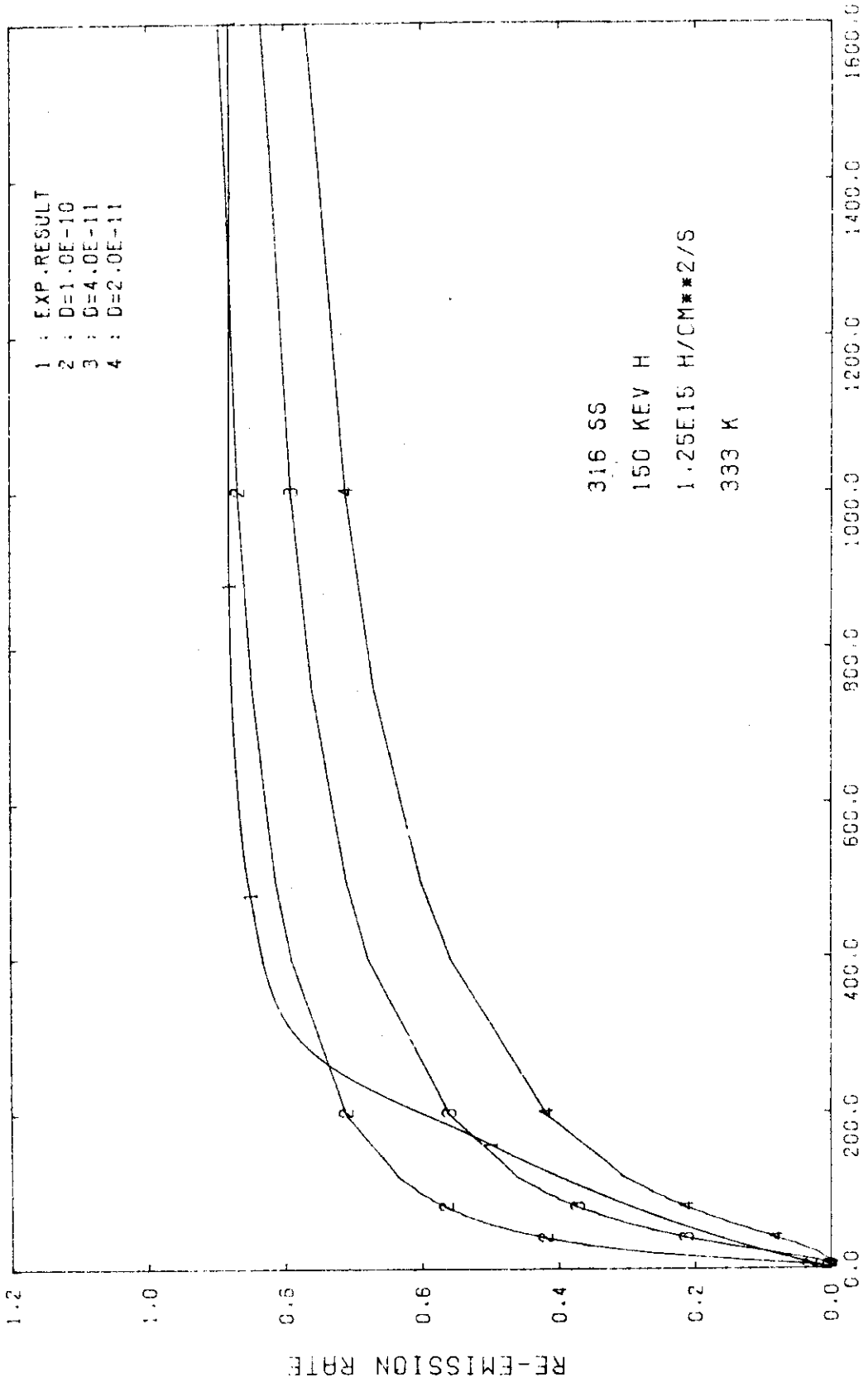

FIG.1 RE-EMISSION RATE FOR VARIOUS DIFFUSION CONSTANTS (RE01)

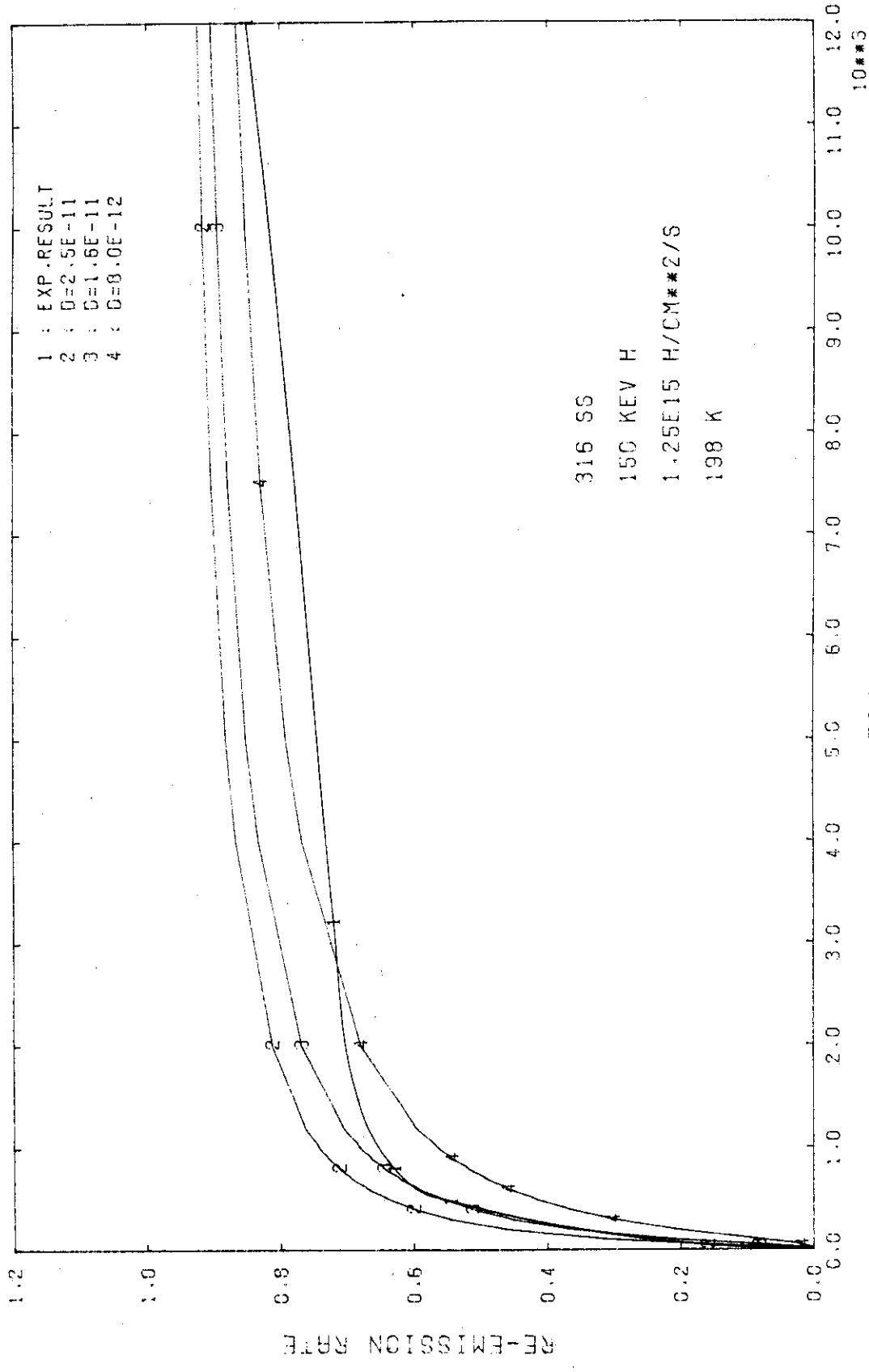

FIG.2 RE-EMISSION RATE FOR VARIOUS DIFFUSION CONSTANTS (RE01)

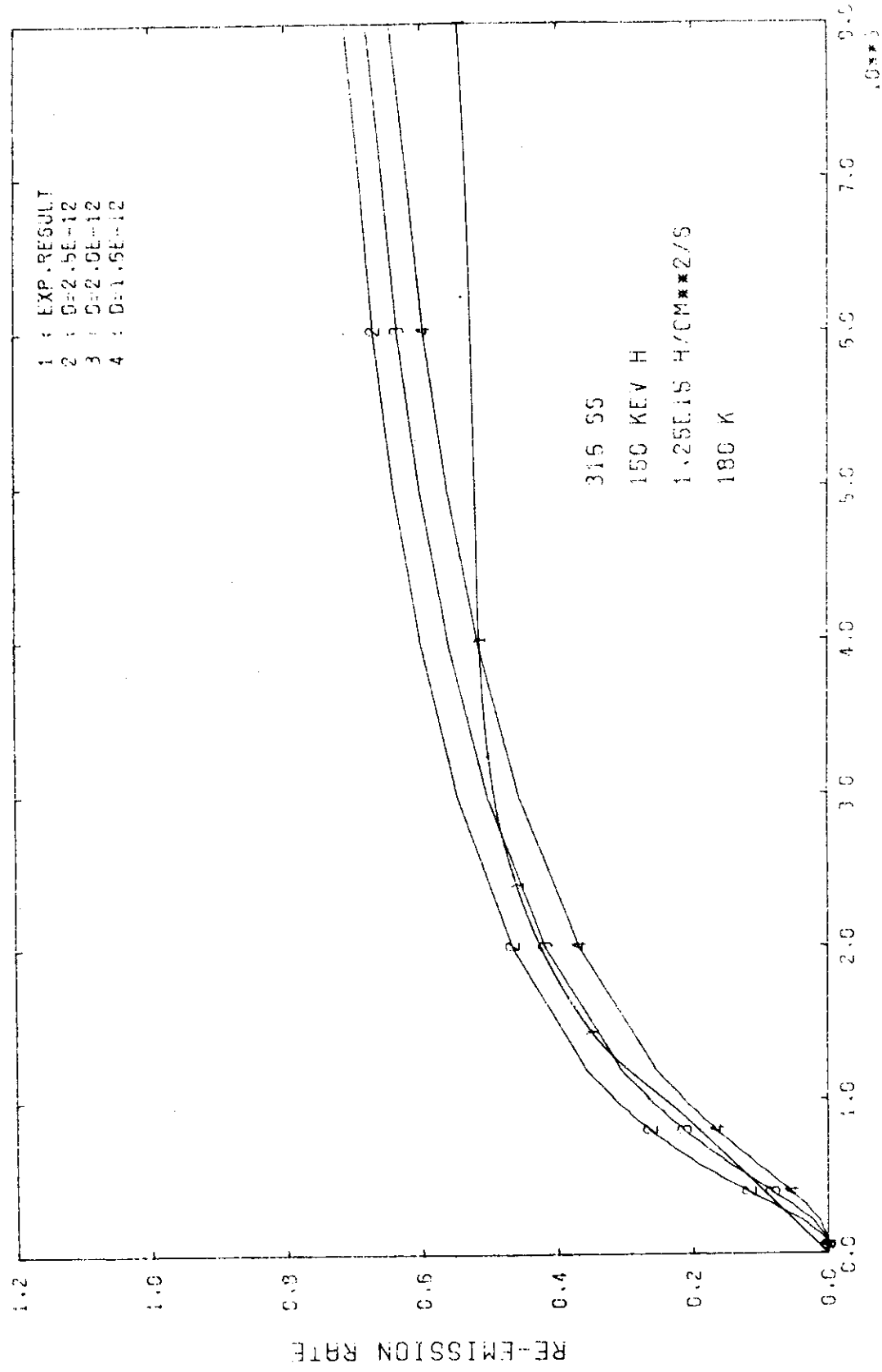

FIG.3 RE-EMISSION RATE FOR VARIOUS DIFFUSION CONSTANTS (RESULT)

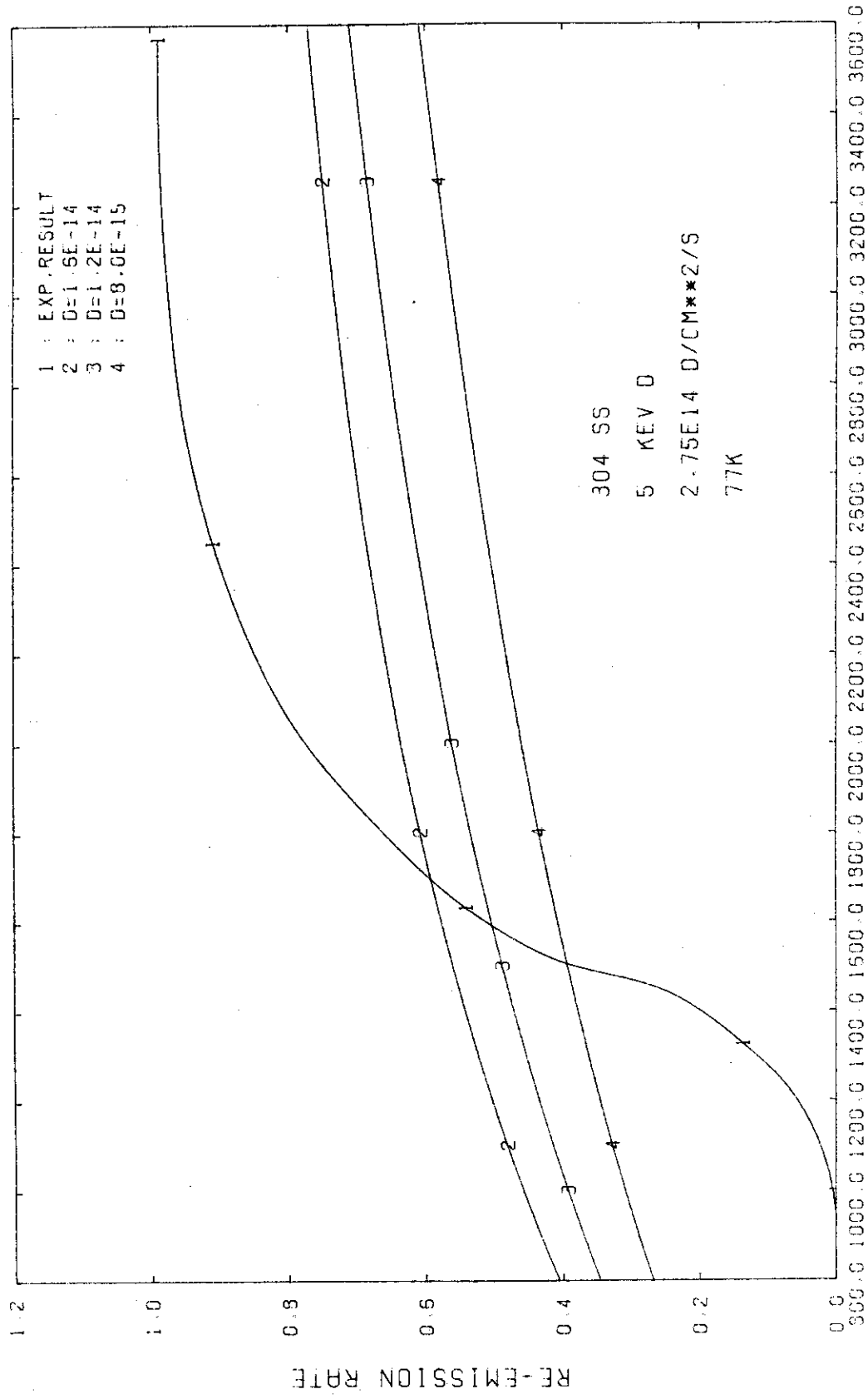

FIG.4 RE-EMISSION RATE FOR VARIOUS DIFFUSION CONSTANTS (RE02)

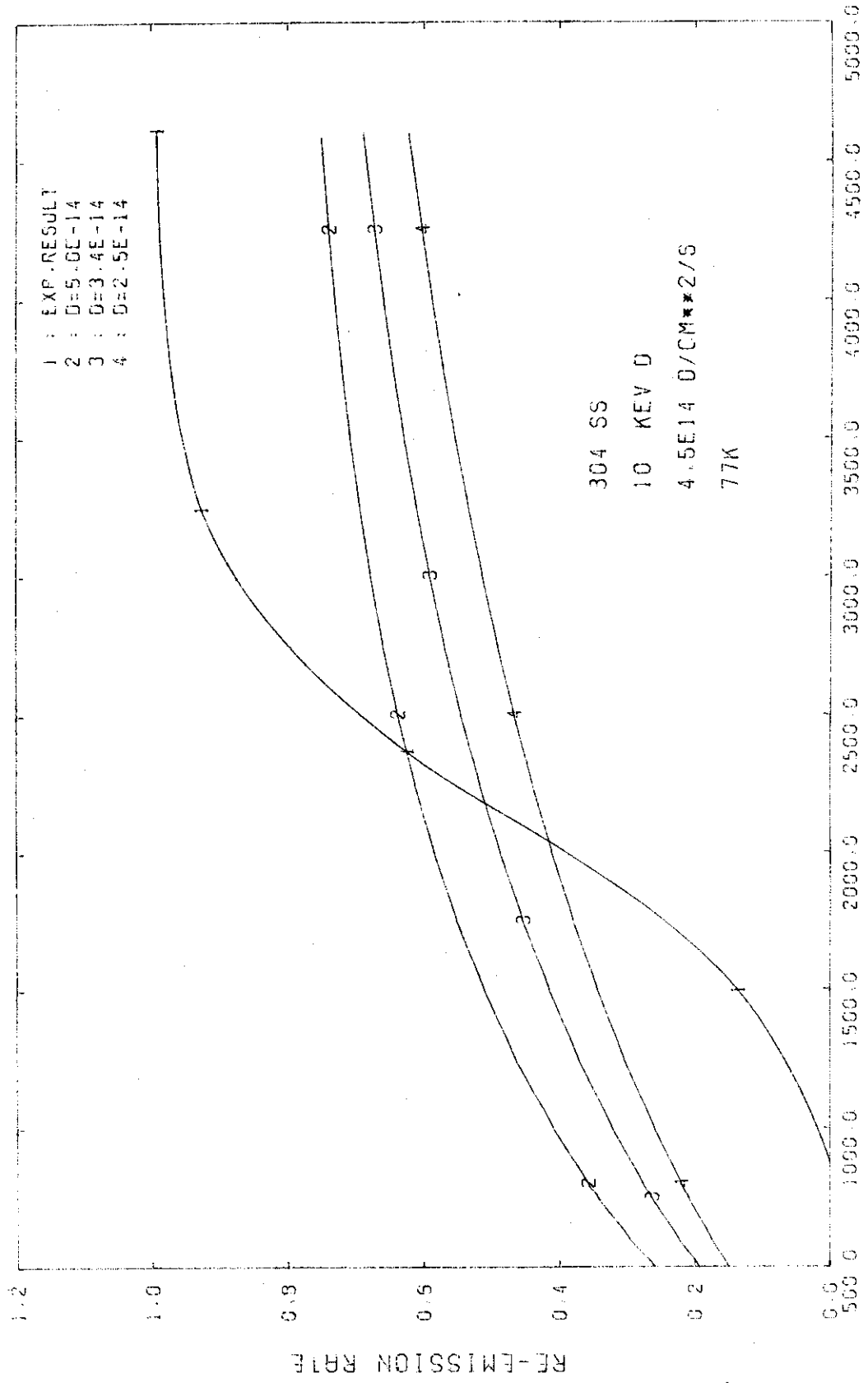

FIG.5 RE-EMISSION RATE FOR VARIOUS DIFFUSION CONSTANTS (RE02)

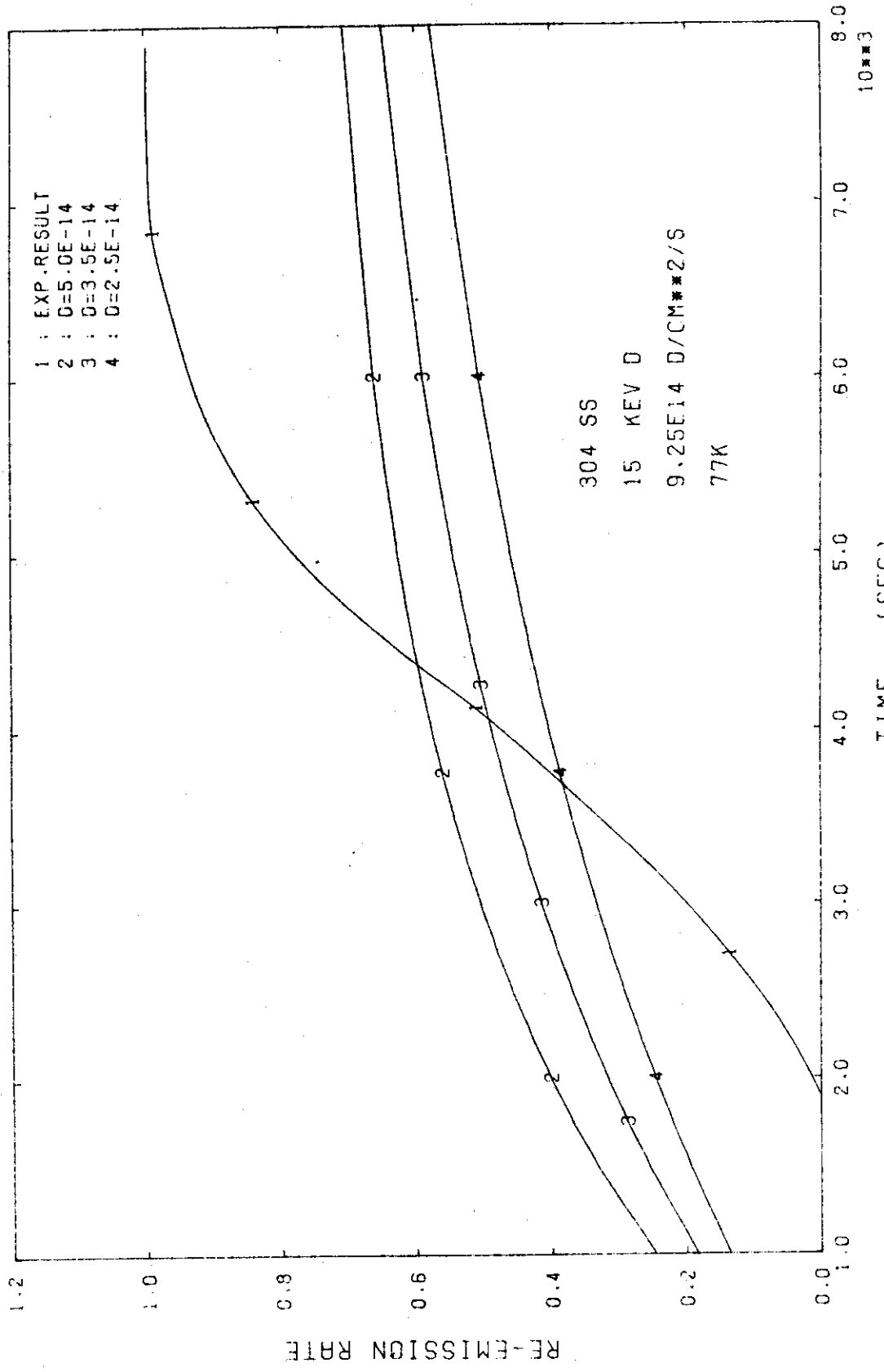

FIG.6 RE-EMISSION RATE FOR VARIOUS DIFFUSION CONSTANTS (REO2)

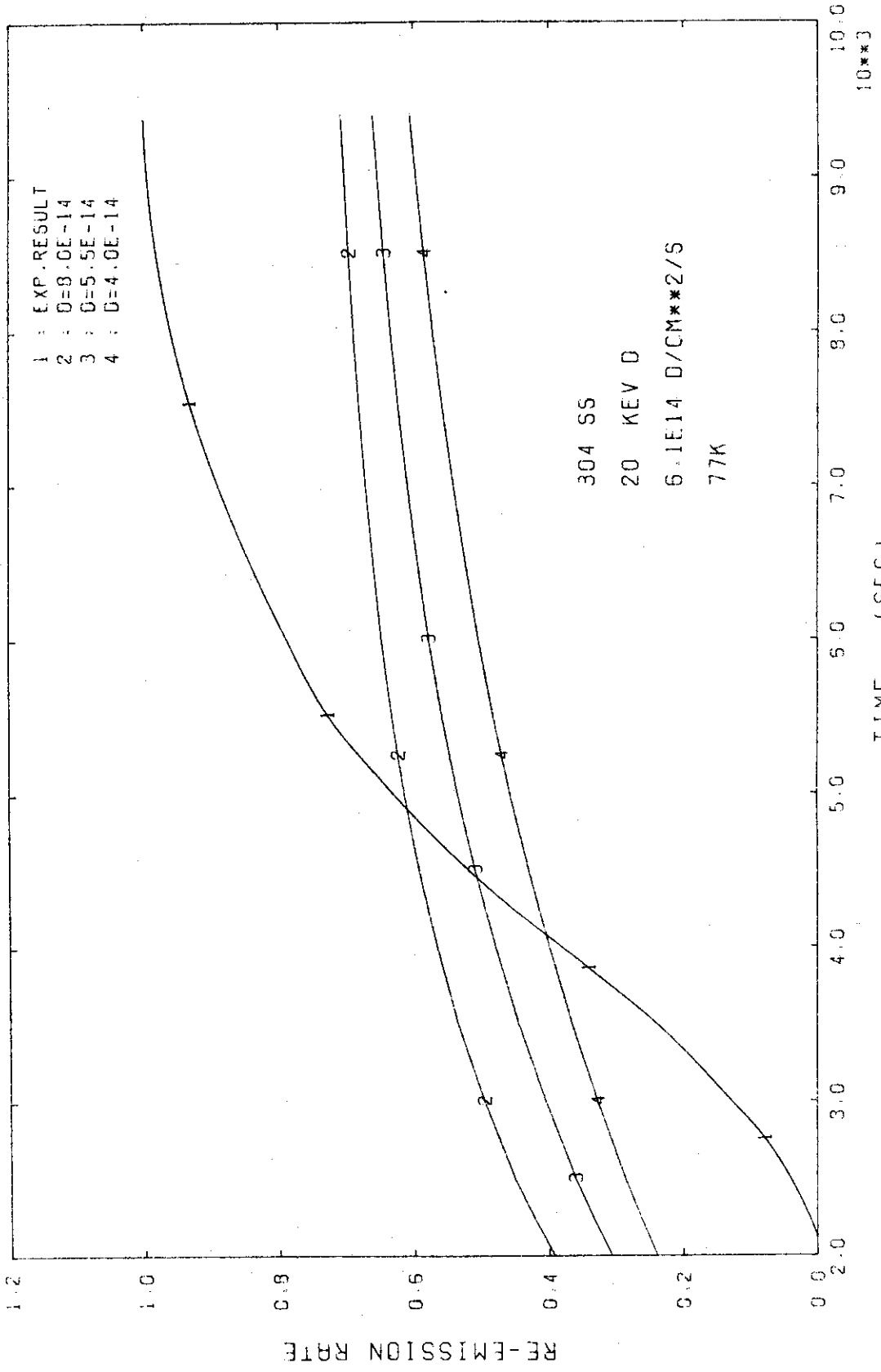

FIG.7 RE-EMISSION RATE FOR VARIOUS DIFFUSION CONSTANTS (RE02)

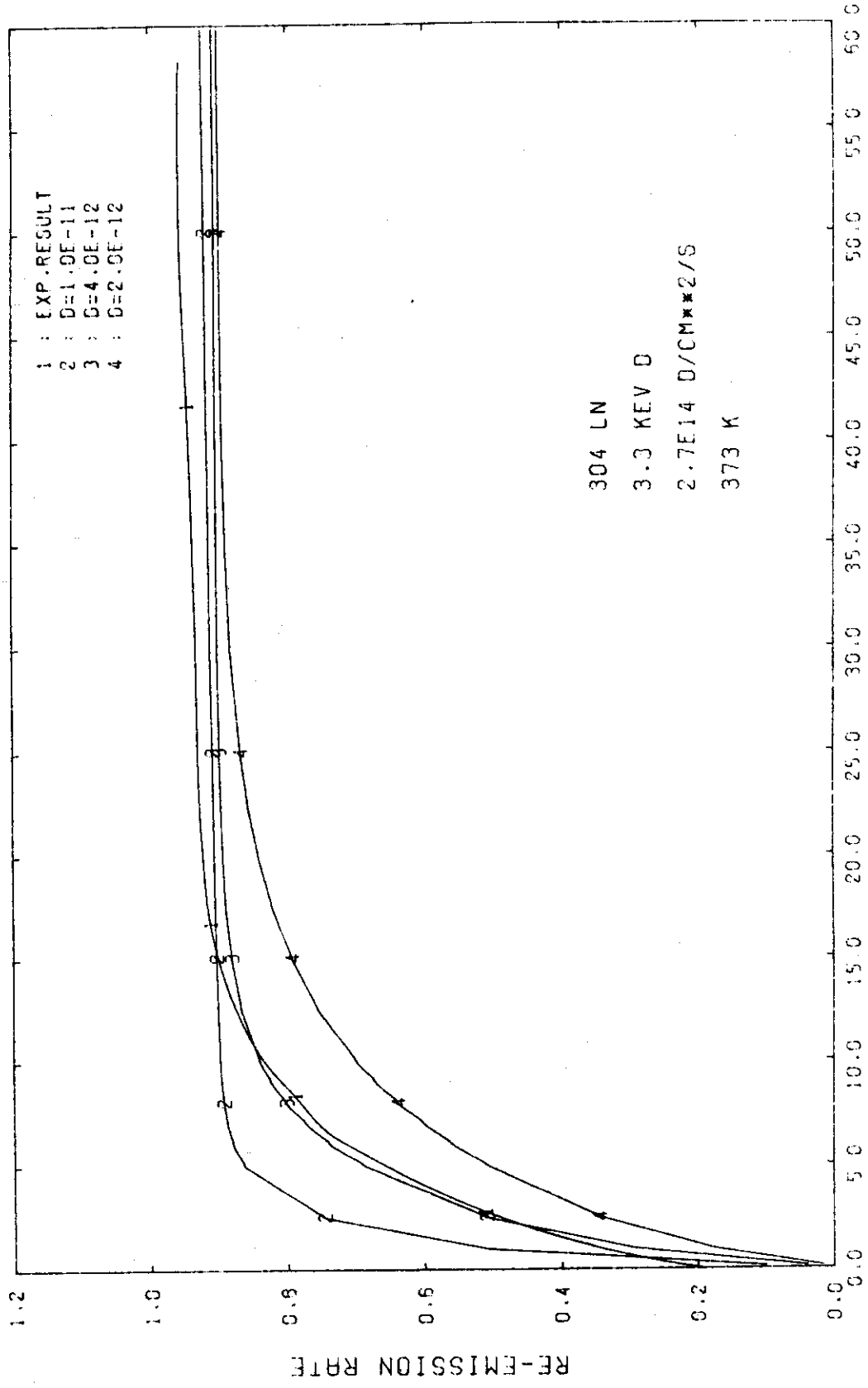

FIG.8 RE-EMISSION RATE FOR VARIOUS DIFFUSION CONSTANTS (REF06)

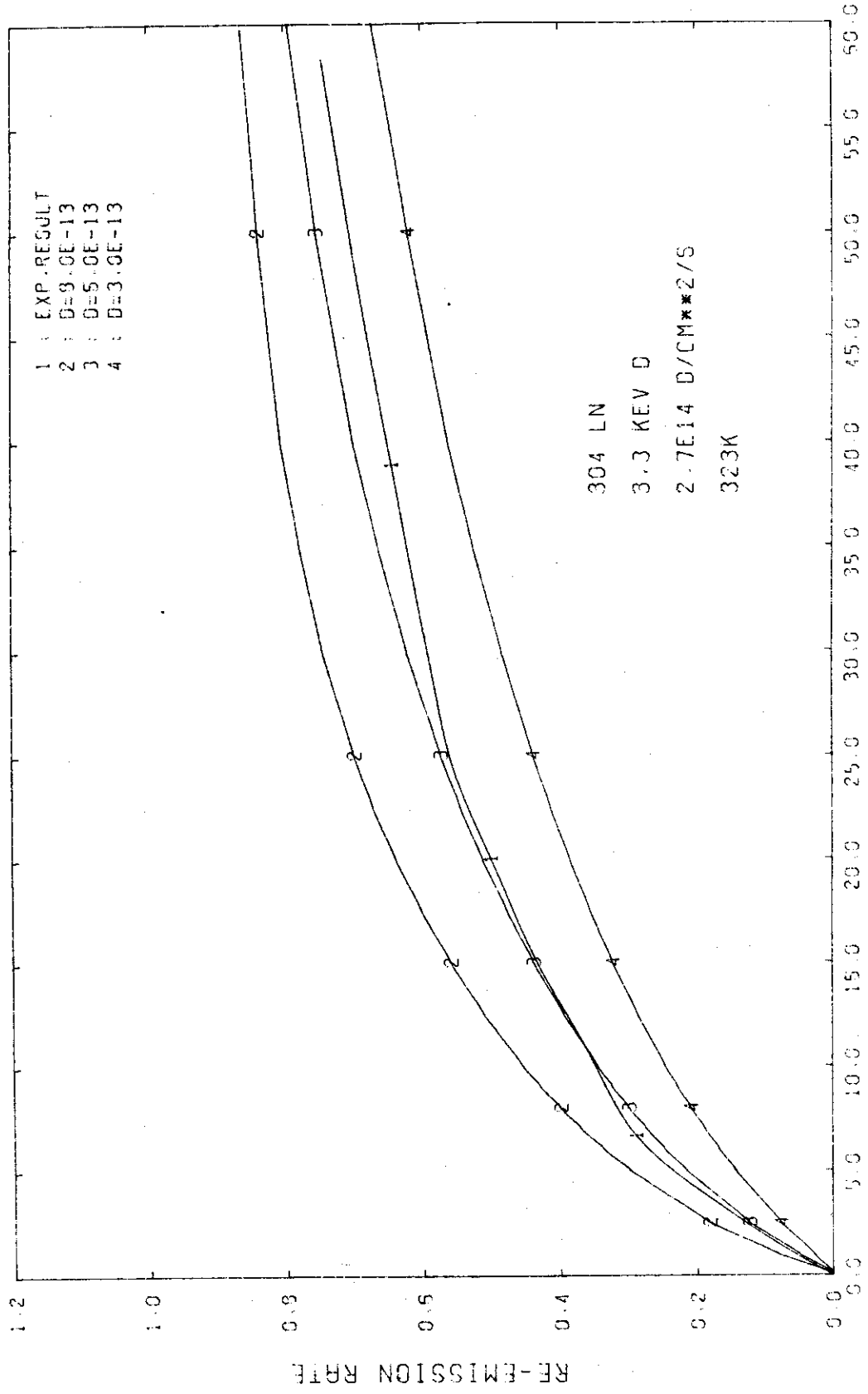

FIG.9 RE-EMISSION RATE FOR VARIOUS DIFFUSION CONSTANTS (REOS)

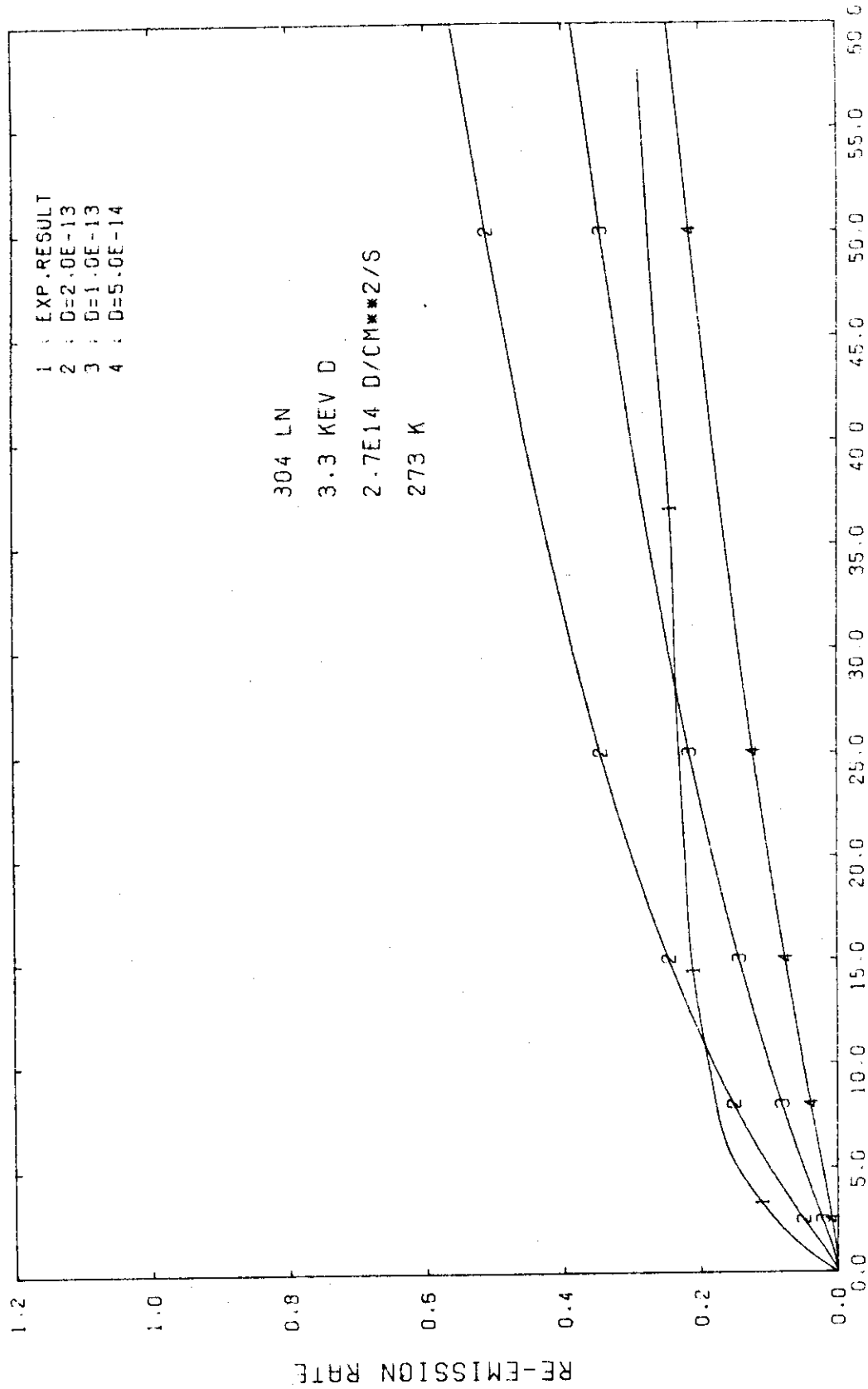

FIG.10 RE-EMISSION RATE FOR VARIOUS DIFFUSION CONSTANTS (REOG)

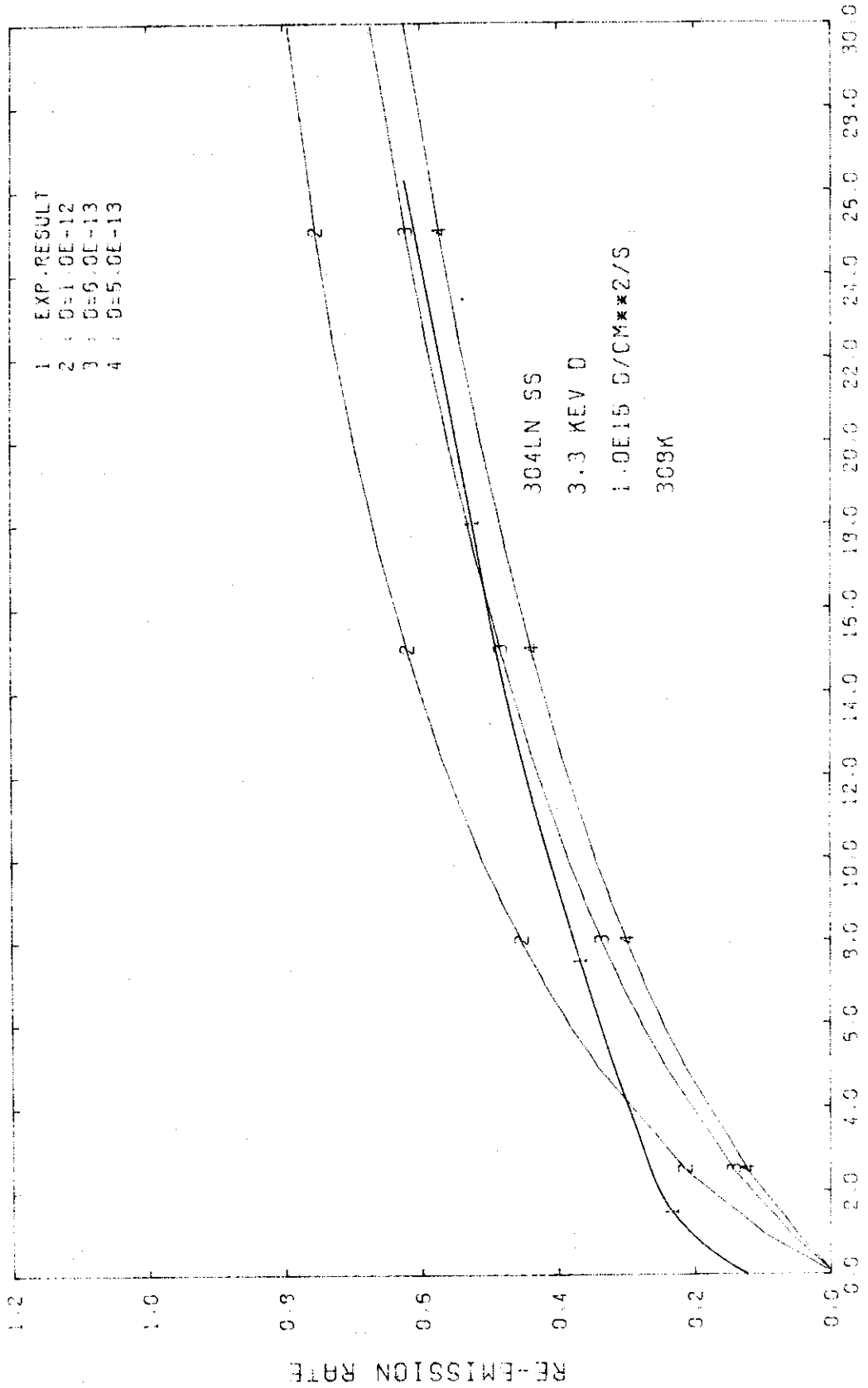

FIG.11 RE-EMISSION RATE FOR VARIOUS DIFFUSION CONSTANTS (REQ7)

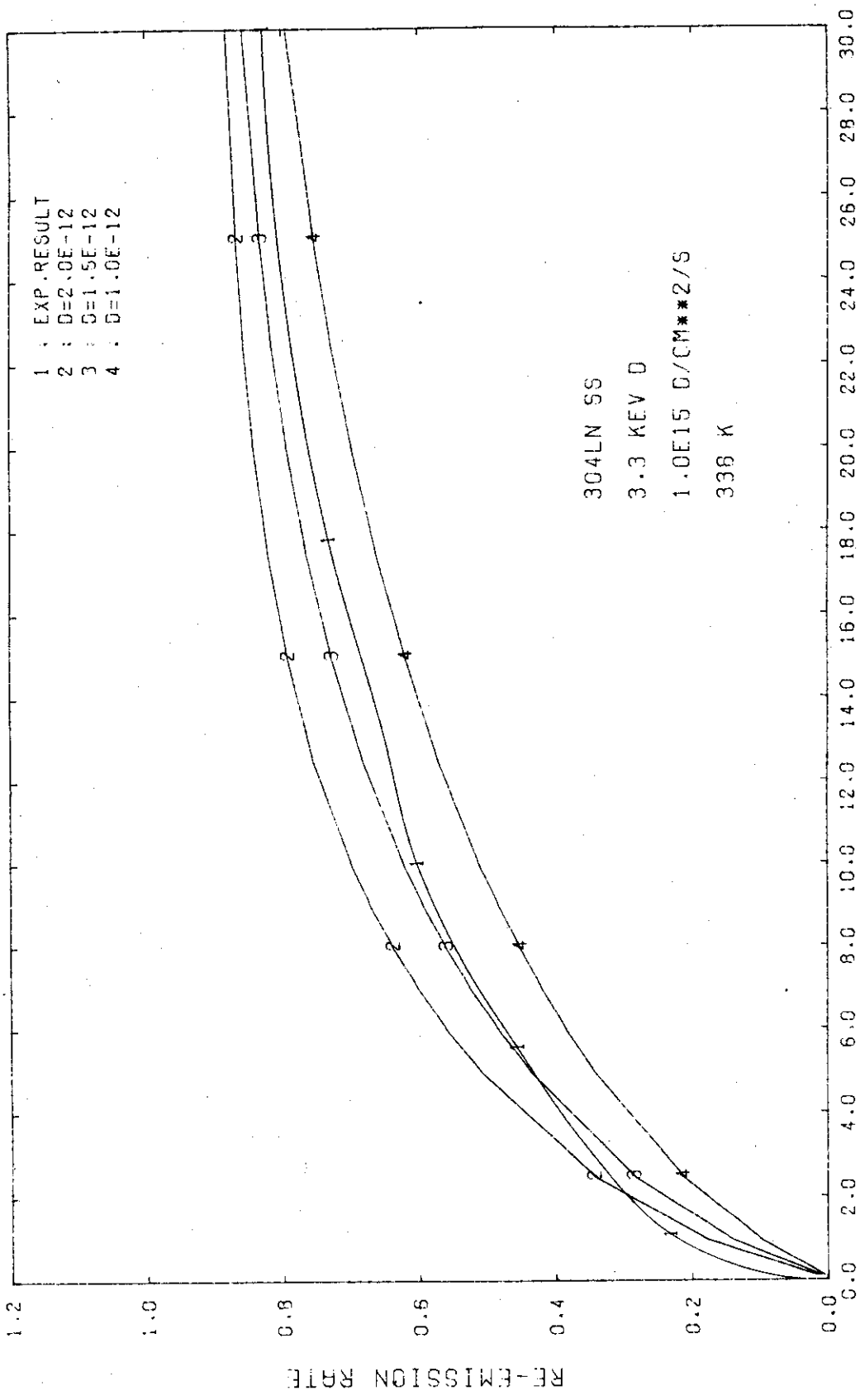

FIG.12 RE-EMISSION RATE FOR VARIOUS DIFFUSION CONSTANTS (RE07)

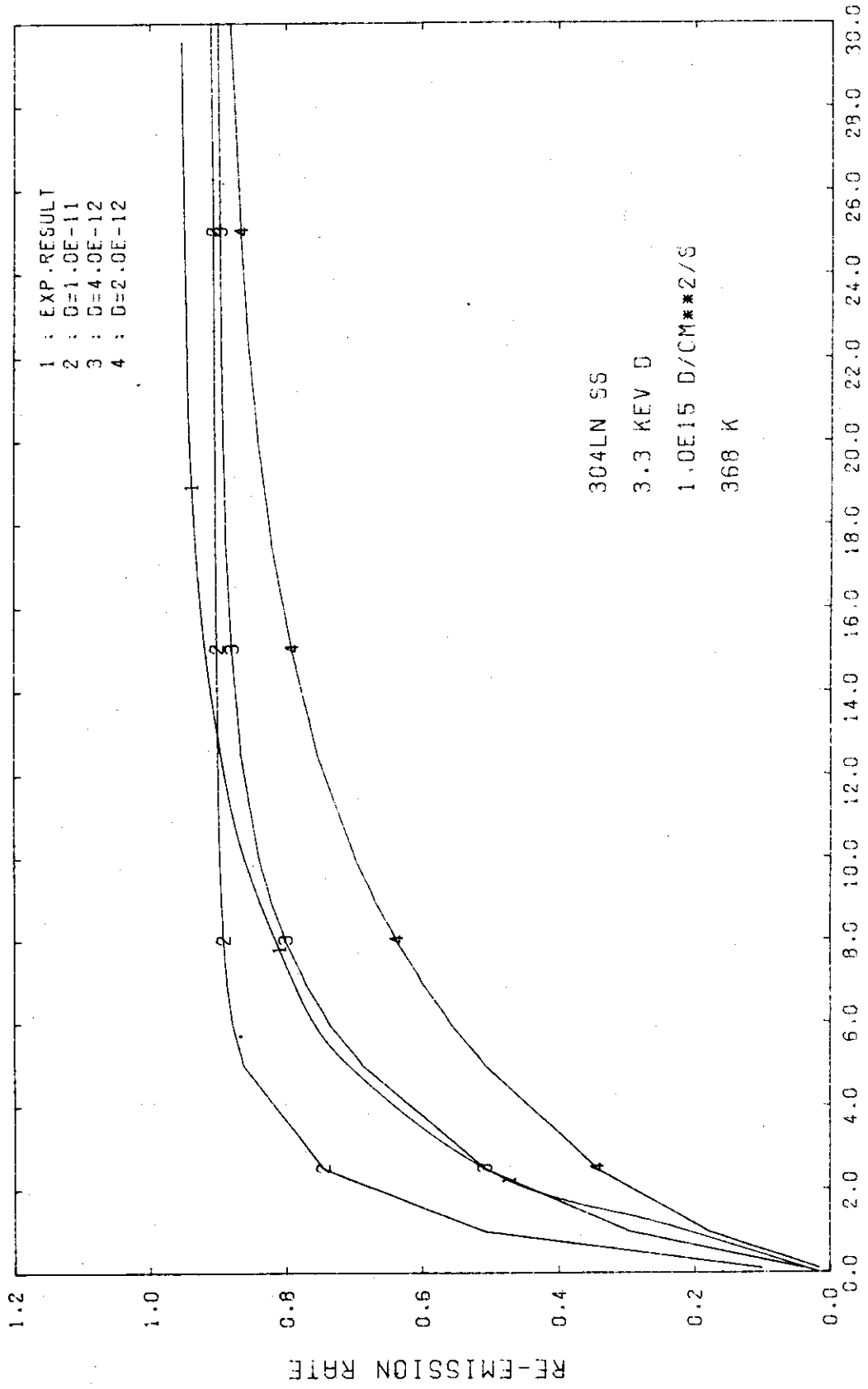

FIG.13 RE-EMISSION RATE FOR VARIOUS DIFFUSION CONSTANTS (RE07)

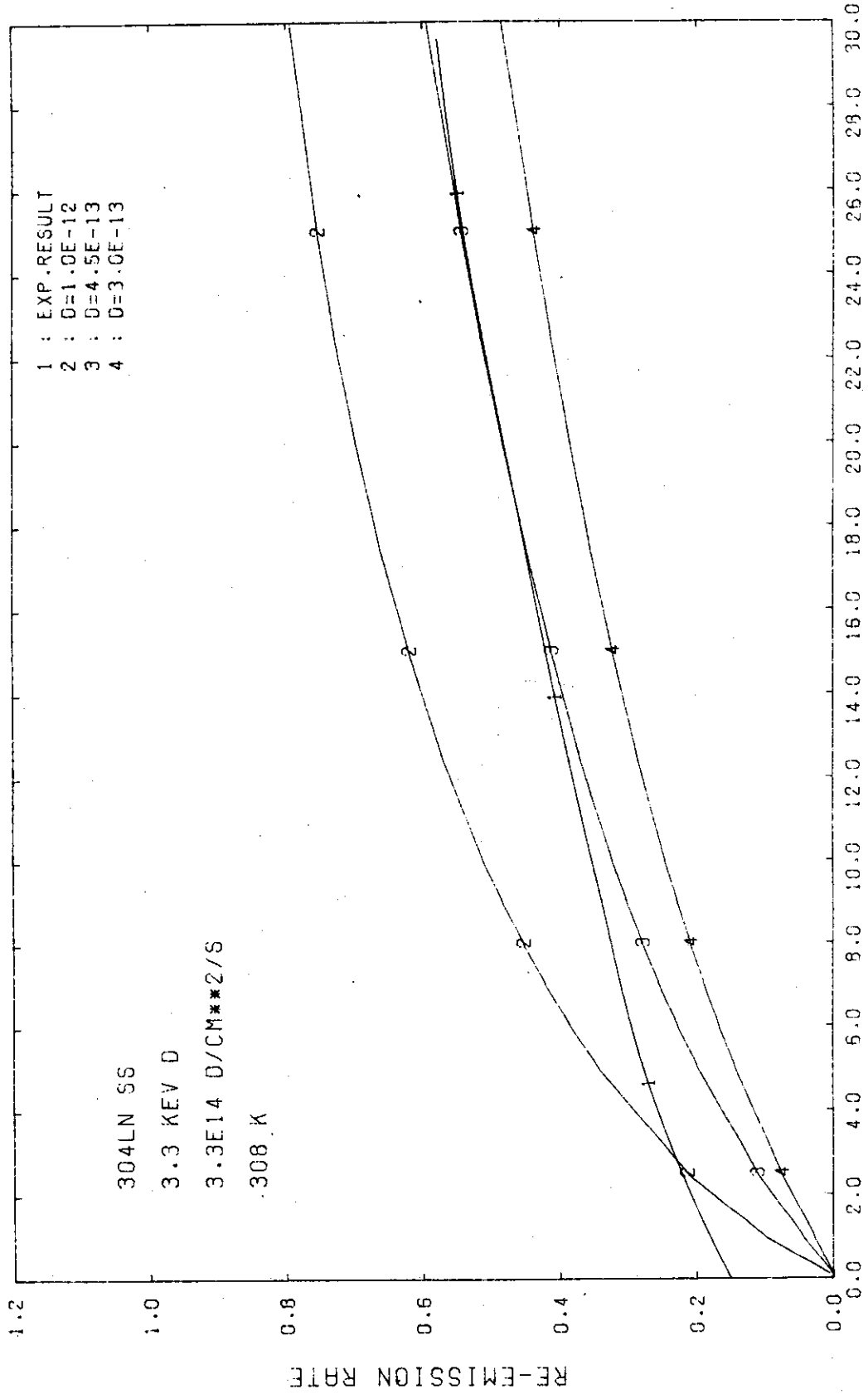

FIG.14 RE-EMISSION RATE FOR VARIOUS DIFFUSION CONSTANTS (REQ7)

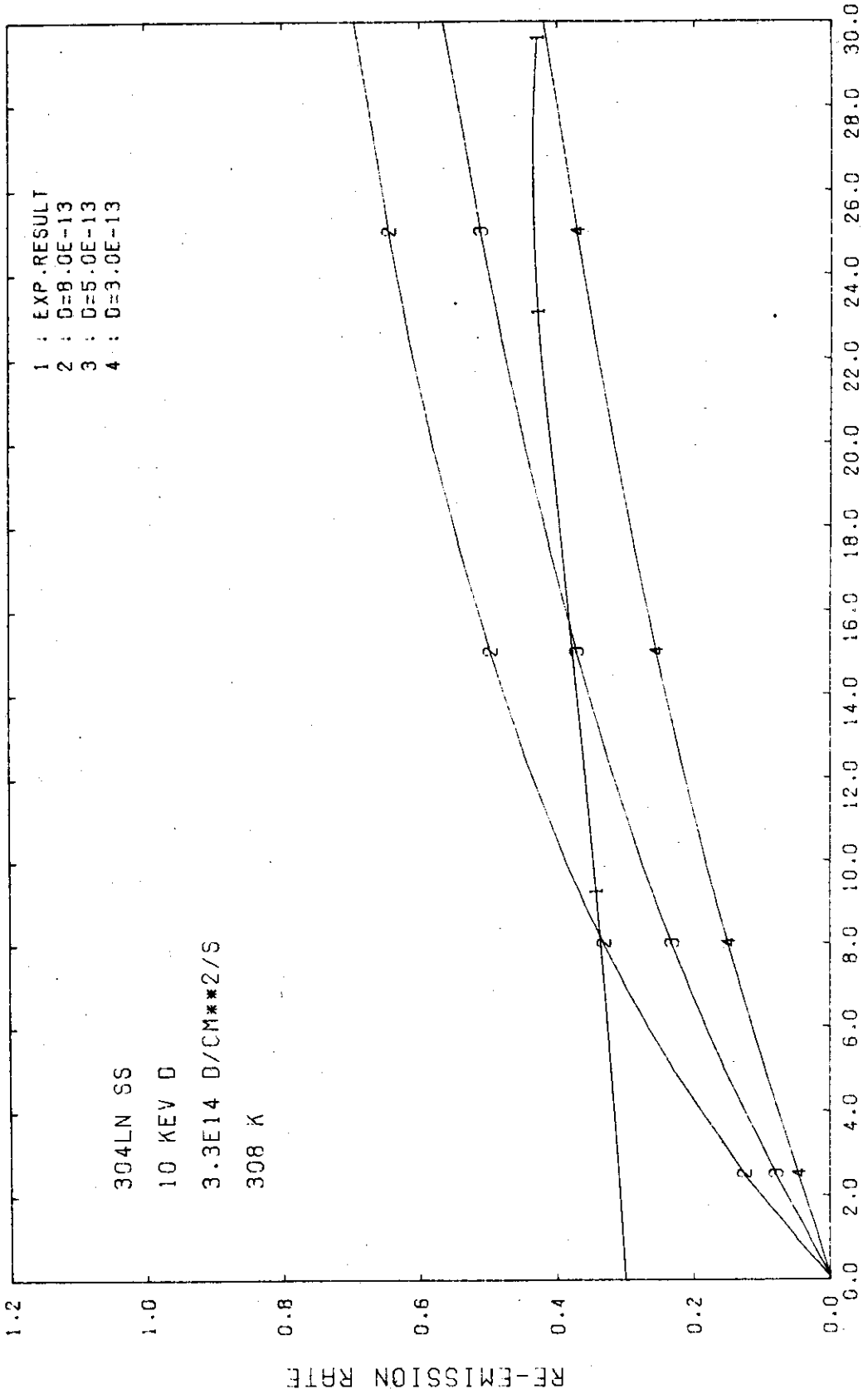

FIG.15 RE-EMISSION RATE FOR VARIOUS DIFFUSION CONSTANTS (RE07)

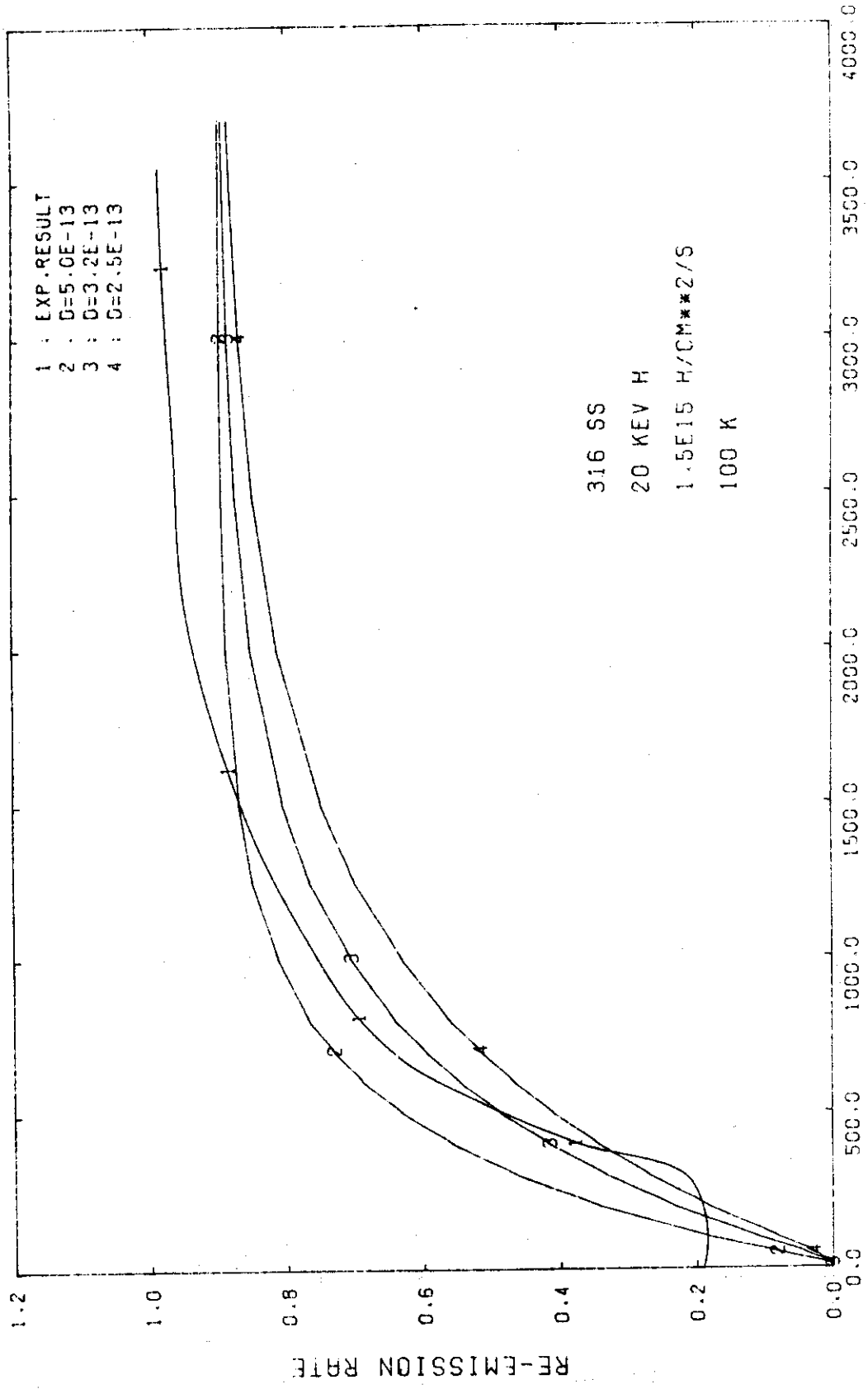

FIG.16 RE-EMISSION RATE FOR VARIOUS DIFFUSION CONSTANTS (REO3)

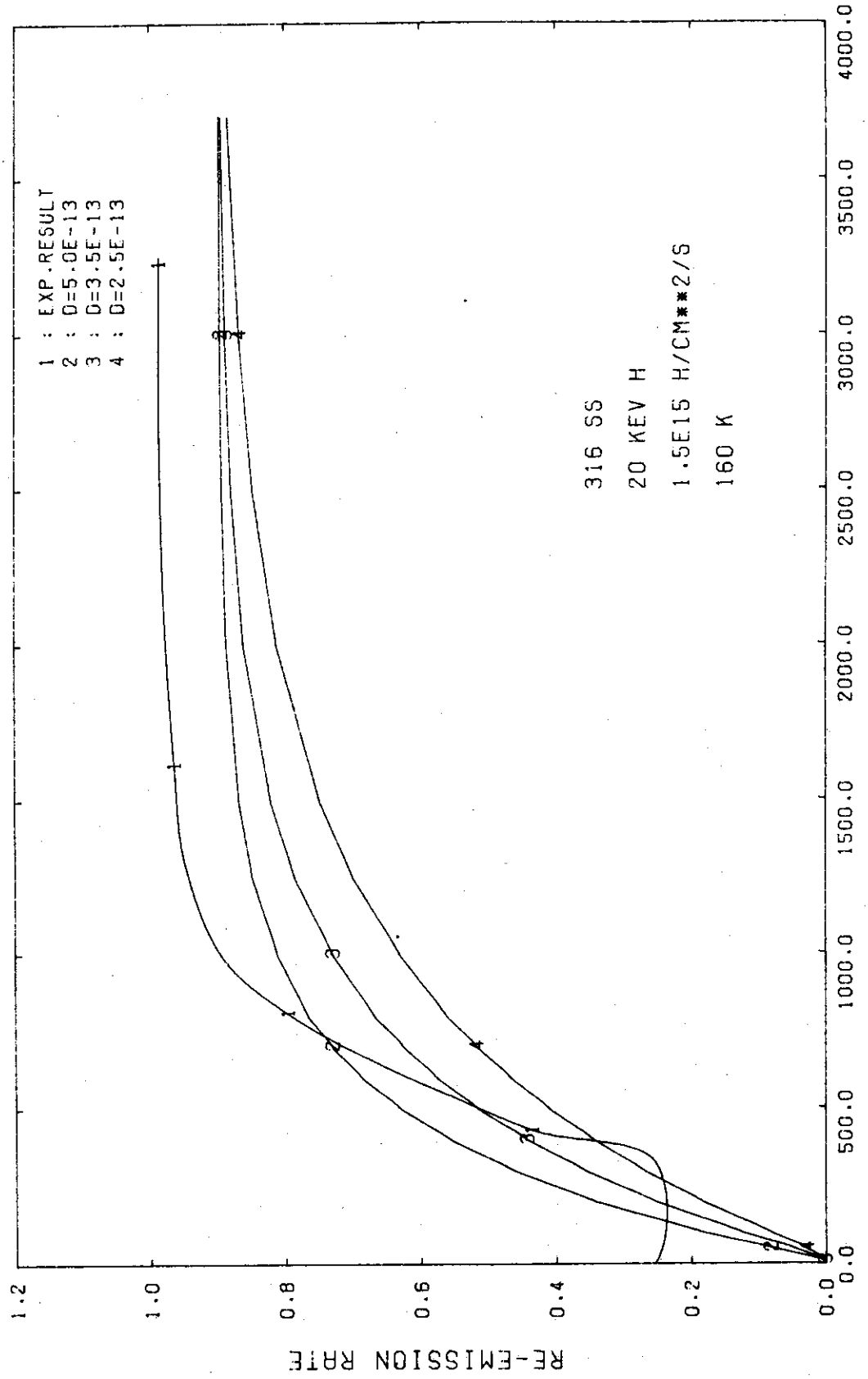

FIG.17 RE-EMISSION RATE FOR VARIOUS DIFFUSION CONSTANTS (RE09)

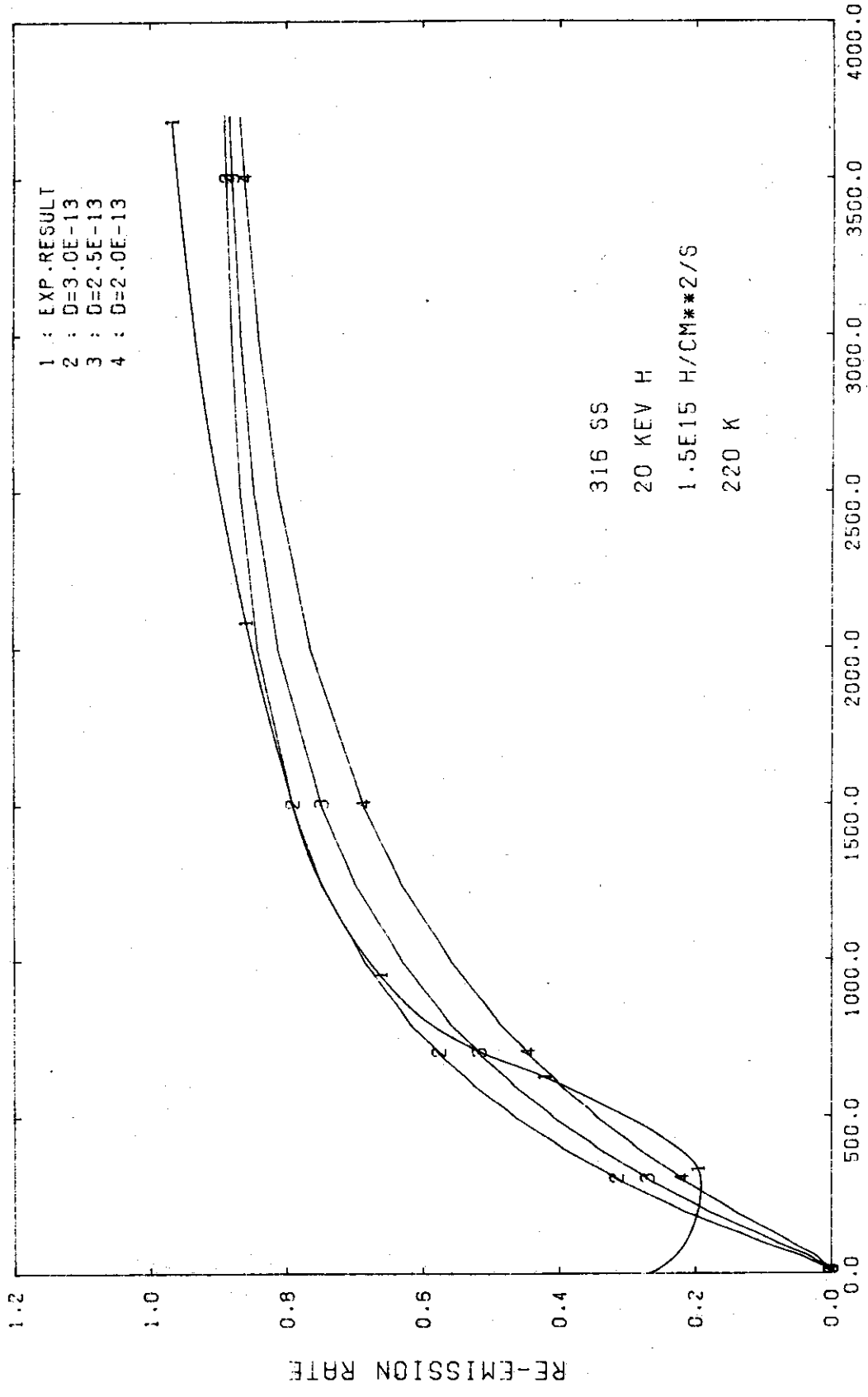

FIG.18 RE-EMISSION RATE FOR VARIOUS DIFFUSION CONSTANTS (RE09)

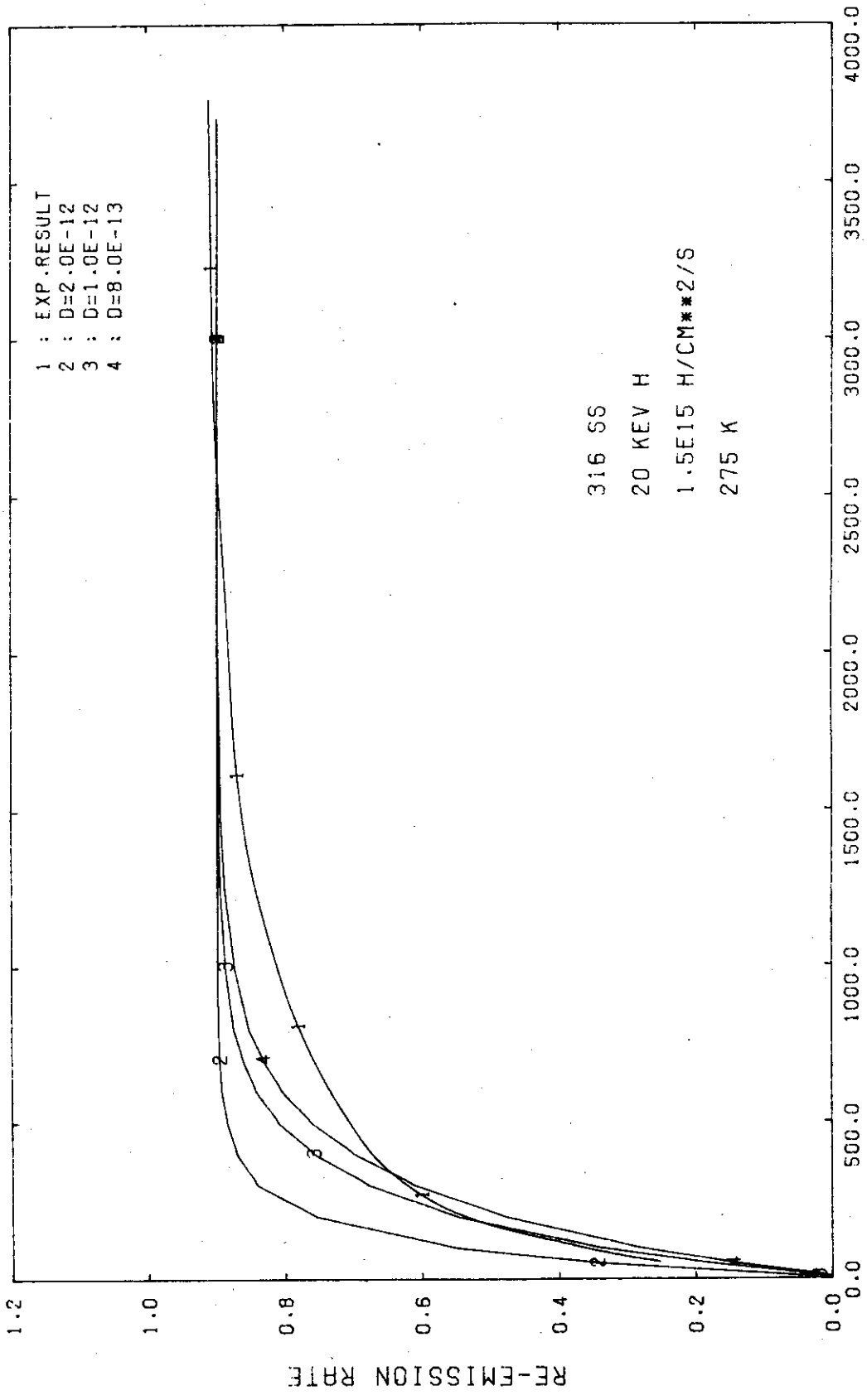

FIG.19 RE-EMISSION RATE FOR VARIOUS DIFFUSION CONSTANTS (RE09)

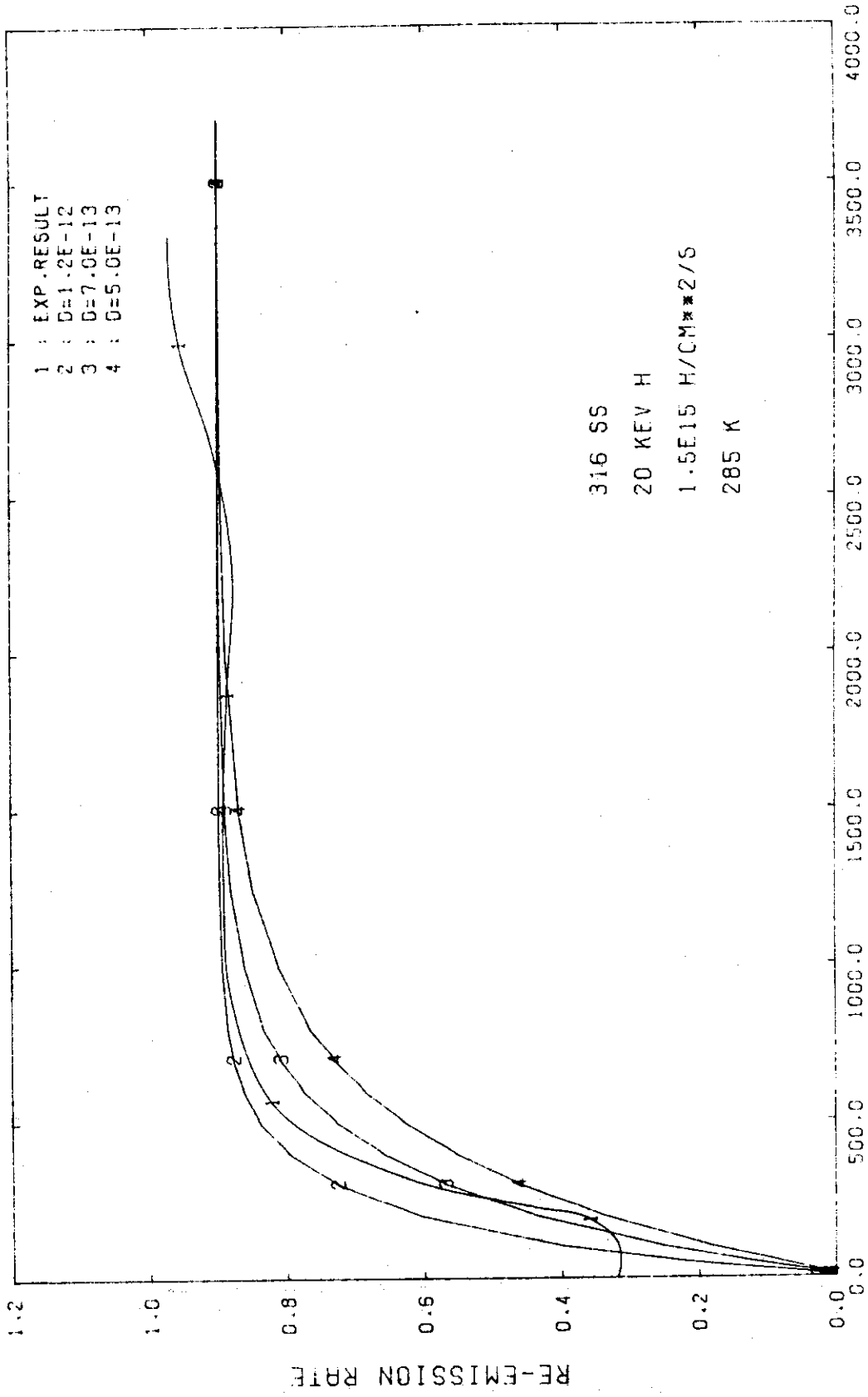

FIG.20 RE-EMISSION RATE FOR VARIOUS DIFFUSION CONSTANTS (REO9)

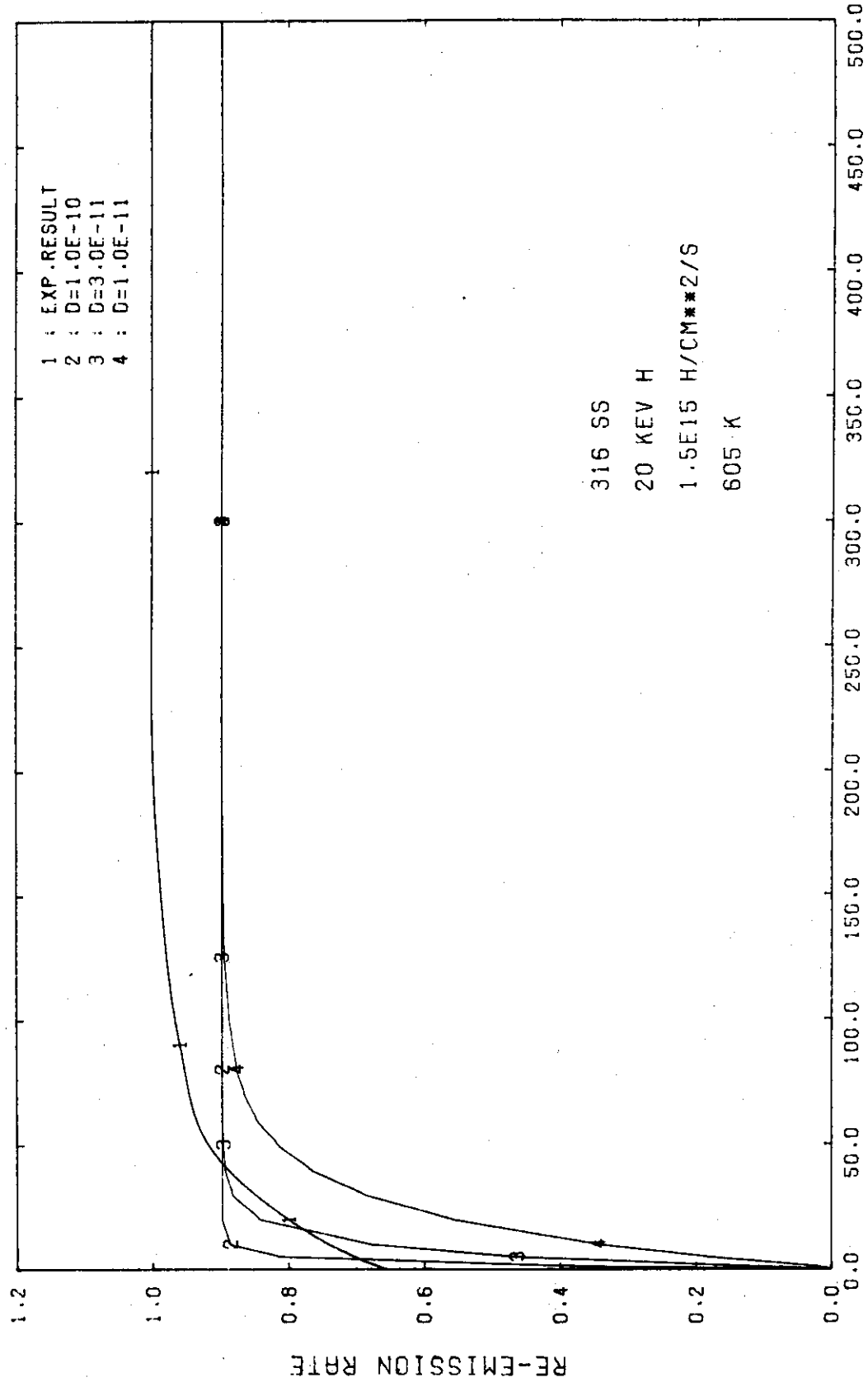

FIG.21 RE-EMISSION RATE FOR VARIOUS DIFFUSION CONSTANTS (RE09)

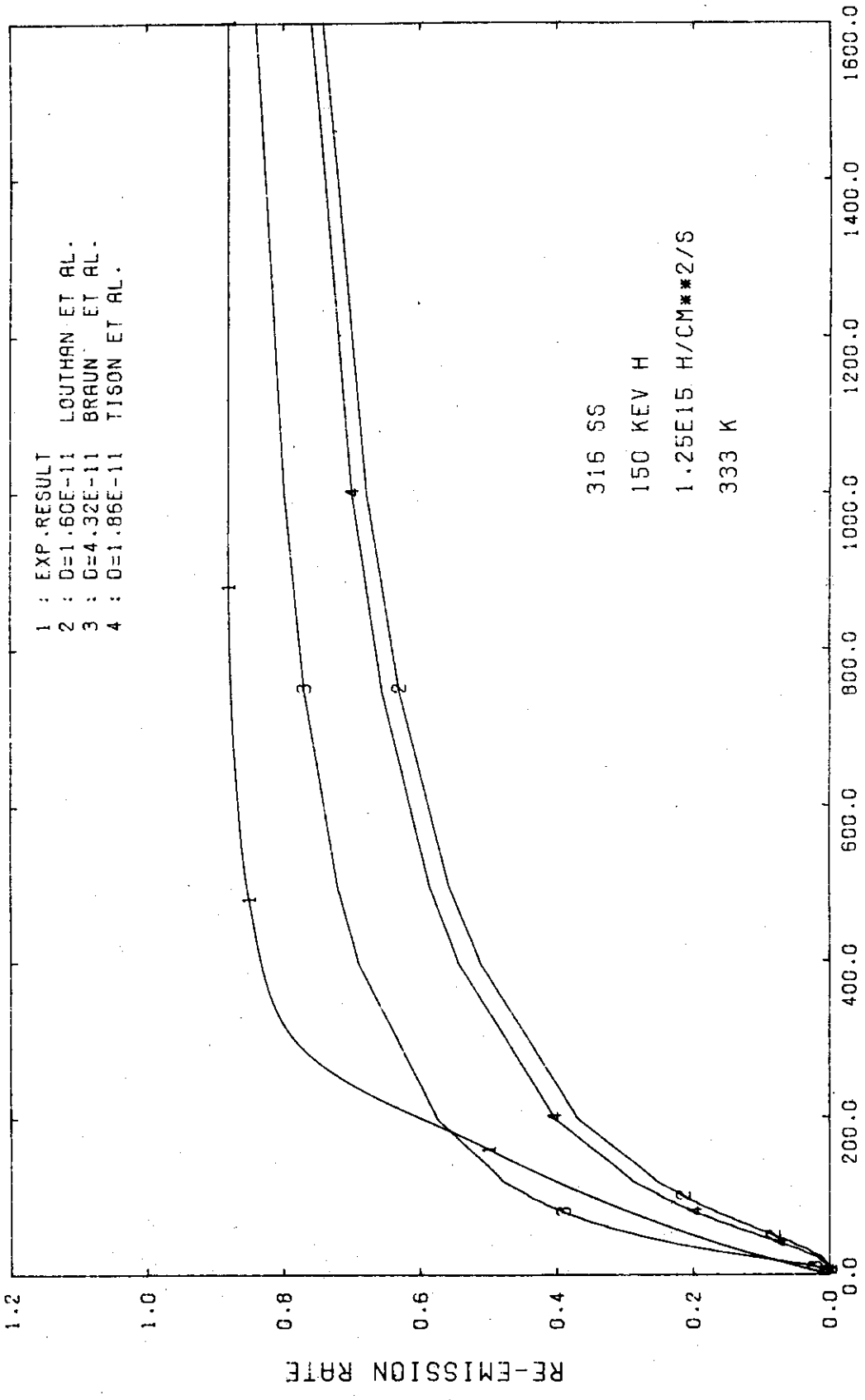

FIG.22 RE-EMISSION RATE FOR EXPERIMENTALLY OBTAINED DIFFUSION CONSTANTS (RE01)

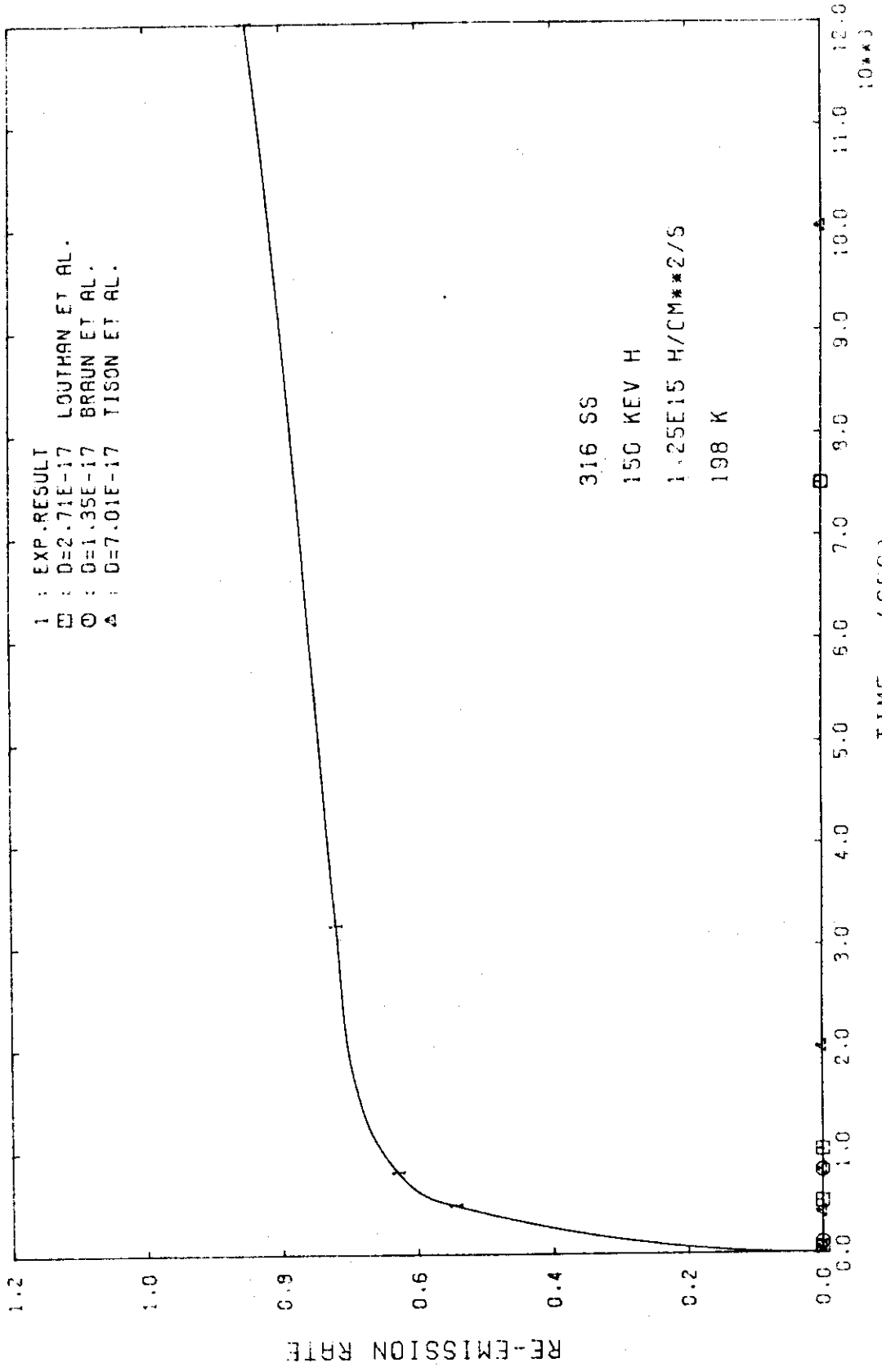

FIG.23 RE-EMISSION RATE FOR EXPERIMENTALLY OBTAINED DIFFUSION CONSTANTS (REF.1)

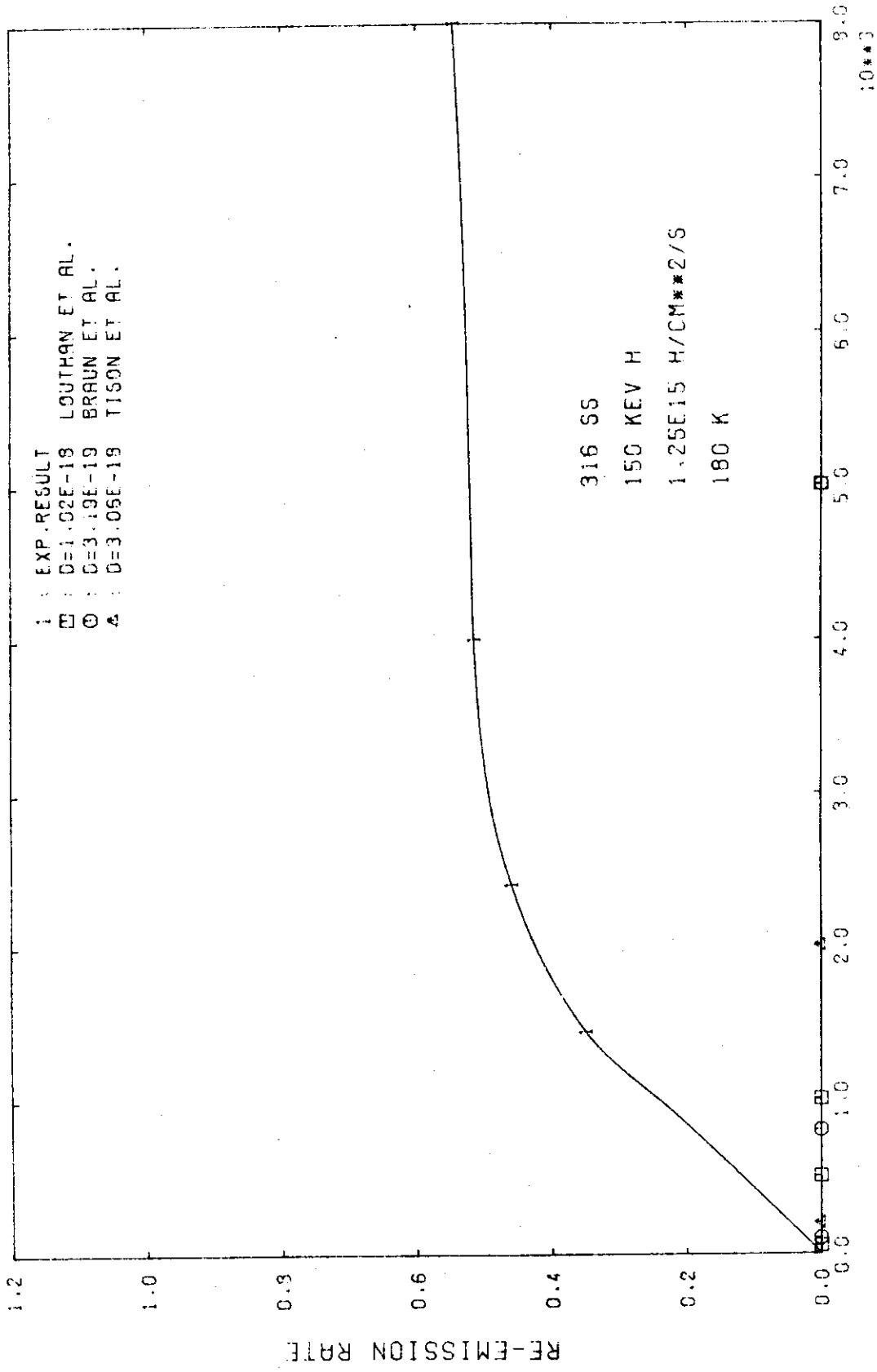

FIG.24 RE-EMISSION RATE FOR EXPERIMENTALLY OBTAINED DIFFUSION CONSTANTS (REF.11)

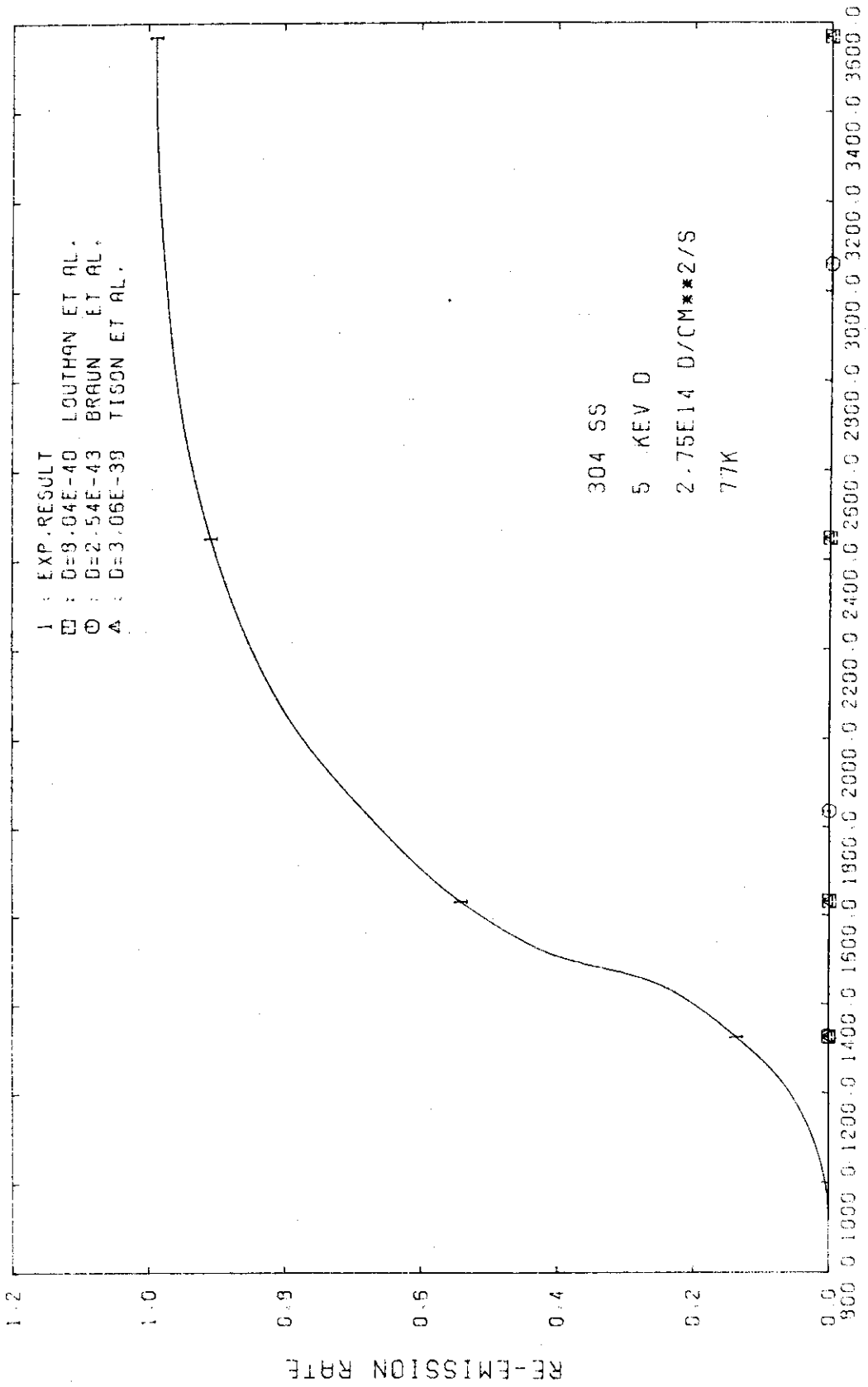

FIG.25 RE-EMISSION RATE FOR EXPERIMENTALLY OBTAINED DIFFUSION CONSTANTS (RE02)

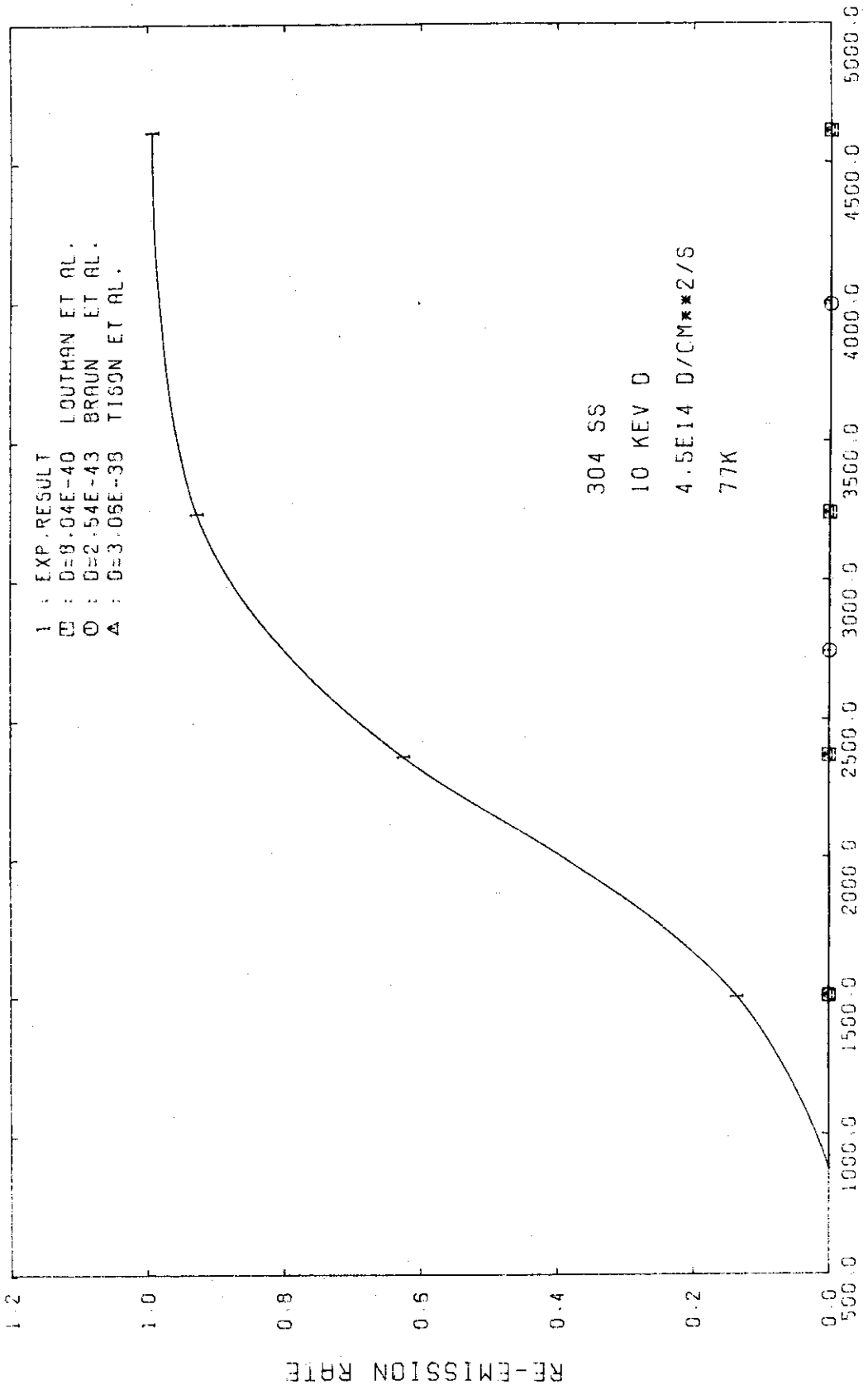

FIG.26 RE-EMISSION RATE FOR EXPERIMENTALLY OBTAINED DIFFUSION CONSTANTS (RE02)

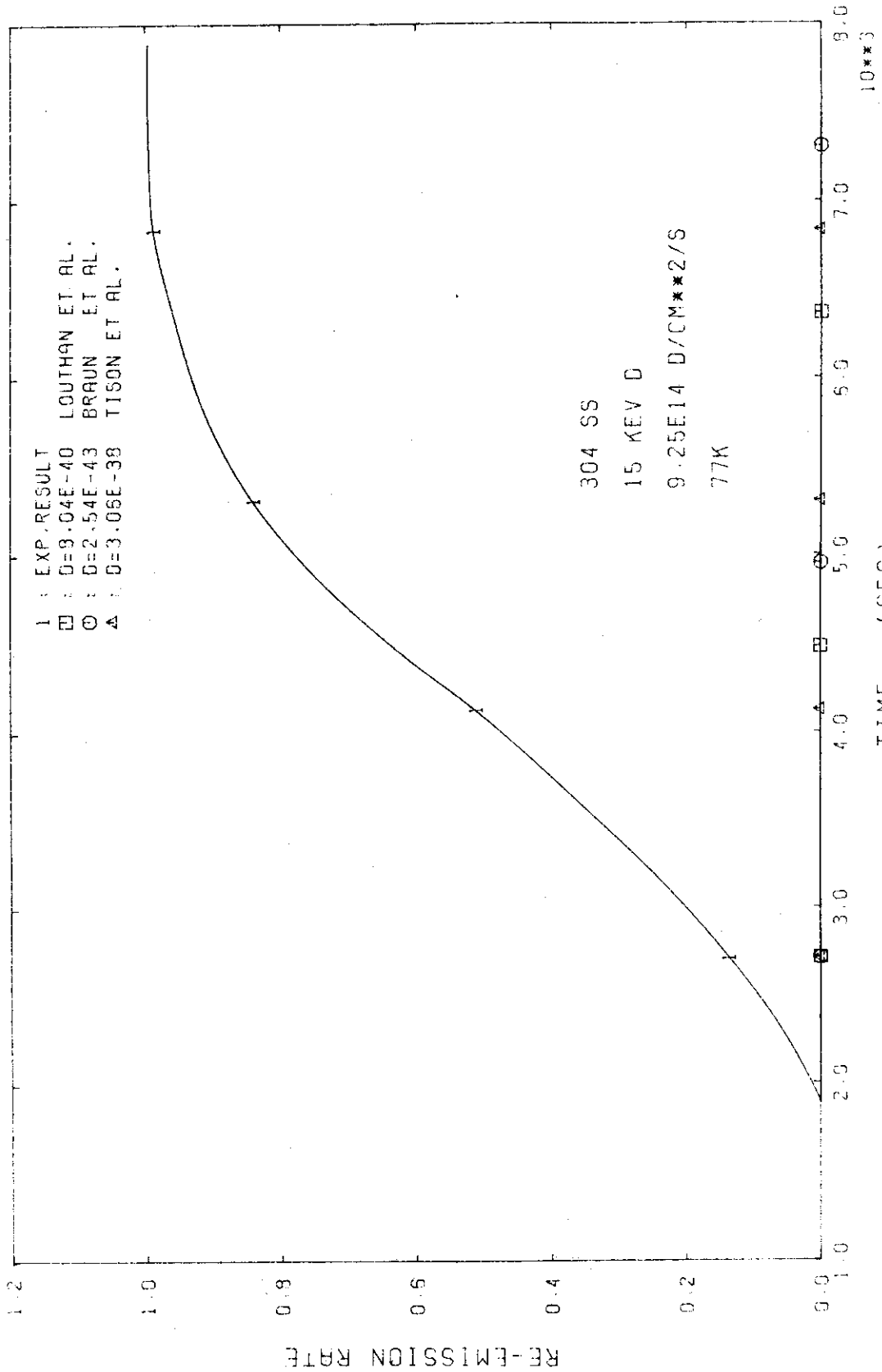

FIG.27 RE-EMISSION RATE FOR EXPERIMENTALLY OBTAINED DIFFUSION CONSTANTS (RE02)

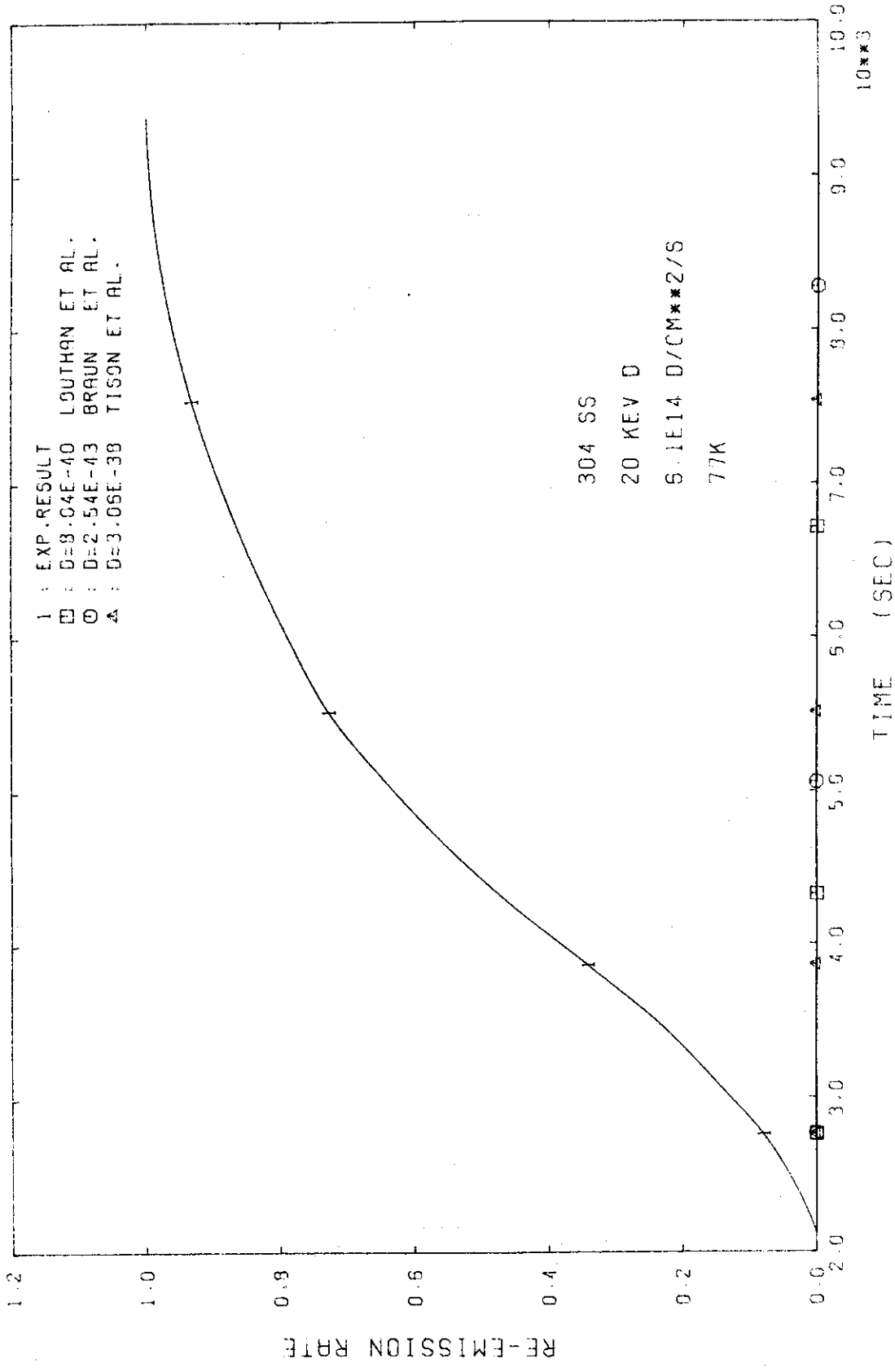

FIG.28 RE-EMISSION RATE FOR EXPERIMENTALLY OBTAINED DIFFUSION CONSTANTS (RE02)

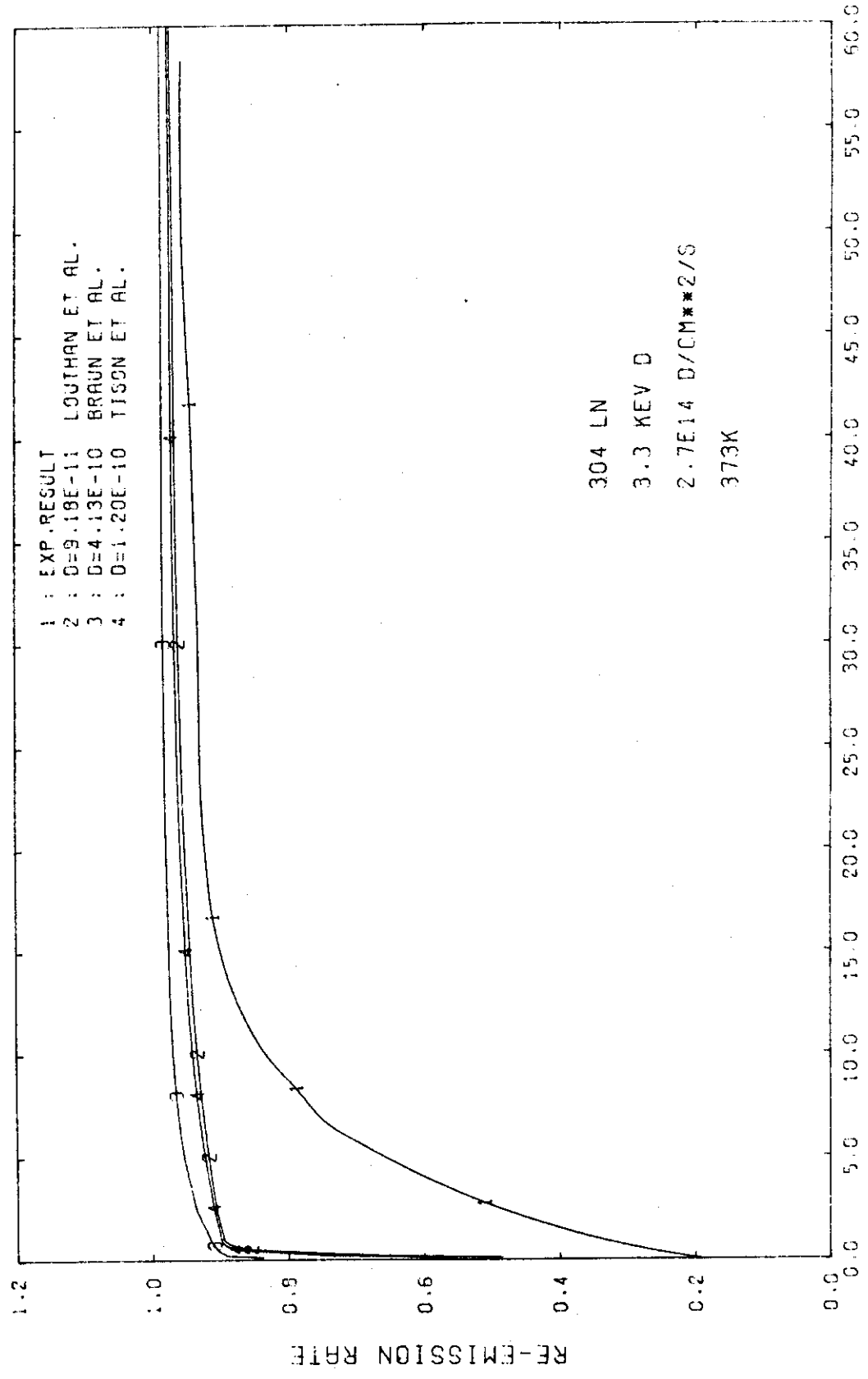

FIG.29 RE-EMISSION RATE FOR EXPERIMENTALLY OBTAINED DIFFUSION CONSTANTS
(REO6)

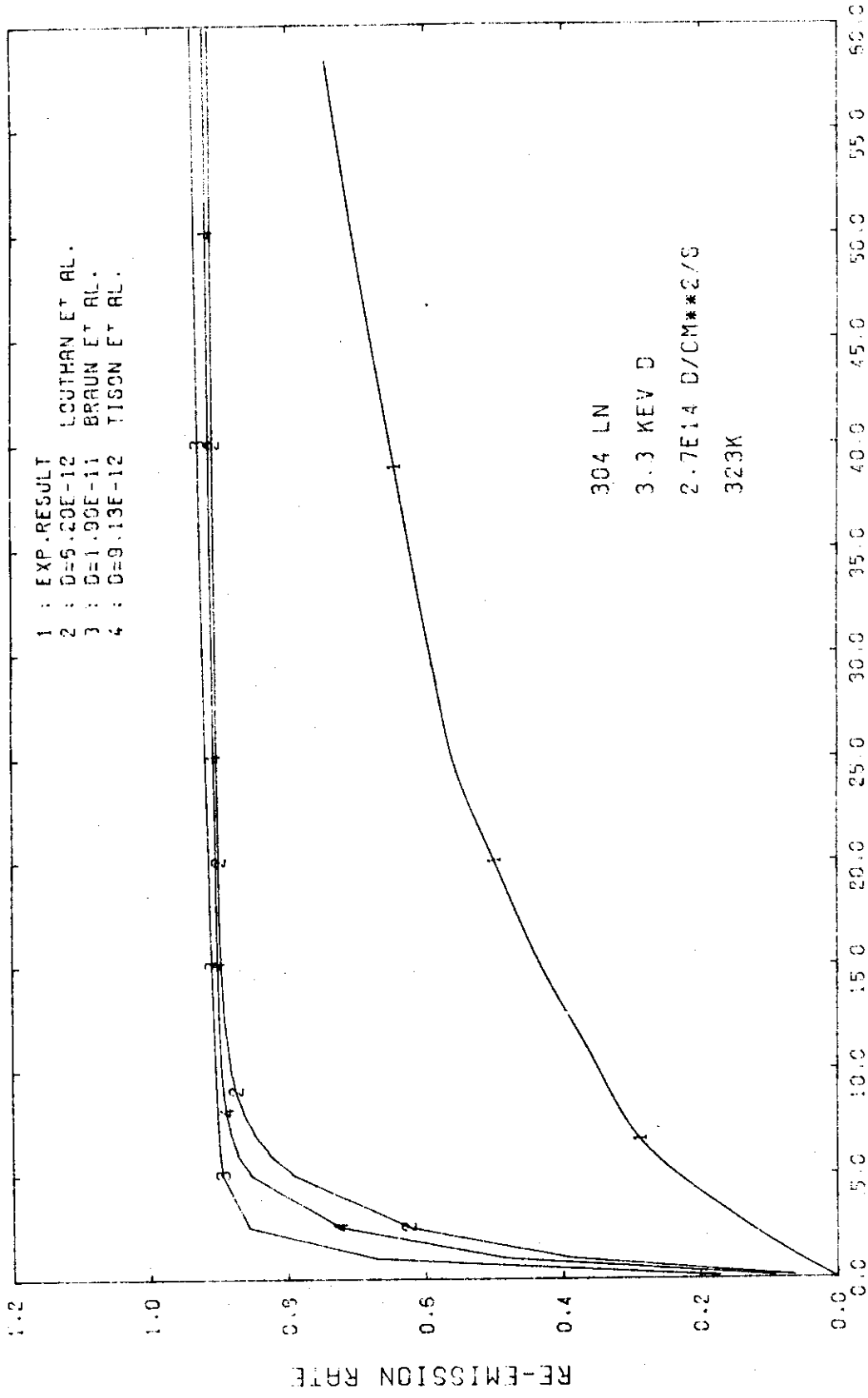

FIG.30 RE-EMISSION RATE FOR EXPERIMENTALLY OBTAINED DIFFUSION CONSTANTS (REOS)

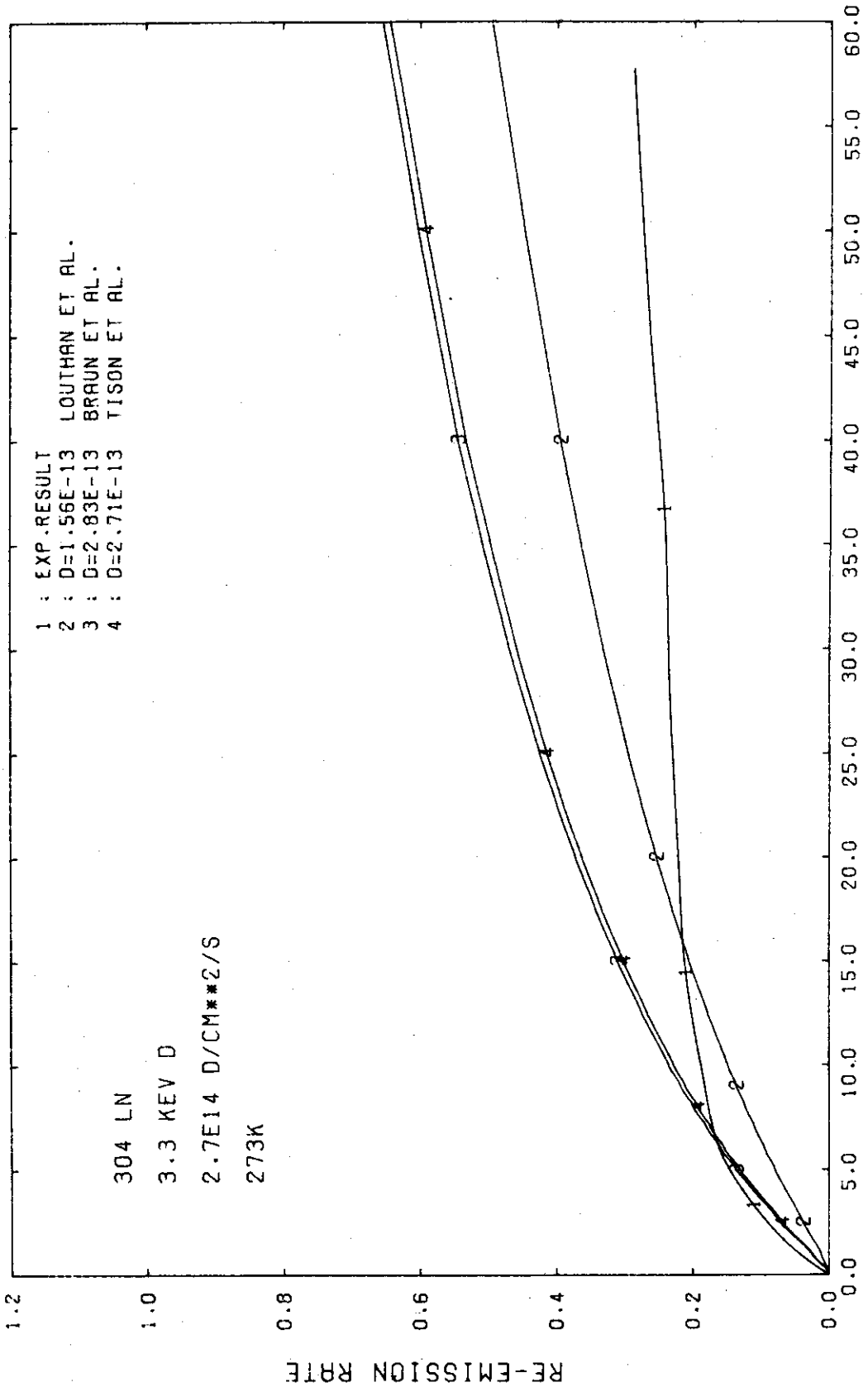

FIG.31 RE-EMISSION RATE FOR EXPERIMENTALLY OBTAINED DIFFUSION CONSTANTS
(RE06)

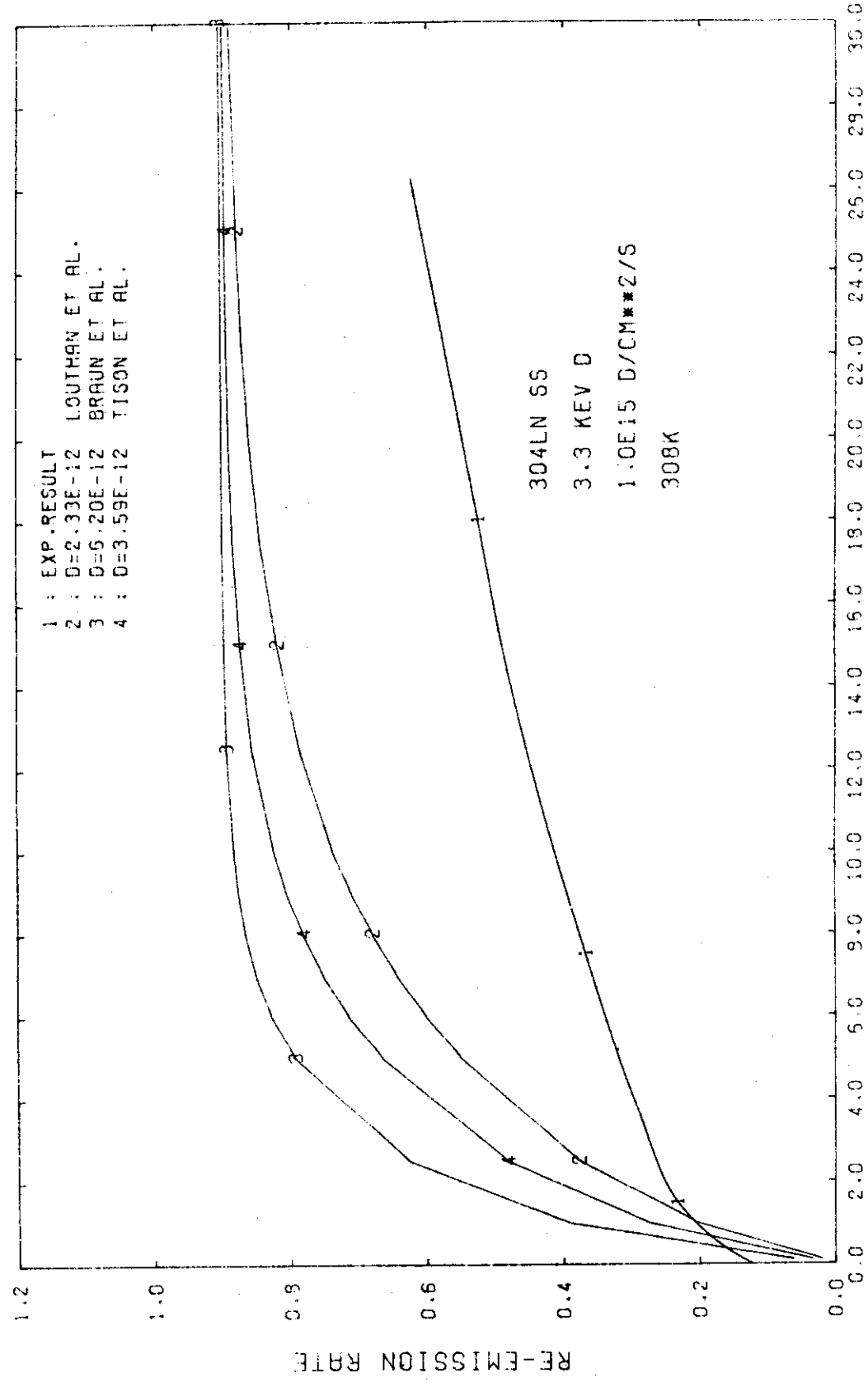

FIG.32 RE-EMISSION RATE FOR EXPERIMENTALLY OBTAINED DIFFUSION CONSTANTS (REO7)

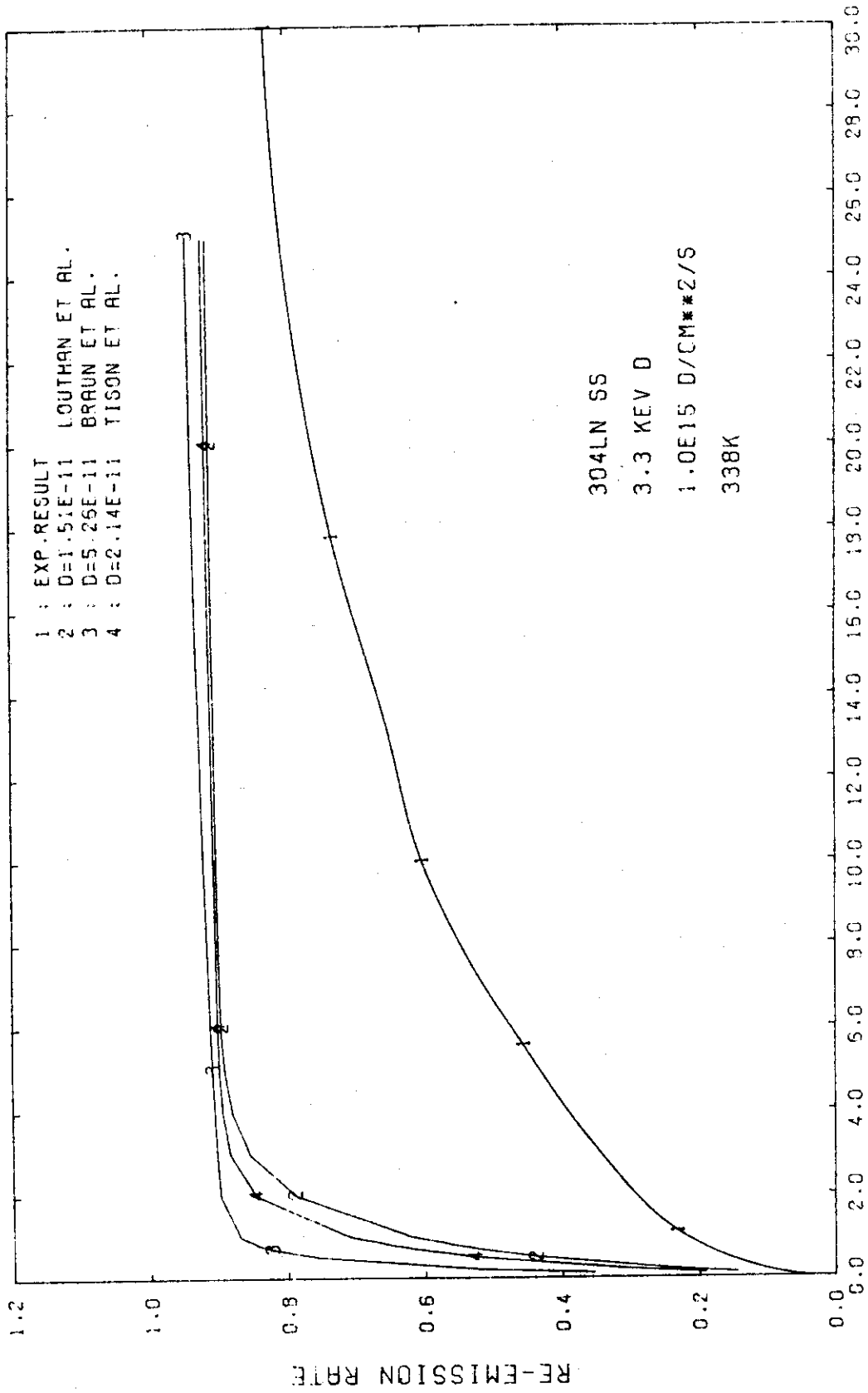

FIG.33 RE-EMISSION RATE FOR EXPERIMENTALLY OBTAINED DIFFUSION CONSTANTS (RE07)

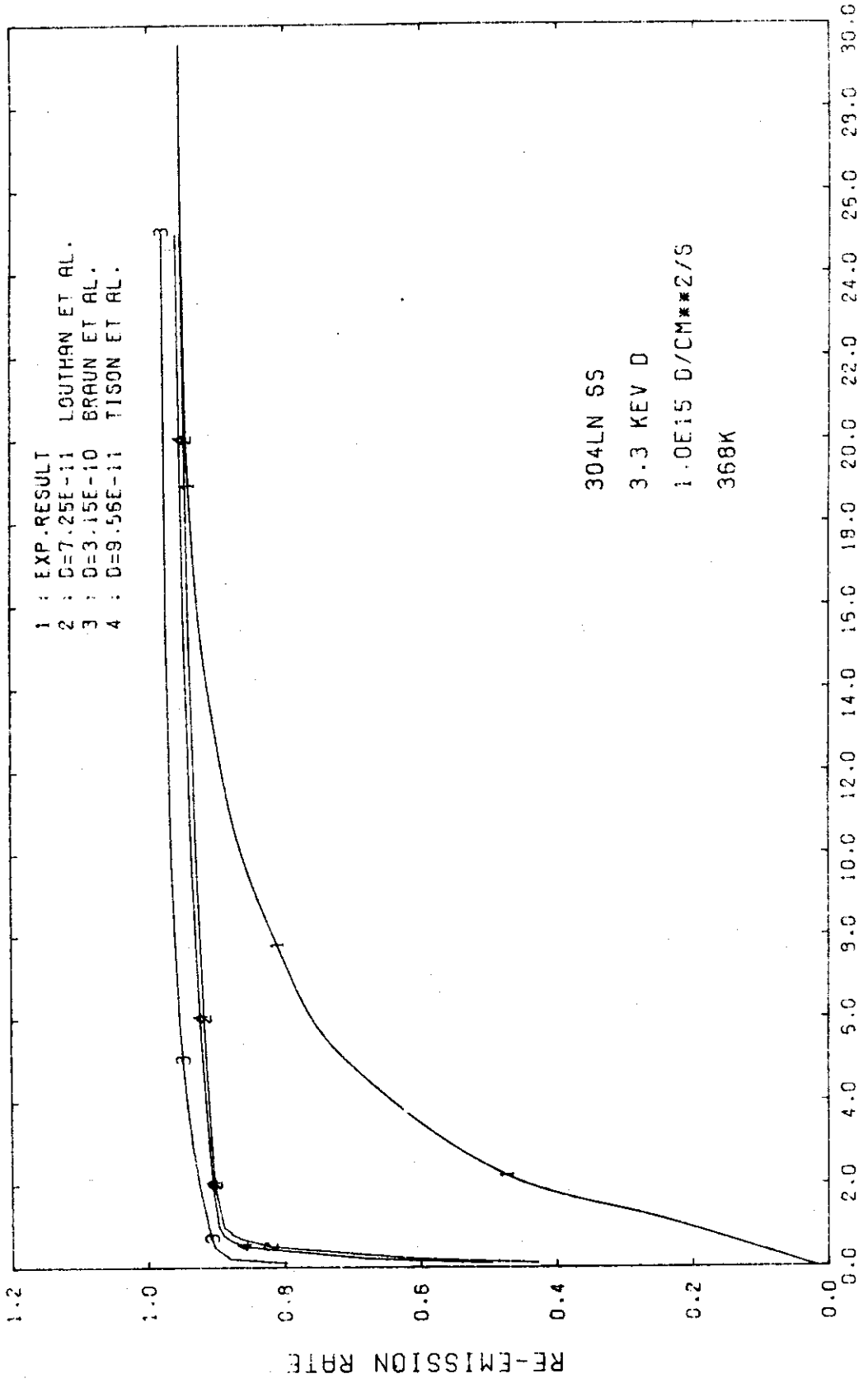

FIG.34 RE-EMISSION RATE FOR EXPERIMENTALLY OBTAINED DIFFUSION CONSTANTS (REO7)

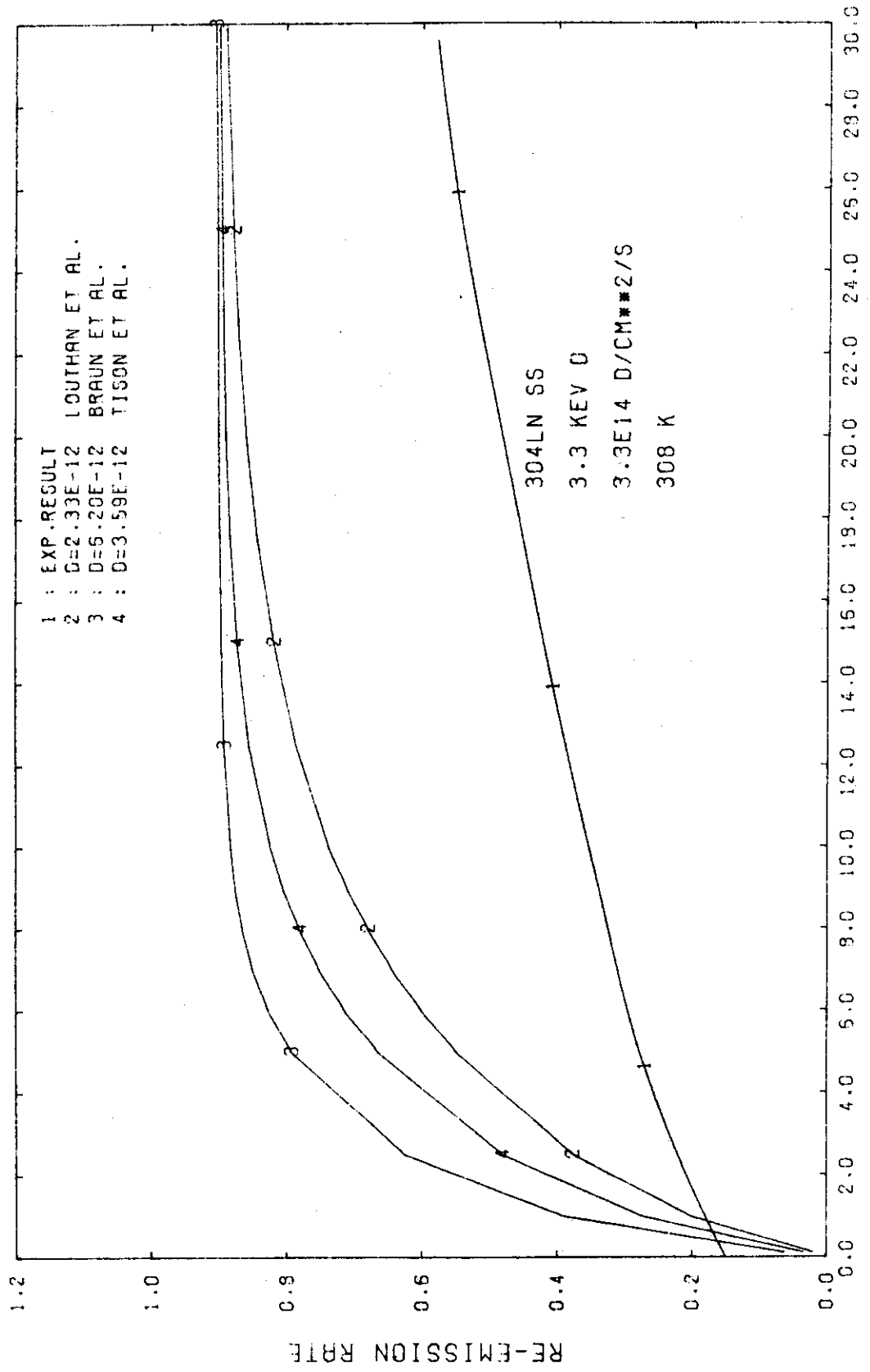

FIG.35 RE-EMISSION RATE FOR EXPERIMENTALLY OBTAINED DIFFUSION CONSTANTS (RE07)

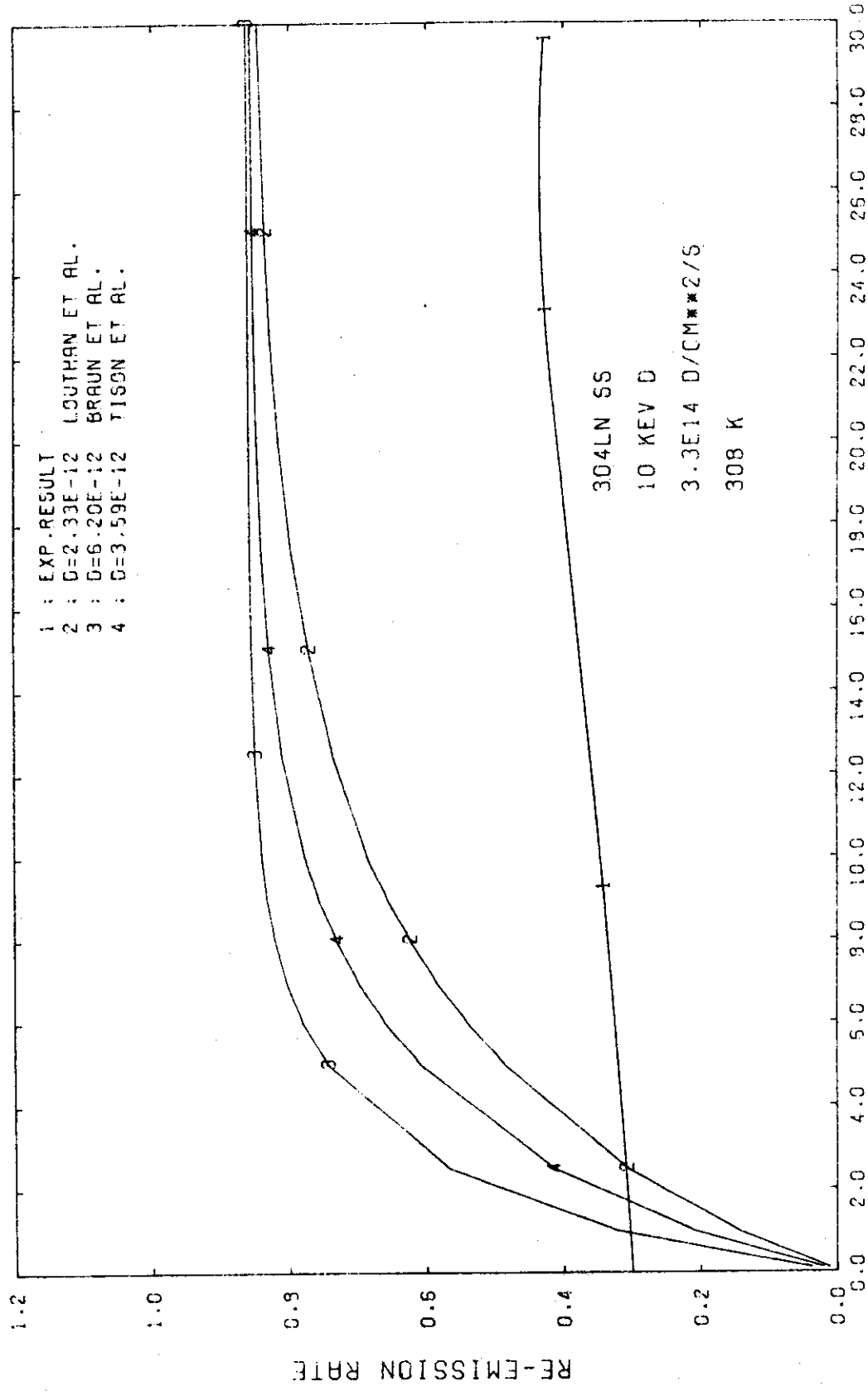

FIG.36 RE-EMISSION RATE FOR EXPERIMENTALLY OBTAINED DIFFUSION CONSTANTS (REF07)

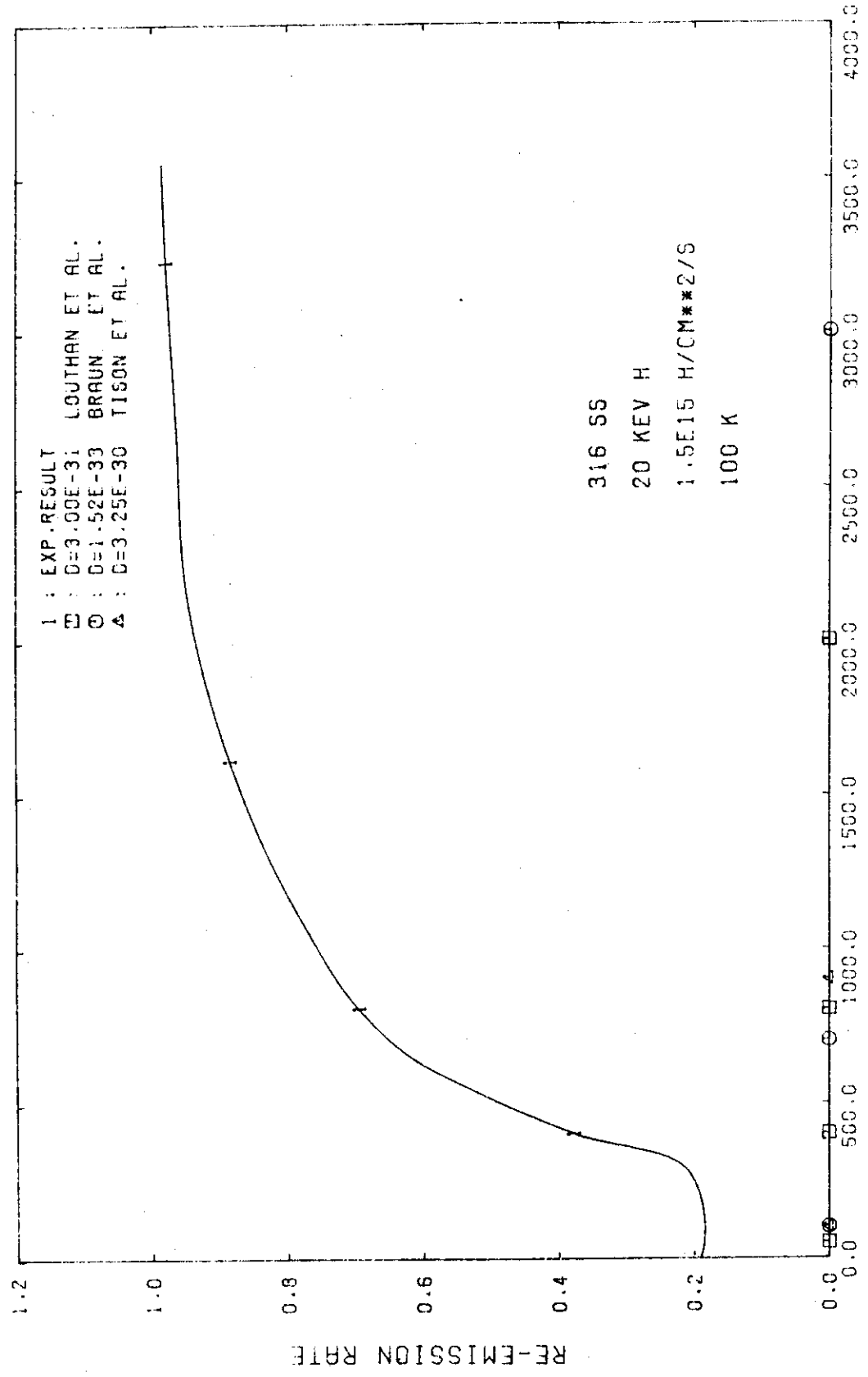

FIG.37 RE-EMISSION RATE FOR EXPERIMENTALLY OBTAINED DIFFUSION CONSTANTS (REF09)

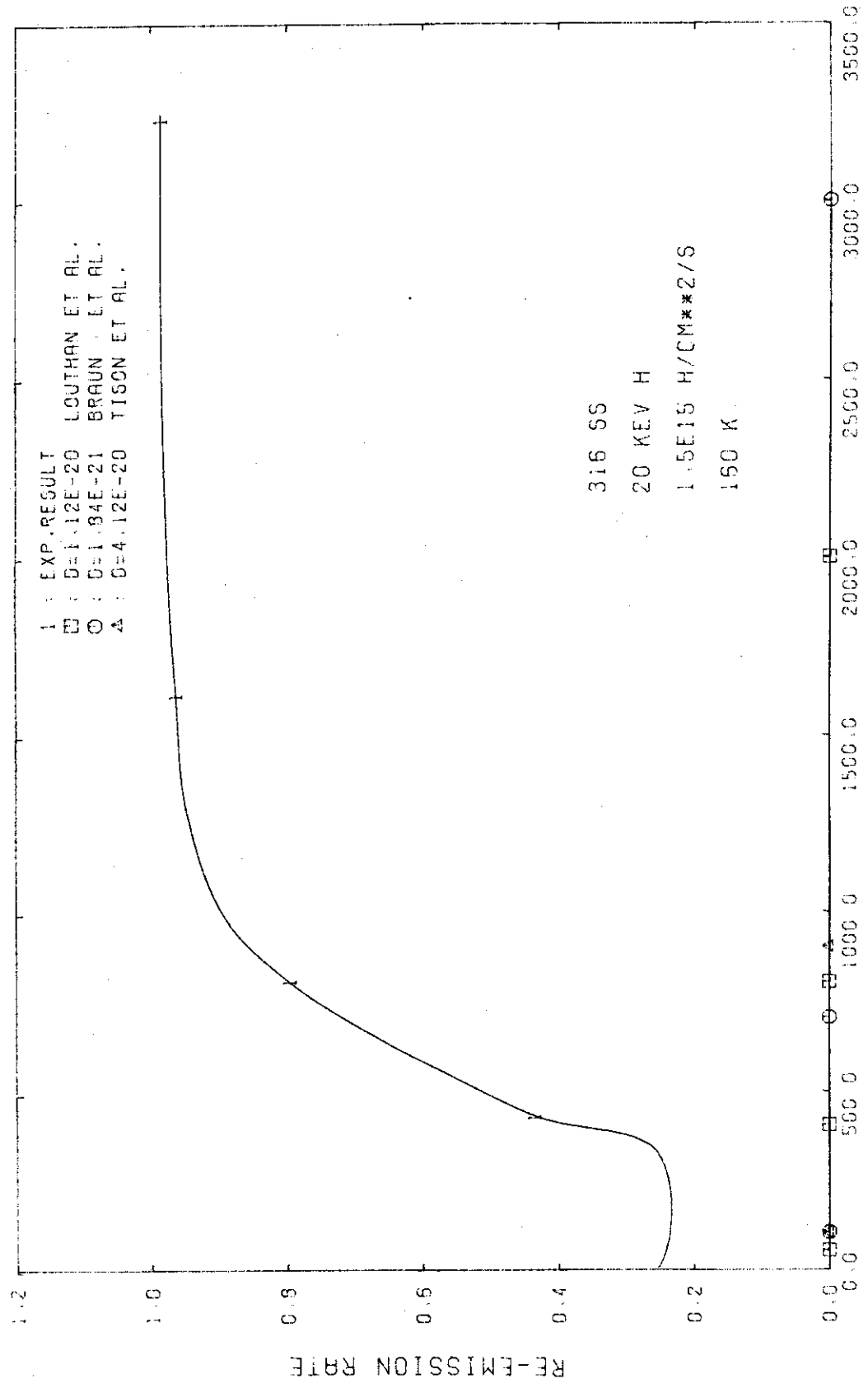

FIG.38 RE-EMISSION RATE FOR EXPERIMENTALLY OBTAINED DIFFUSION CONSTANTS (REF09)

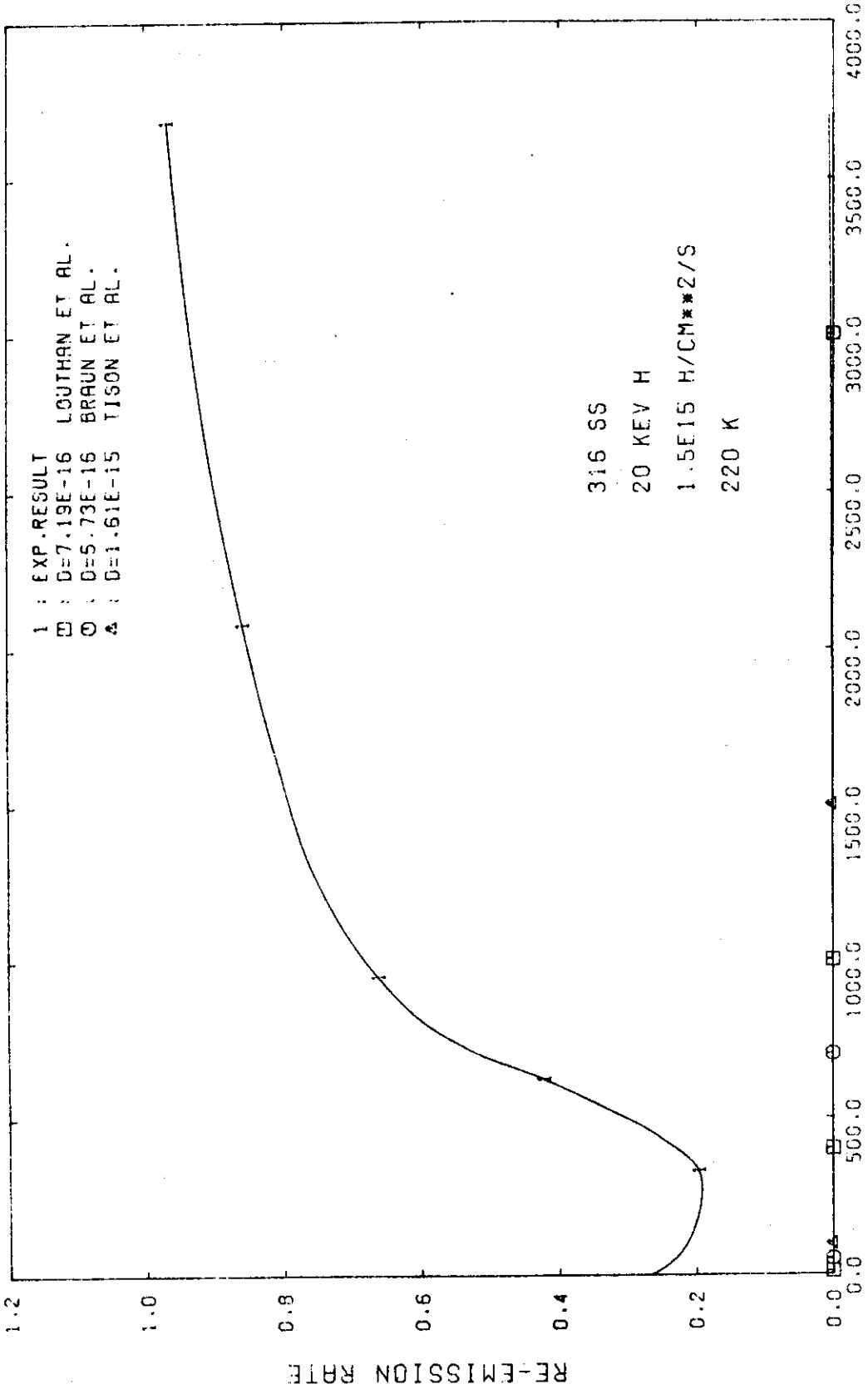

FIG.39 RE-EMISSION RATE FOR EXPERIMENTALLY OBTAINED DIFFUSION CONSTANTS (RE09)

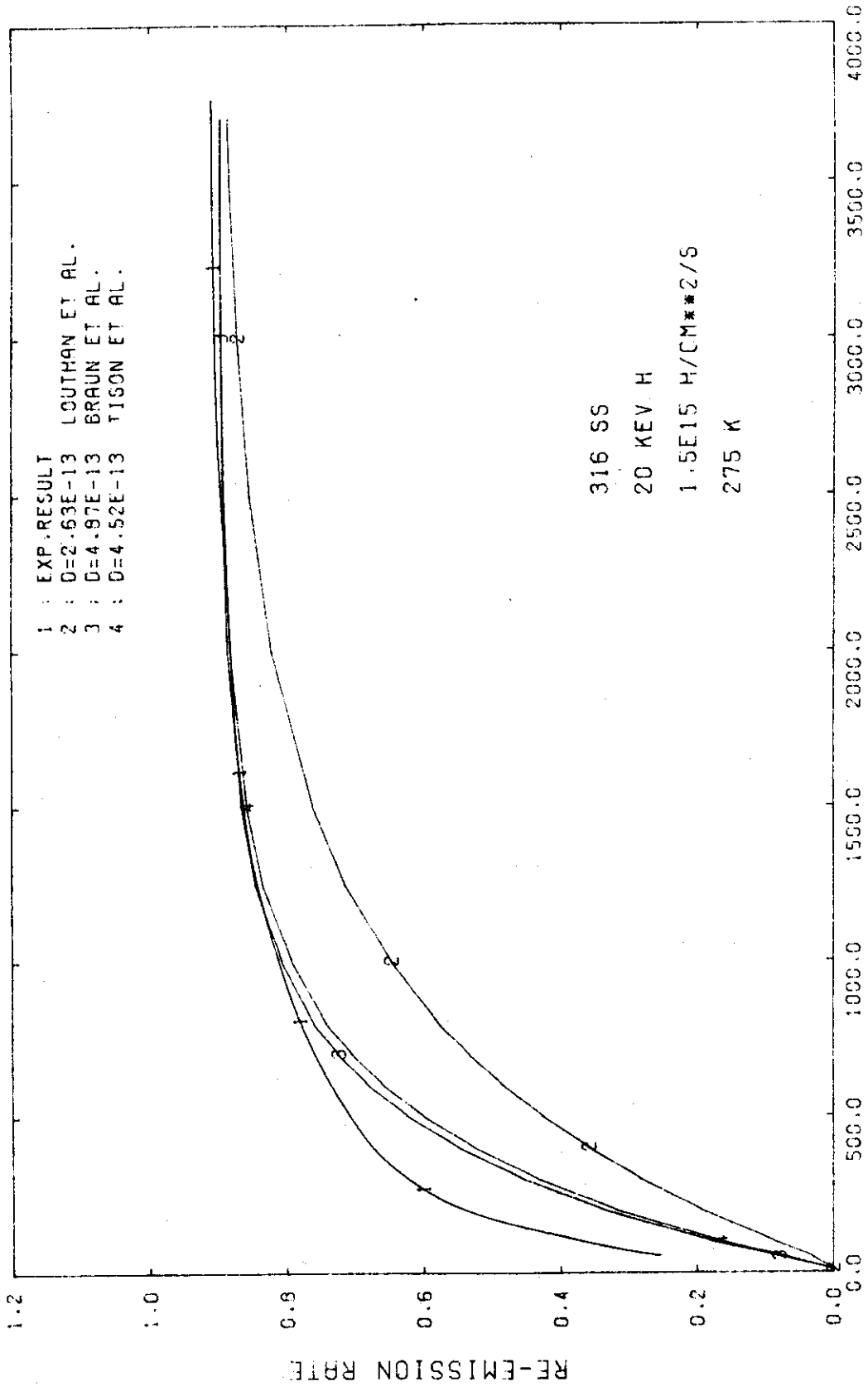

FIG.40 RE-EMISSION RATE FOR EXPERIMENTALLY OBTAINED DIFFUSION CONSTANTS (RE09)

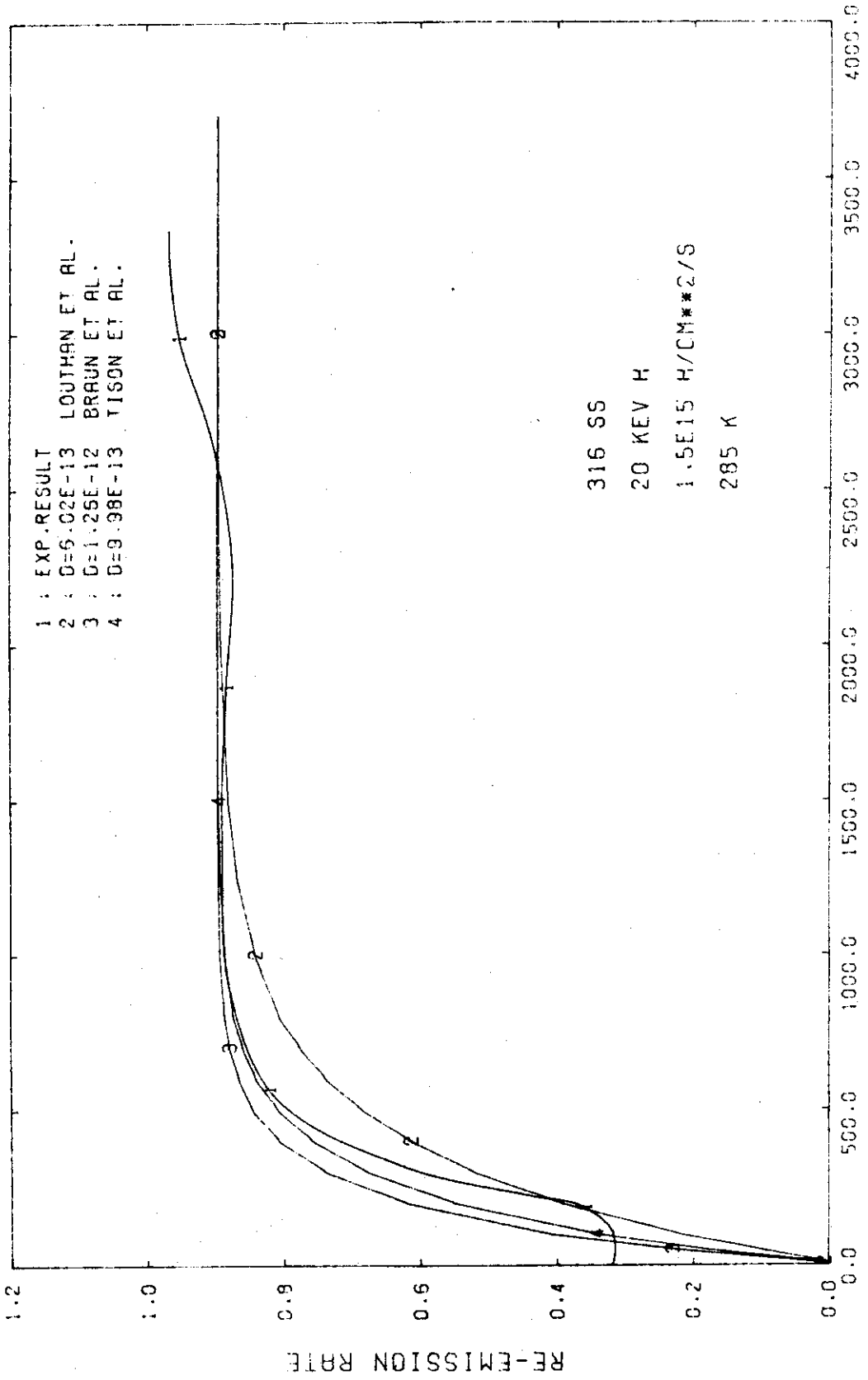

FIG.41 RE-EMISSION RATE FOR EXPERIMENTALLY OBTAINED DIFFUSION CONSTANTS (REO9)

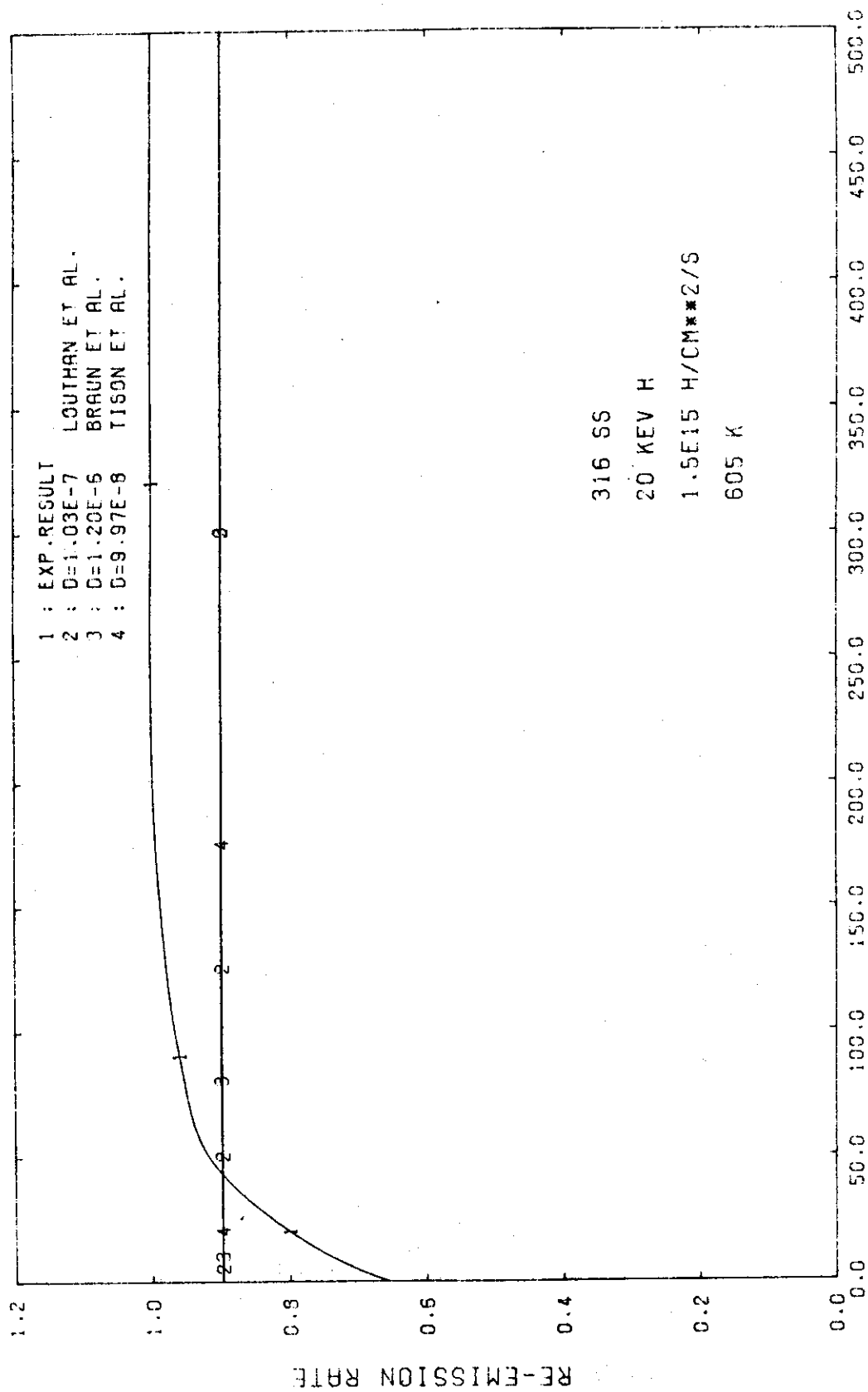

FIG.42 RE-EMISSION RATE FOR EXPERIMENTALLY OBTAINED DIFFUSION CONSTANTS (RE09)

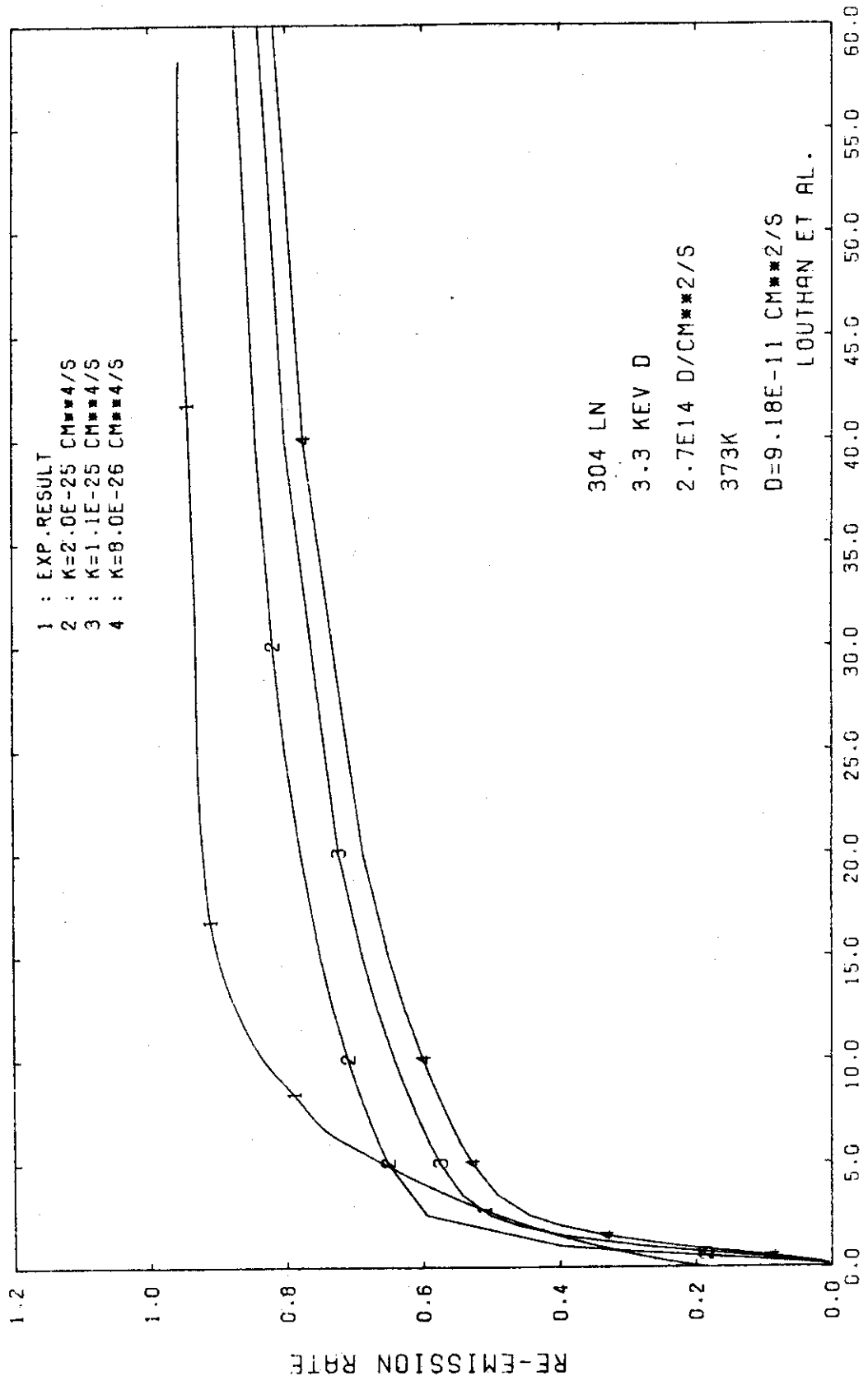

FIG.43 RE-EMISSION RATE FOR VARIOUS RECOMBINATION CONSTANTS WITH EXPERIMENTALLY OBTAINED DIFFUSION CONSTANT (RE06)

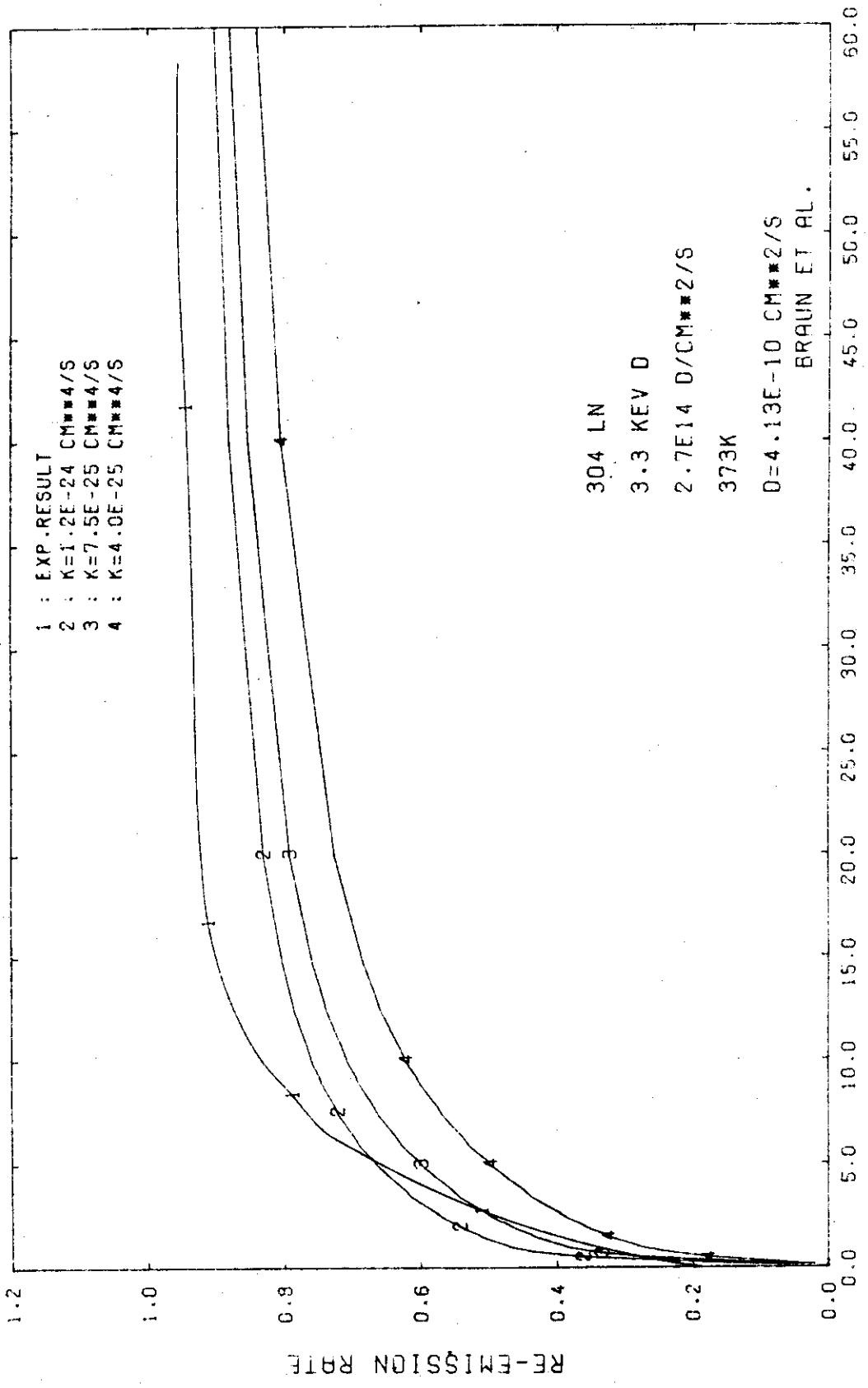

FIG.44 RE-EMISSION RATE FOR VARIOUS RECOMBINATION CONSTANTS WITH EXPERIMENTALLY OBTAINED DIFFUSION CONSTANT (REF05)

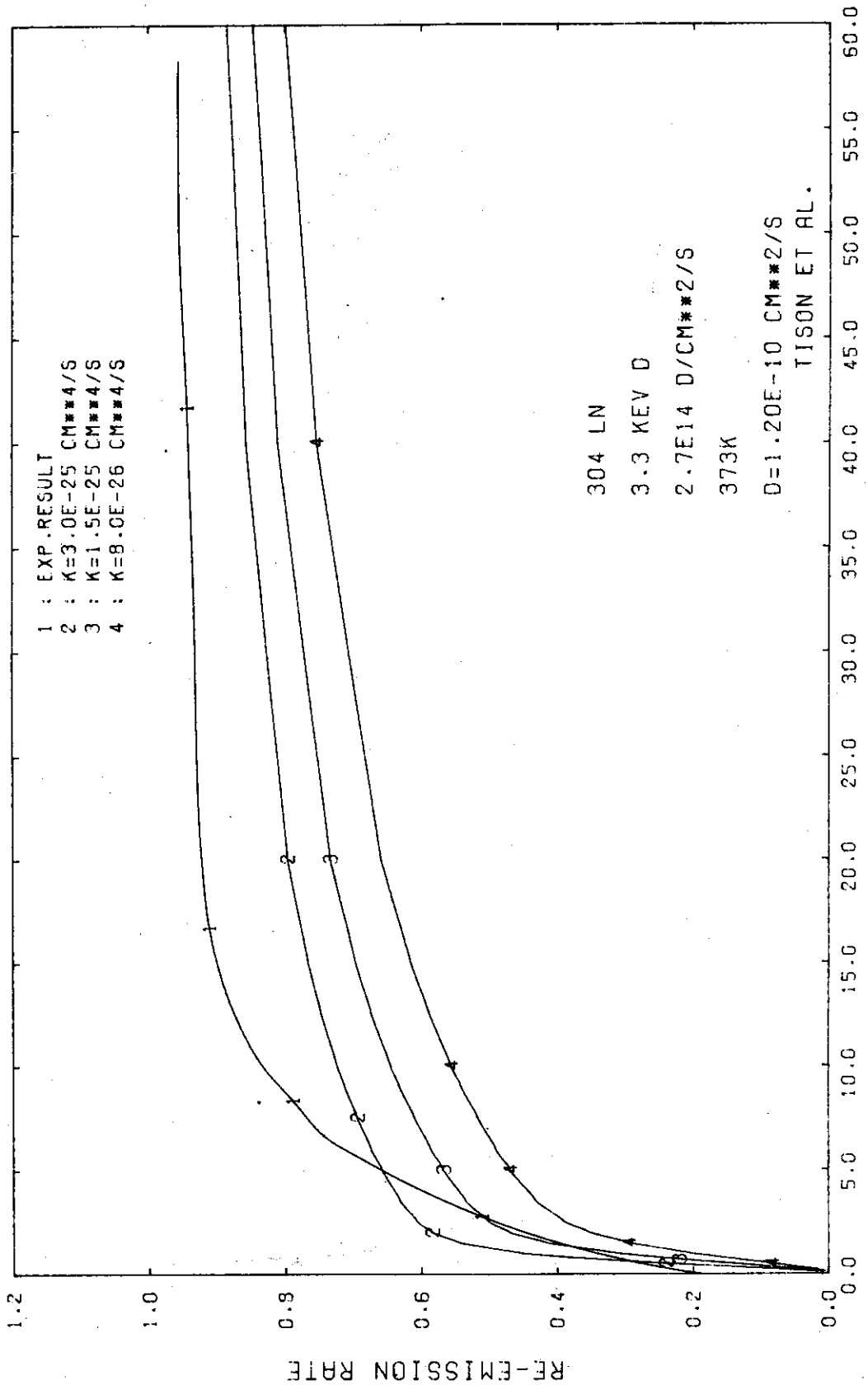

FIG.45 RE-EMISSION RATE FOR VARIOUS RECOMBINATION CONSTANTS WITH EXPERIMENTALLY OBTAINED DIFFUSION CONSTANT (REO6)

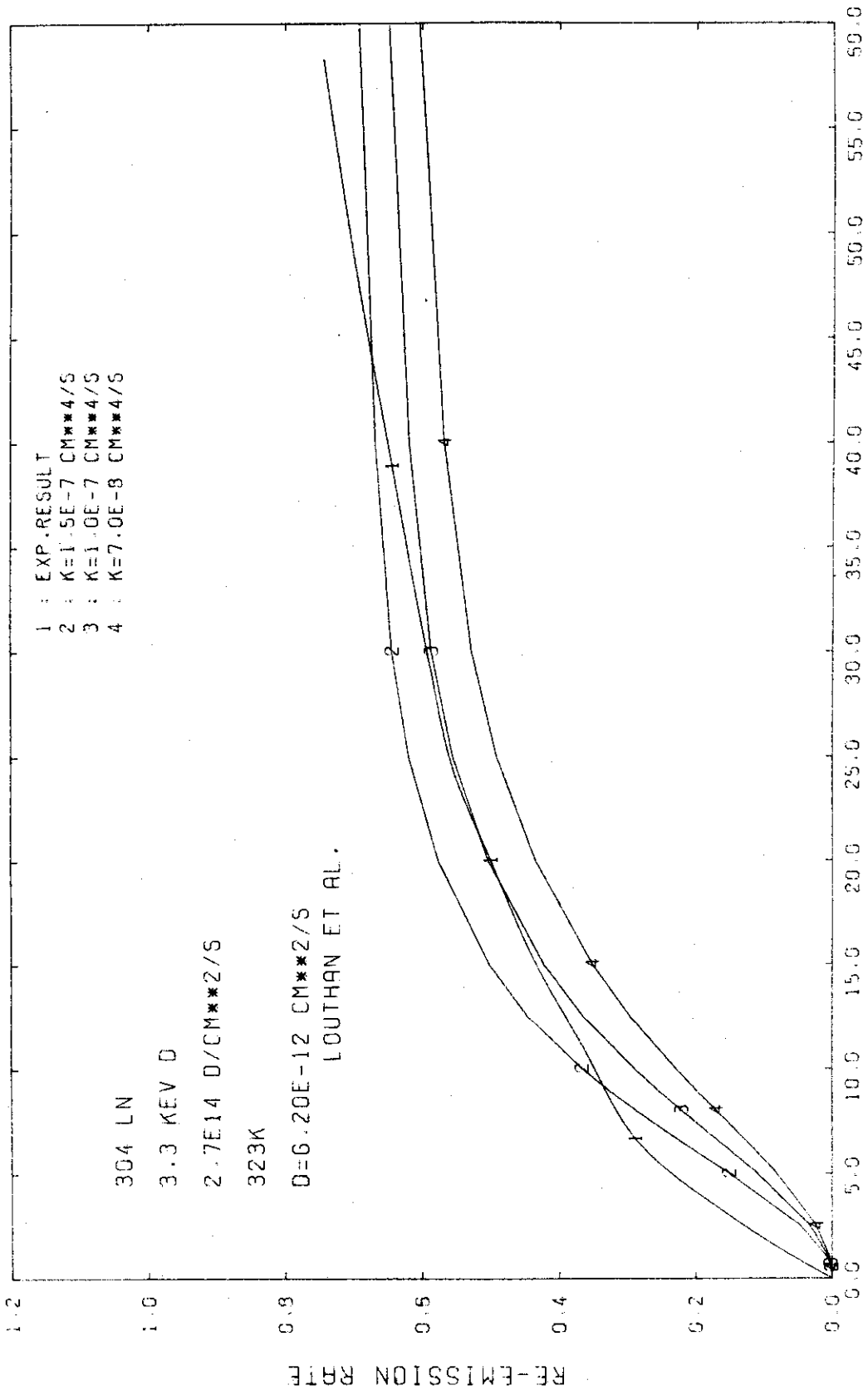

FIG.46 RE-EMISSION RATE FOR VARIOUS RECOMBINATION CONSTANTS WITH EXPERIMENTALLY OBTAINED DIFFUSION CONSTANT (RE06)

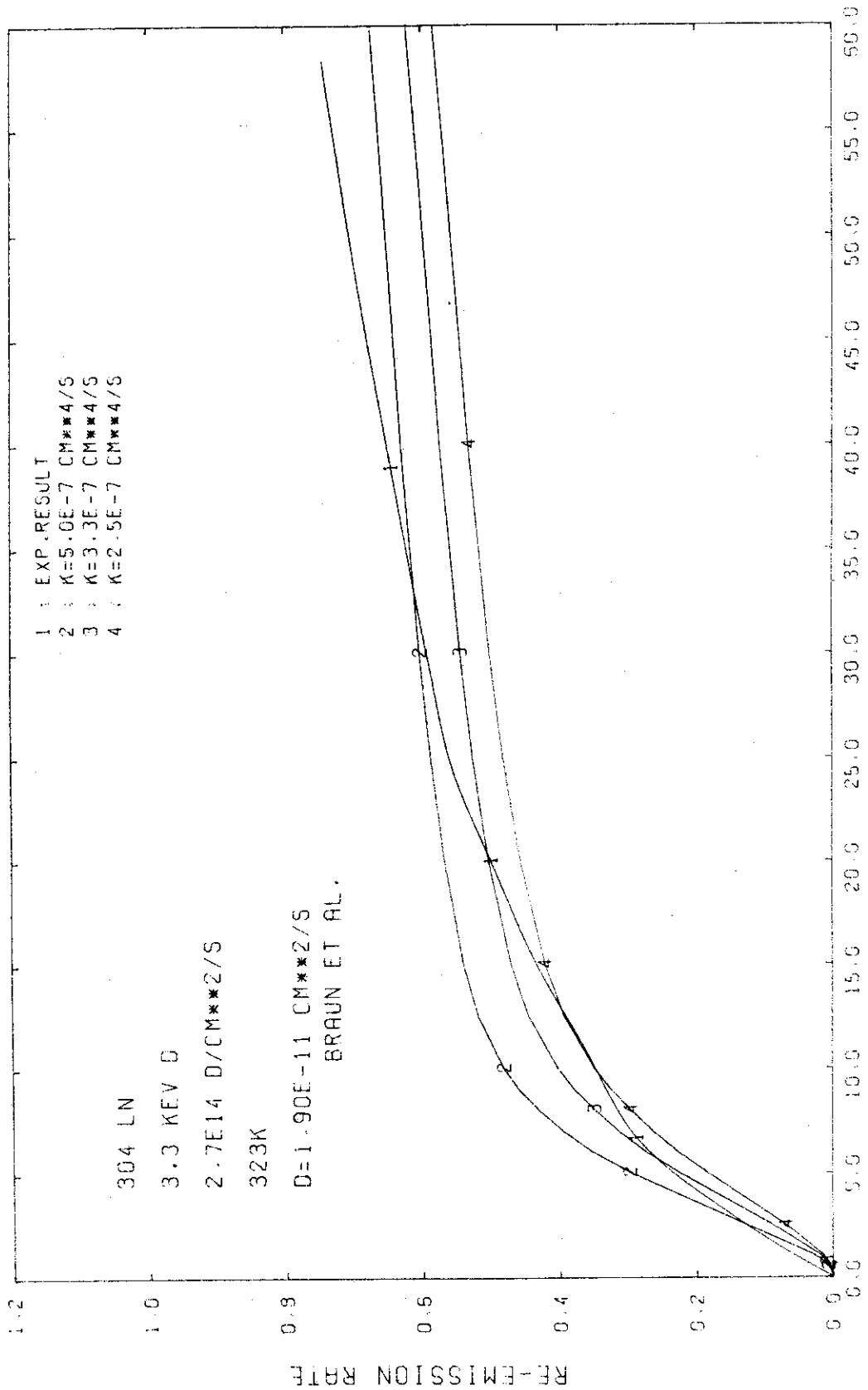

FIG 47 RE-EMISSION RATE FOR VARIOUS RECOMBINATION CONSTANTS WITH EXPERIMENTALLY OBTAINED DIFFUSION CONSTANT (REOS)

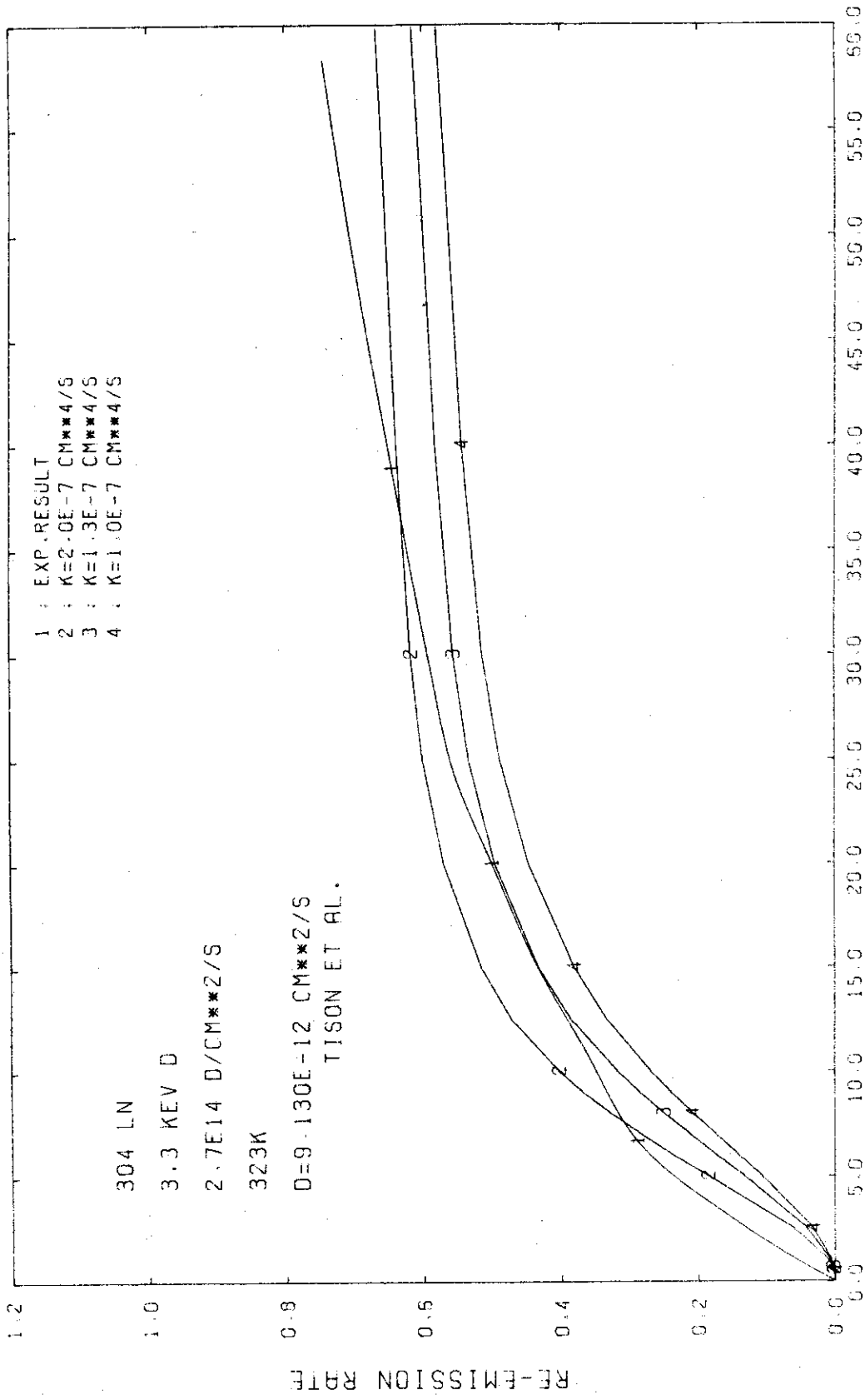

FIG.48 RE-EMISSION RATE FOR VARIOUS RECOMBINATION CONSTANTS WITH EXPERIMENTALLY OBTAINED DIFFUSION CONSTANT (REF05)

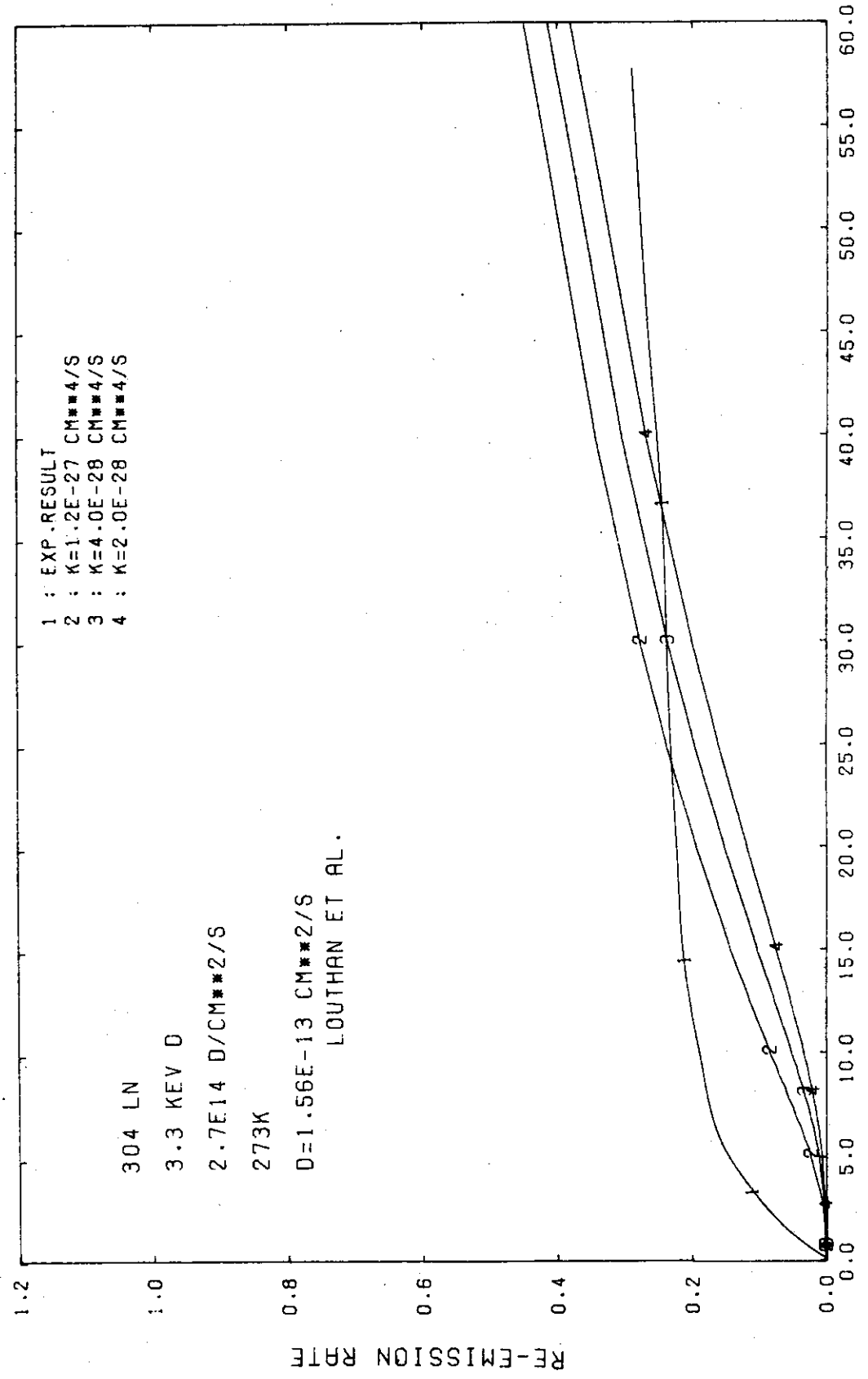

FIG.49 RE-EMISSION RATE FOR VARIOUS RECOMBINATION CONSTANTS WITH EXPERIMENTALLY OBTAINED DIFFUSION CONSTANT (RE06)

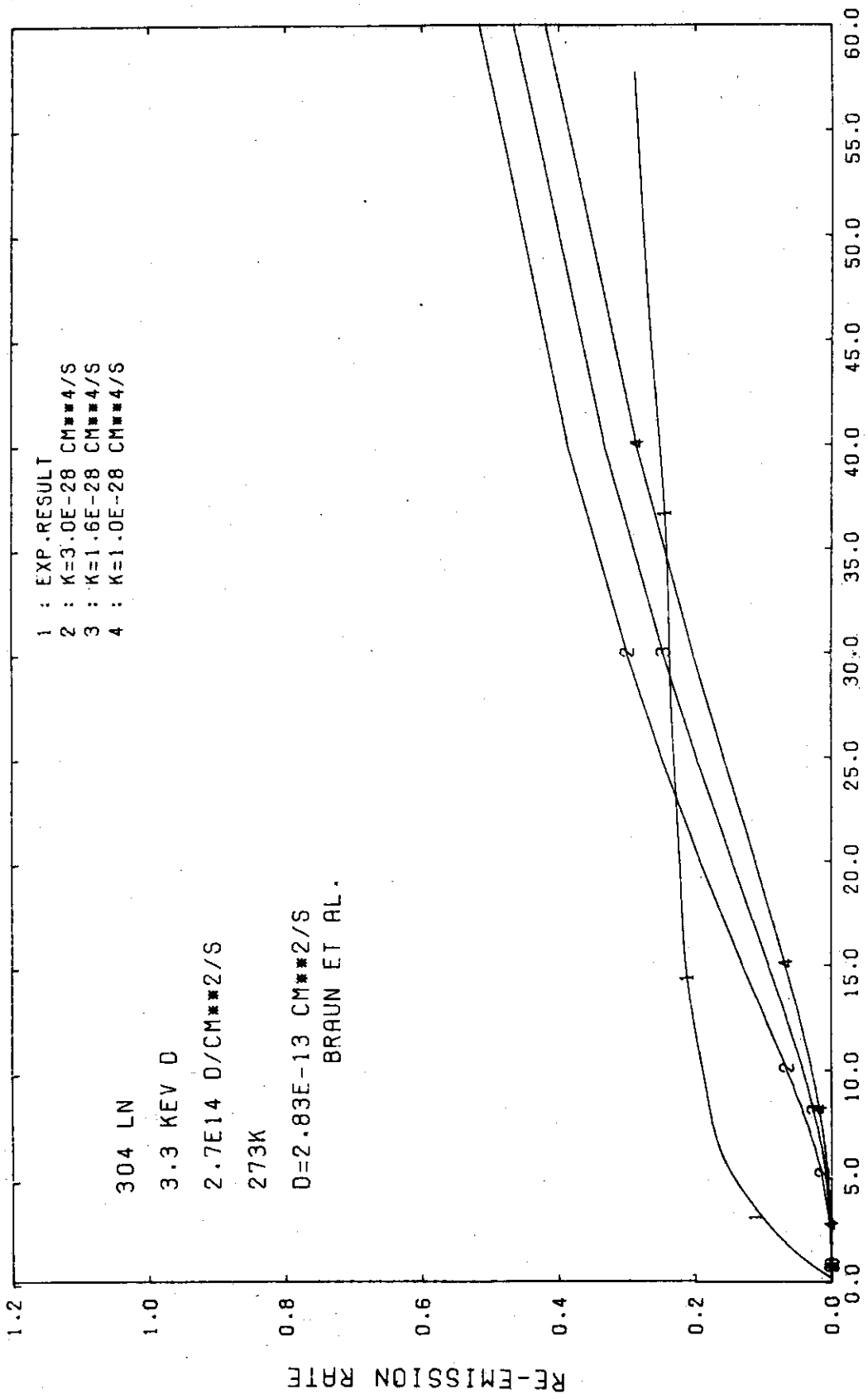

FIG.50 RE-EMISSION RATE FOR VARIOUS RECOMBINATION CONSTANTS WITH EXPERIMENTALLY OBTAINED DIFFUSION CONSTANT (RE06)

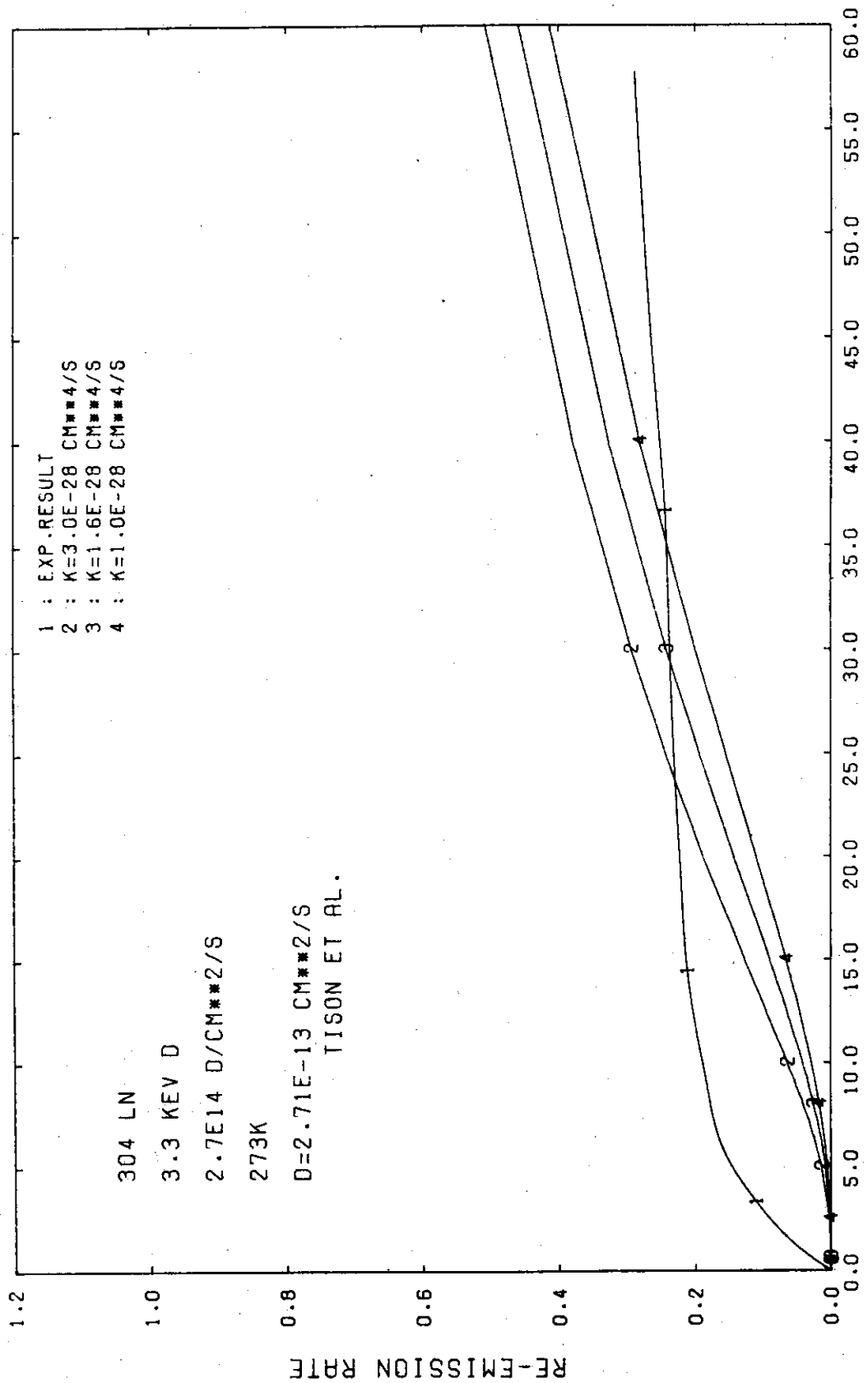

FIG.51 RE-EMISSION RATE FOR VARIOUS RECOMBINATION CONSTANTS WITH EXPERIMENTALLY OBTAINED DIFFUSION CONSTANT (RE06)

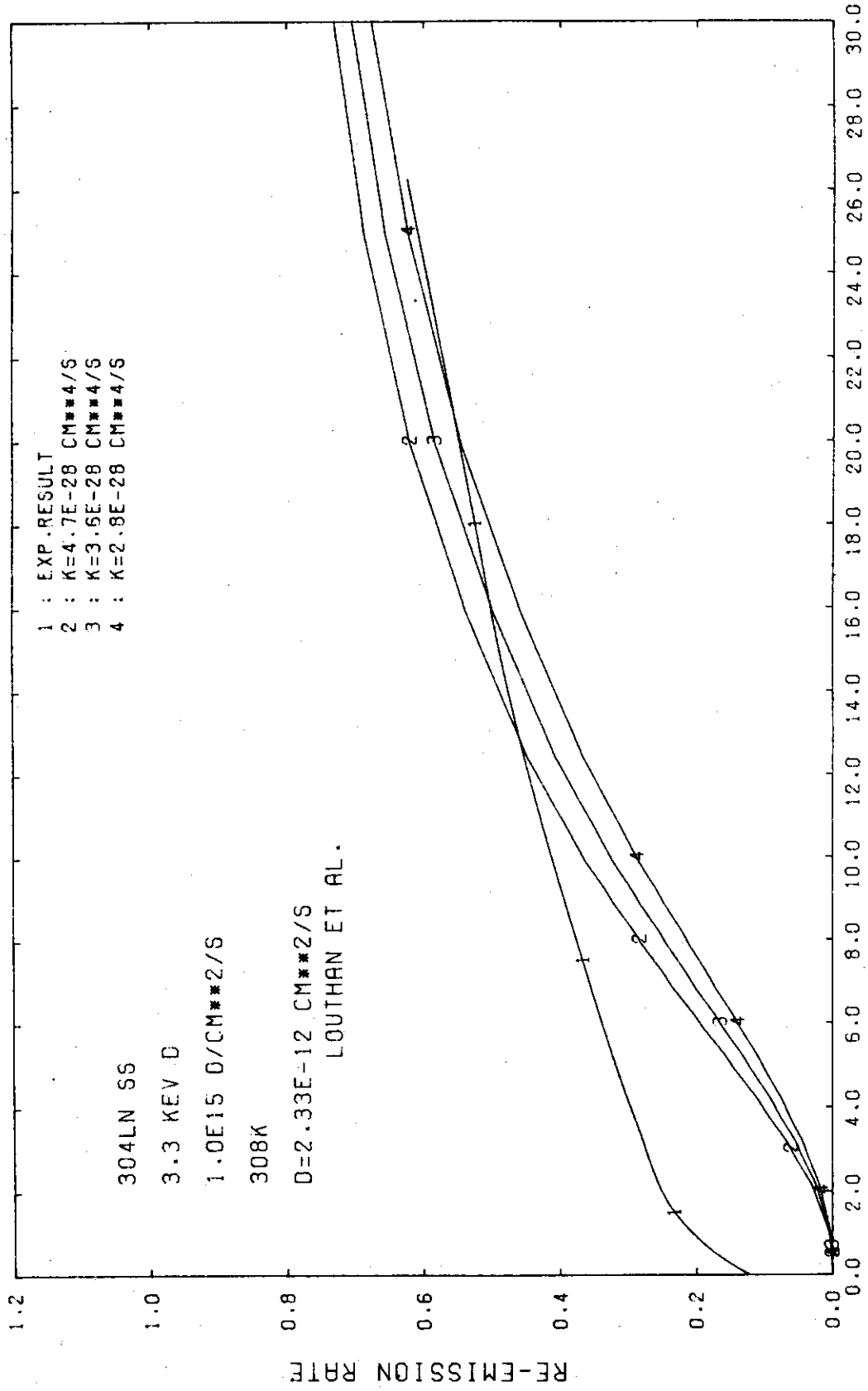

FIG.52 RE-EMISSION RATE FOR VARIOUS RECOMBINATION CONSTANTS WITH EXPERIMENTALLY OBTAINED DIFFUSION CONSTANT (RE07)

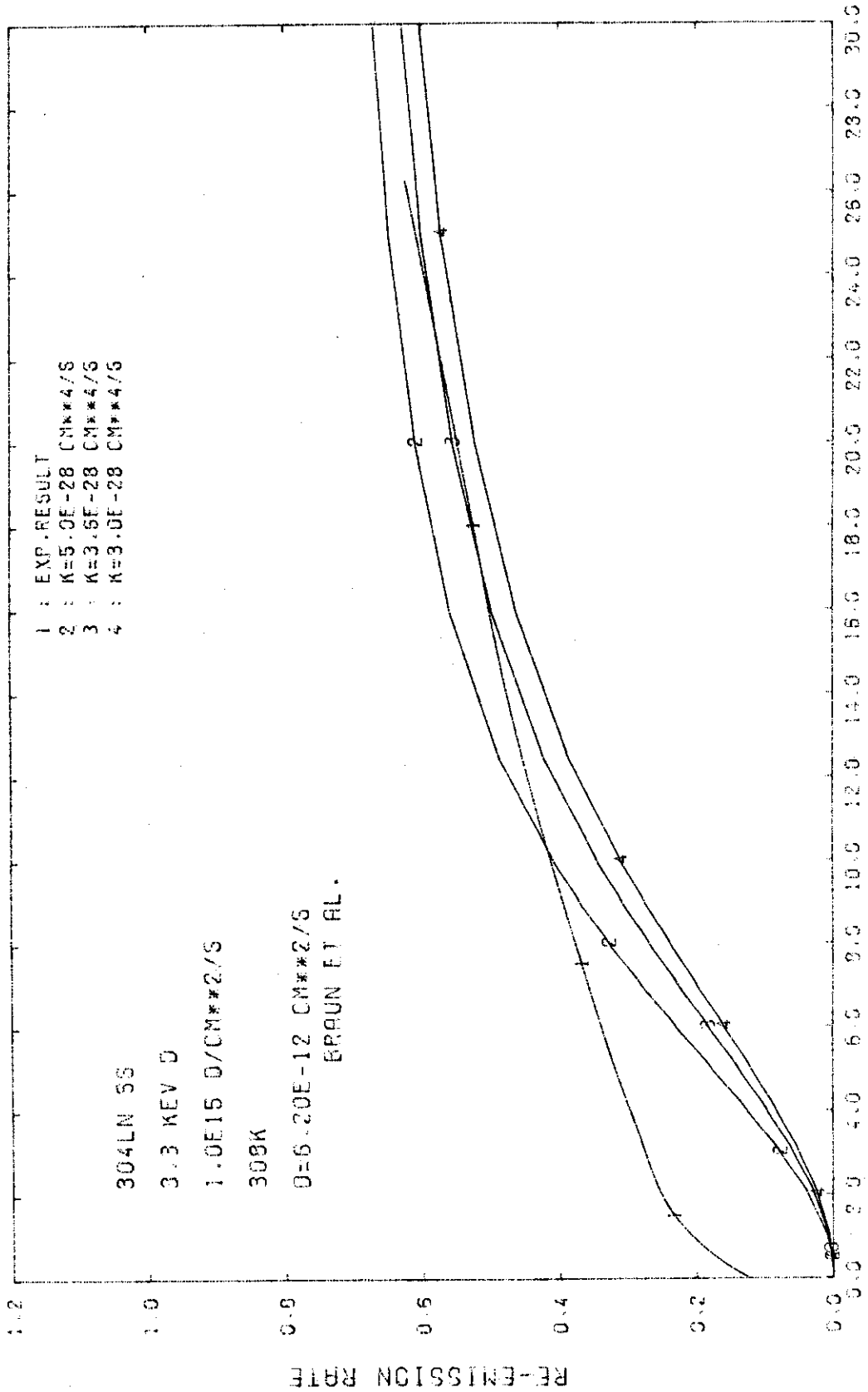

FIG.53 RE-EMISSION RATE FOR VARIOUS RECOMBINATION CONSTANTS WITH EXPERIMENTALLY OBTAINED DIFFUSION CONSTANT (REF7)

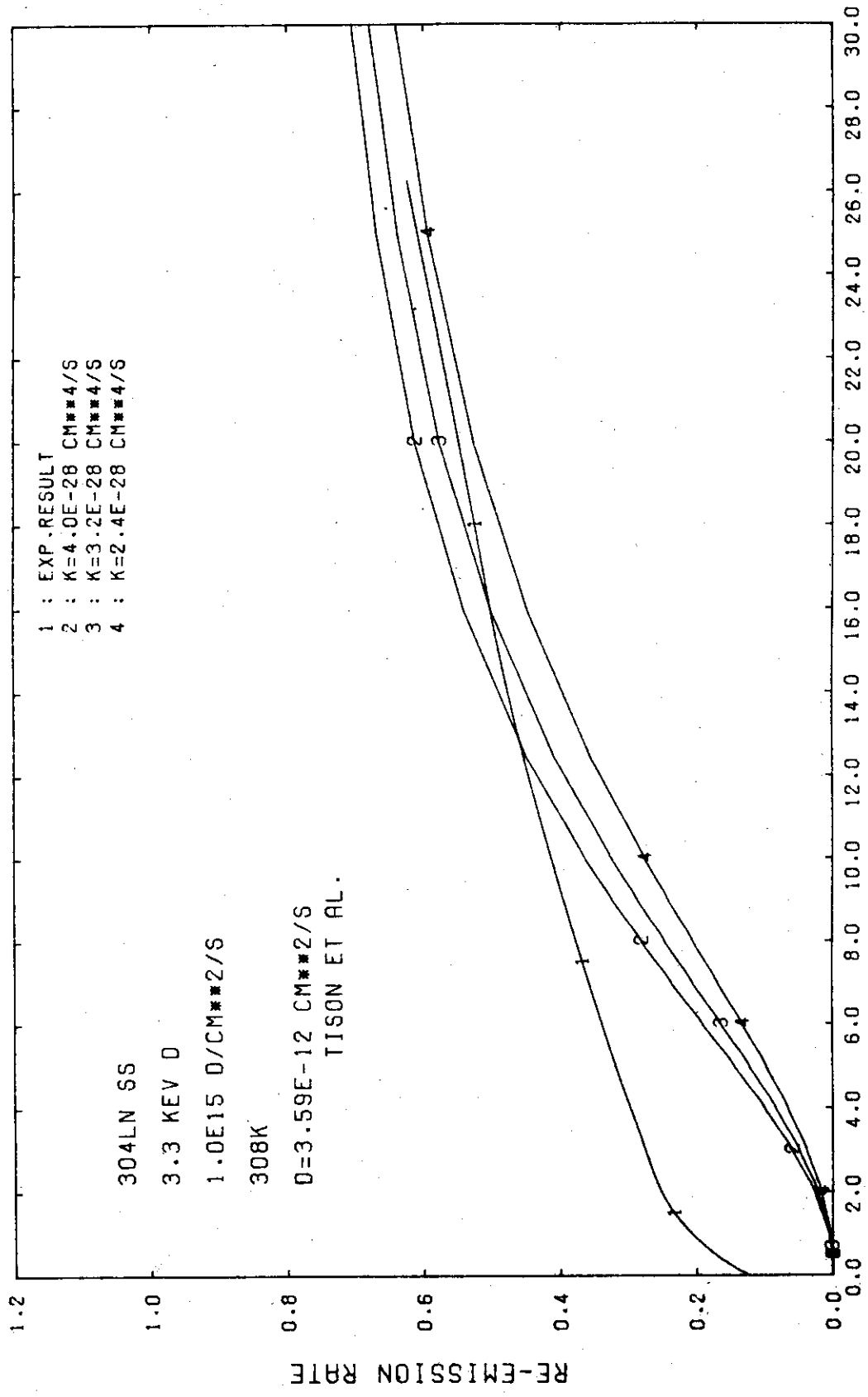

FIG.54 RE-EMISSION RATE FOR VARIOUS RECOMBINATION CONSTANTS WITH EXPERIMENTALLY OBTAINED DIFFUSION CONSTANT (RE07)

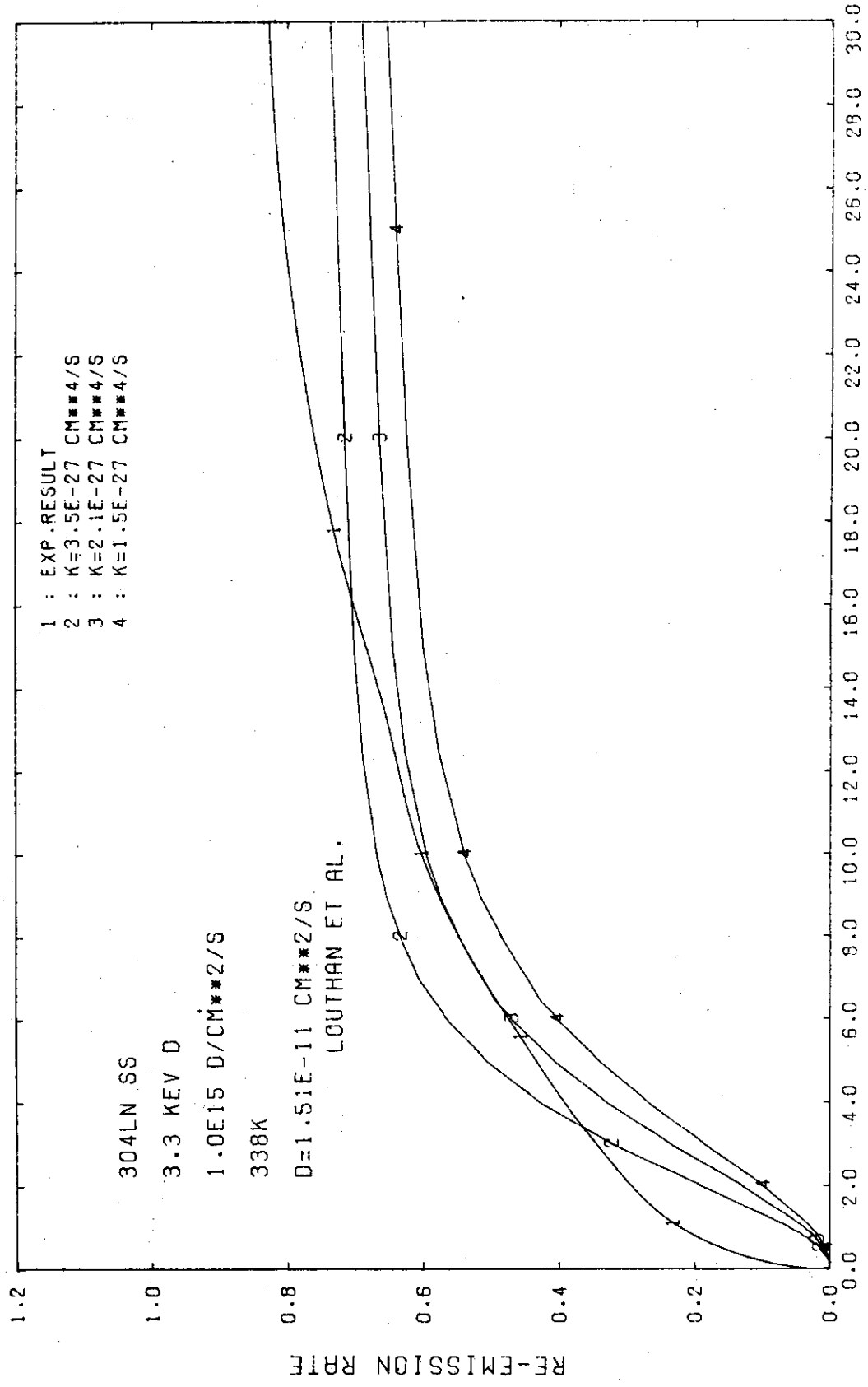

FIG.55 RE-EMISSION RATE FOR VARIOUS RECOMBINATION CONSTANTS WITH EXPERIMENTALLY OBTAINED DIFFUSION CONSTANT (RE07)

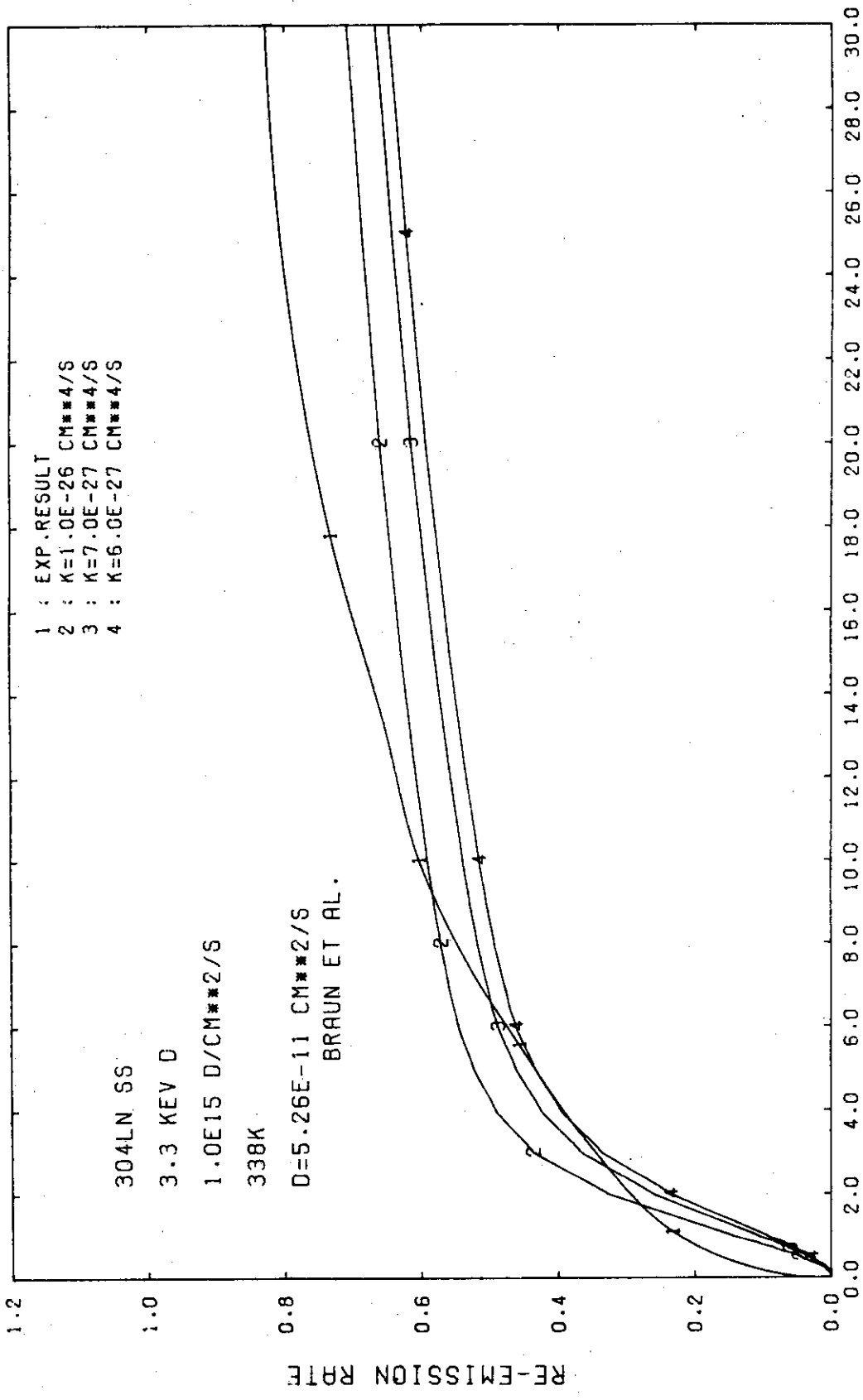

FIG.56 RE-EMISSION RATE FOR VARIOUS RECOMBINATION CONSTANTS WITH EXPERIMENTALLY OBTAINED DIFFUSION CONSTANT (RE07)

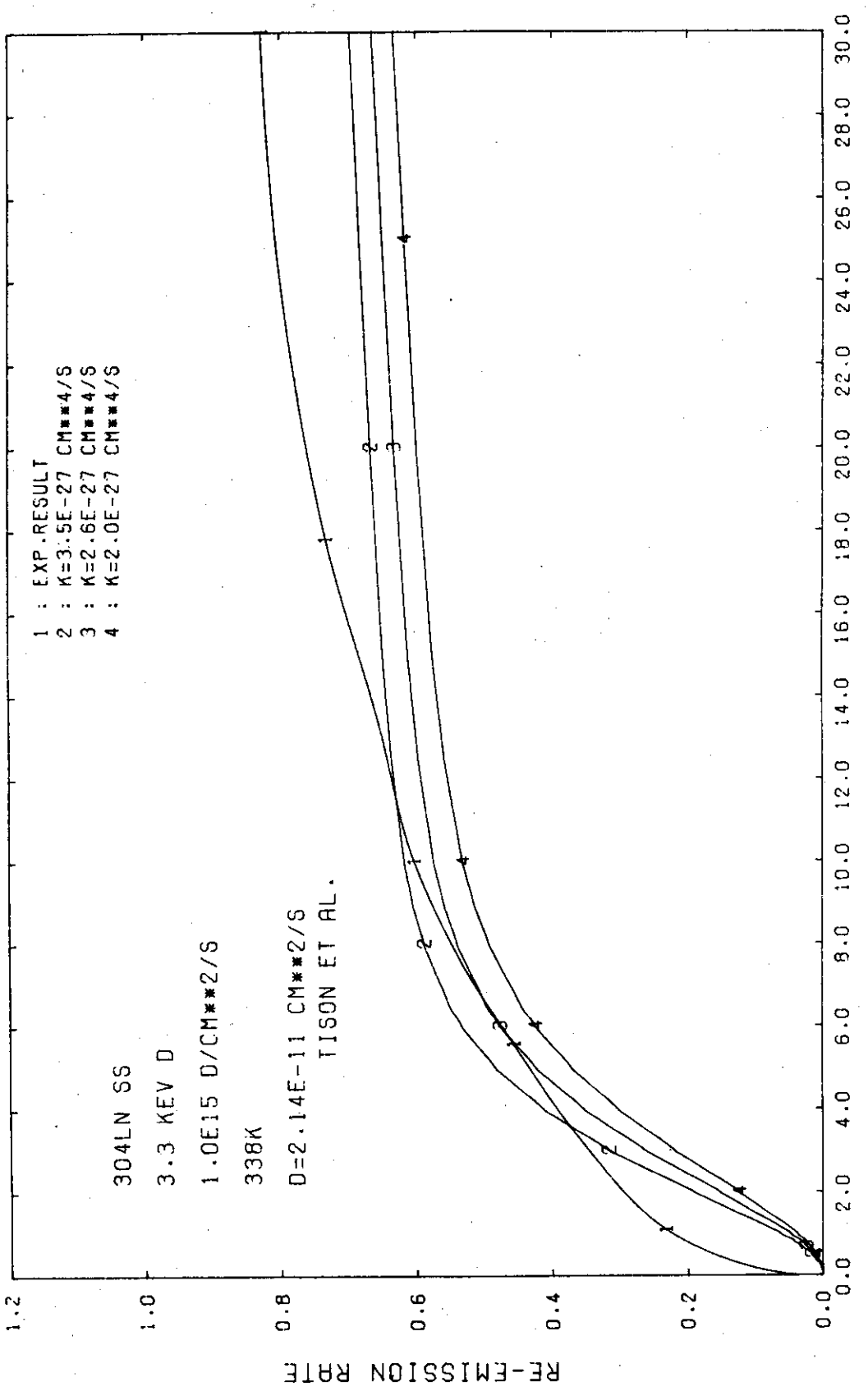

FIG.57 RE-EMISSION RATE FOR VARIOUS RECOMBINATION CONSTANTS WITH EXPERIMENTALLY OBTAINED DIFFUSION CONSTANT (RE07)

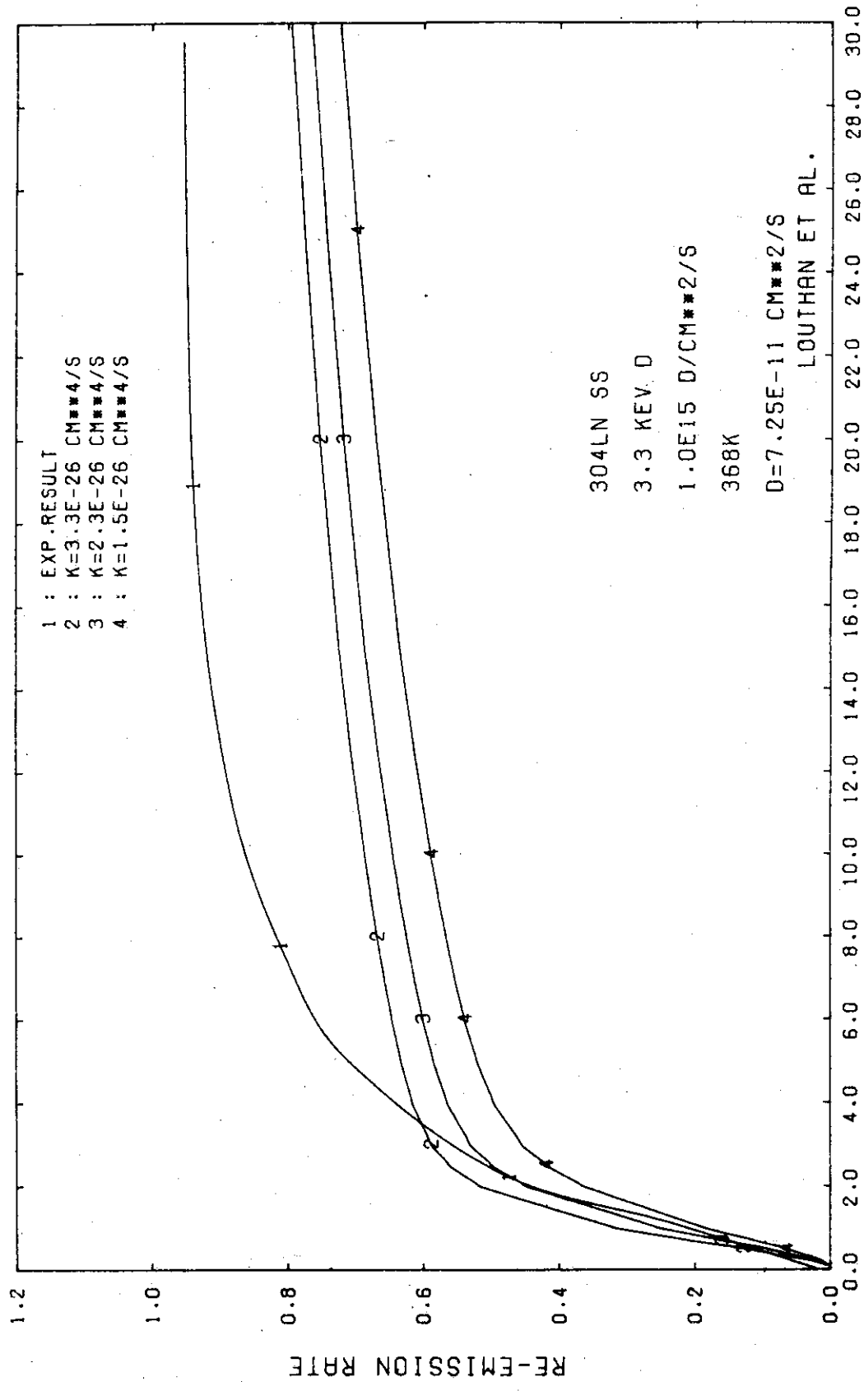

FIG.58 RE-EMISSION RATE FOR VARIOUS RECOMBINATION CONSTANTS WITH EXPERIMENTALLY OBTAINED DIFFUSION CONSTANT (RE07)

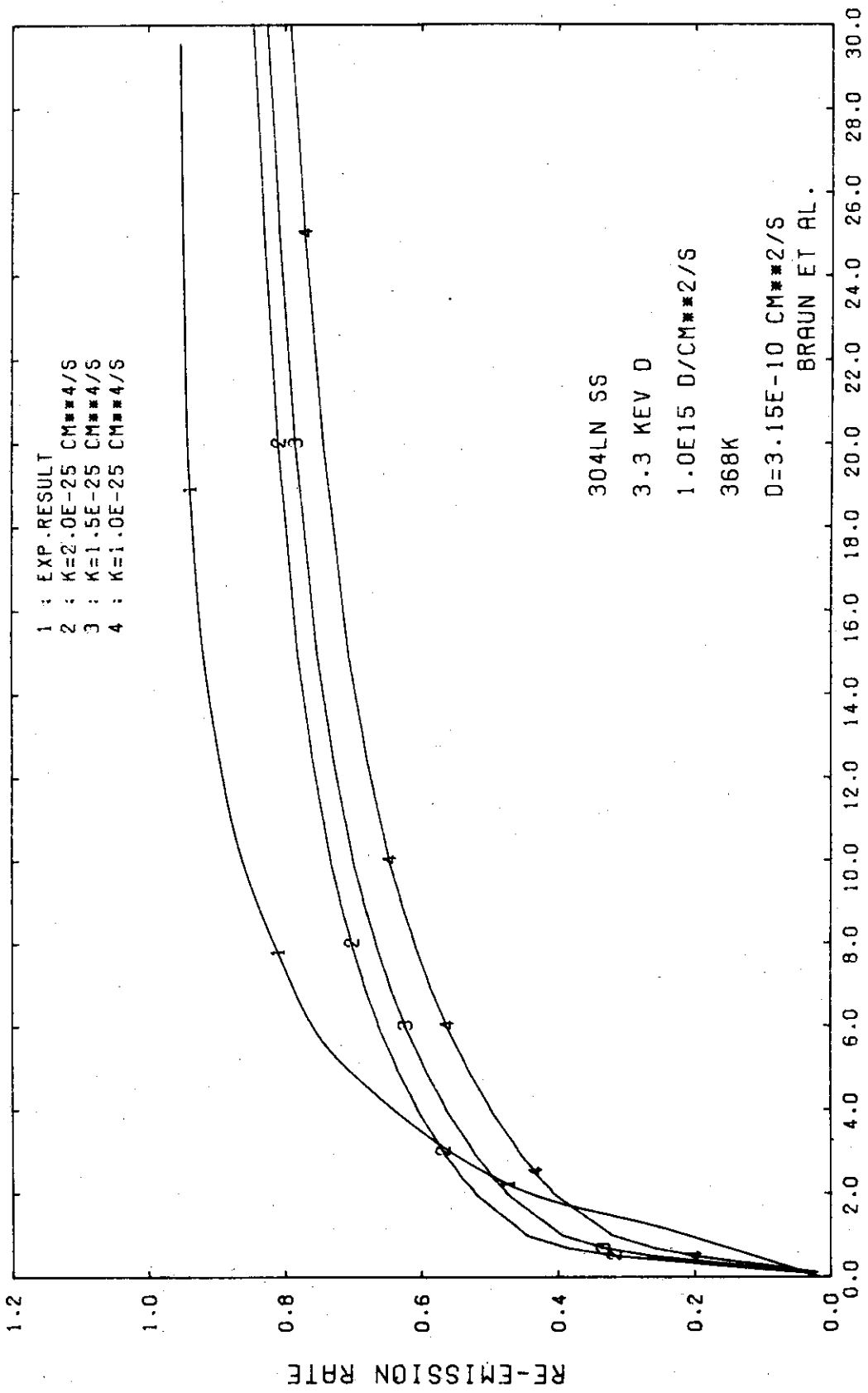

FIG.59 RE-EMISSION RATE FOR VARIOUS RECOMBINATION CONSTANTS WITH EXPERIMENTALLY OBTAINED DIFFUSION CONSTANT (RE07)

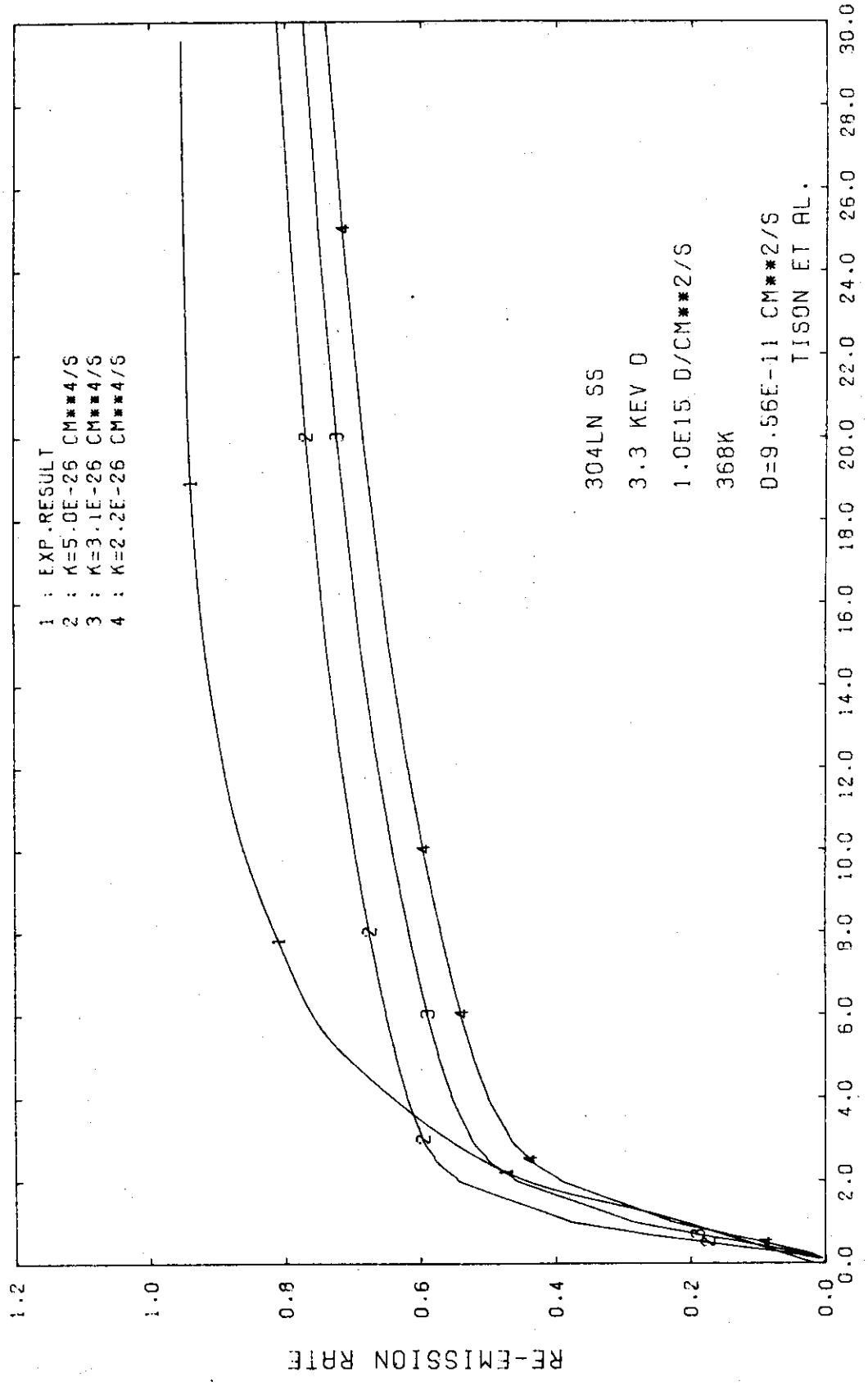

FIG.60 RE-EMISSION RATE FOR VARIOUS RECOMBINATION CONSTANTS WITH EXPERIMENTALLY OBTAINED DIFFUSION CONSTANT (RE07)

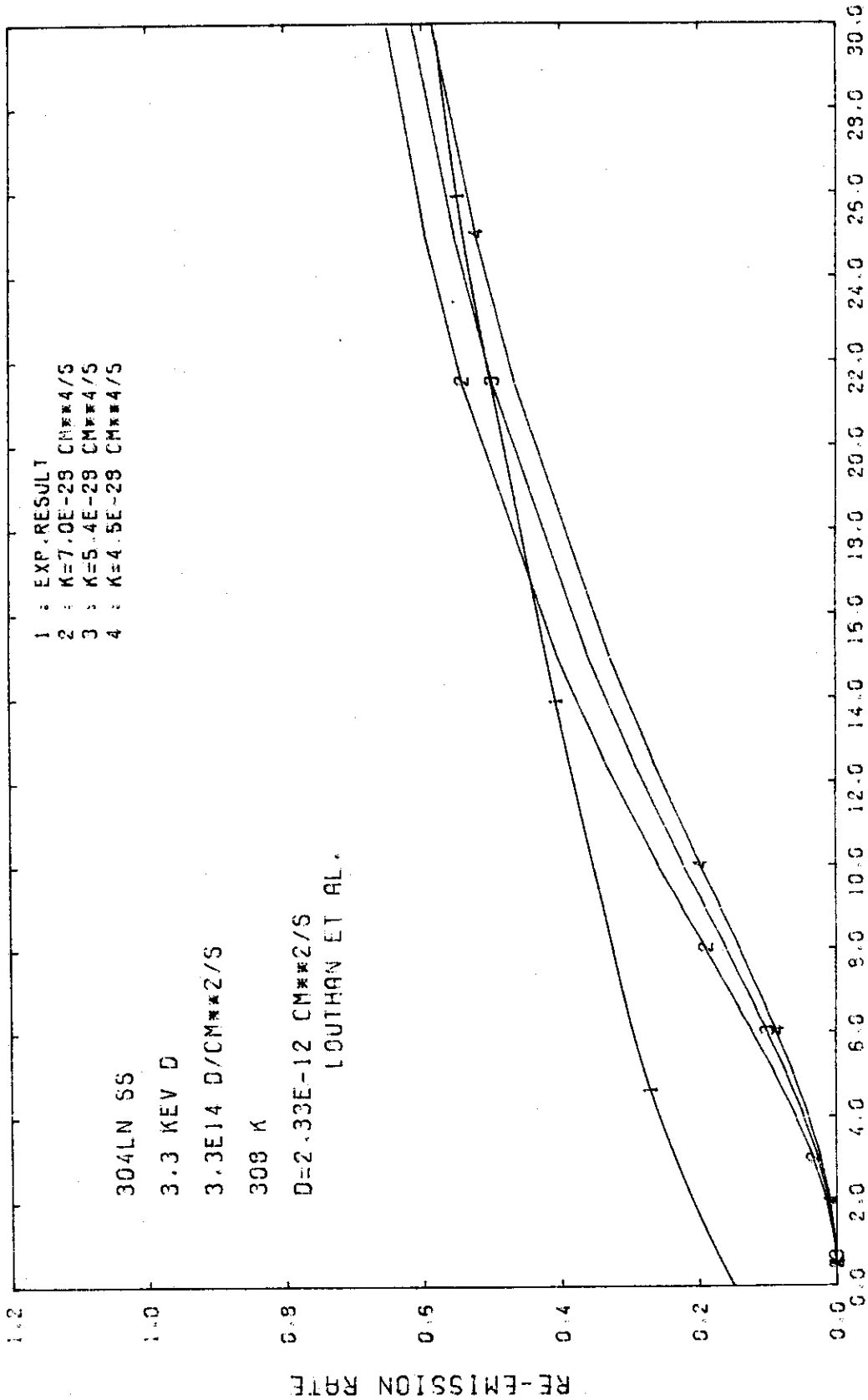

FIG.61 RE-EMISSION RATE FOR VARIOUS RECOMBINATION CONSTANTS WITH EXPERIMENTALLY OBTAINED DIFFUSION CONSTANT (REO7)

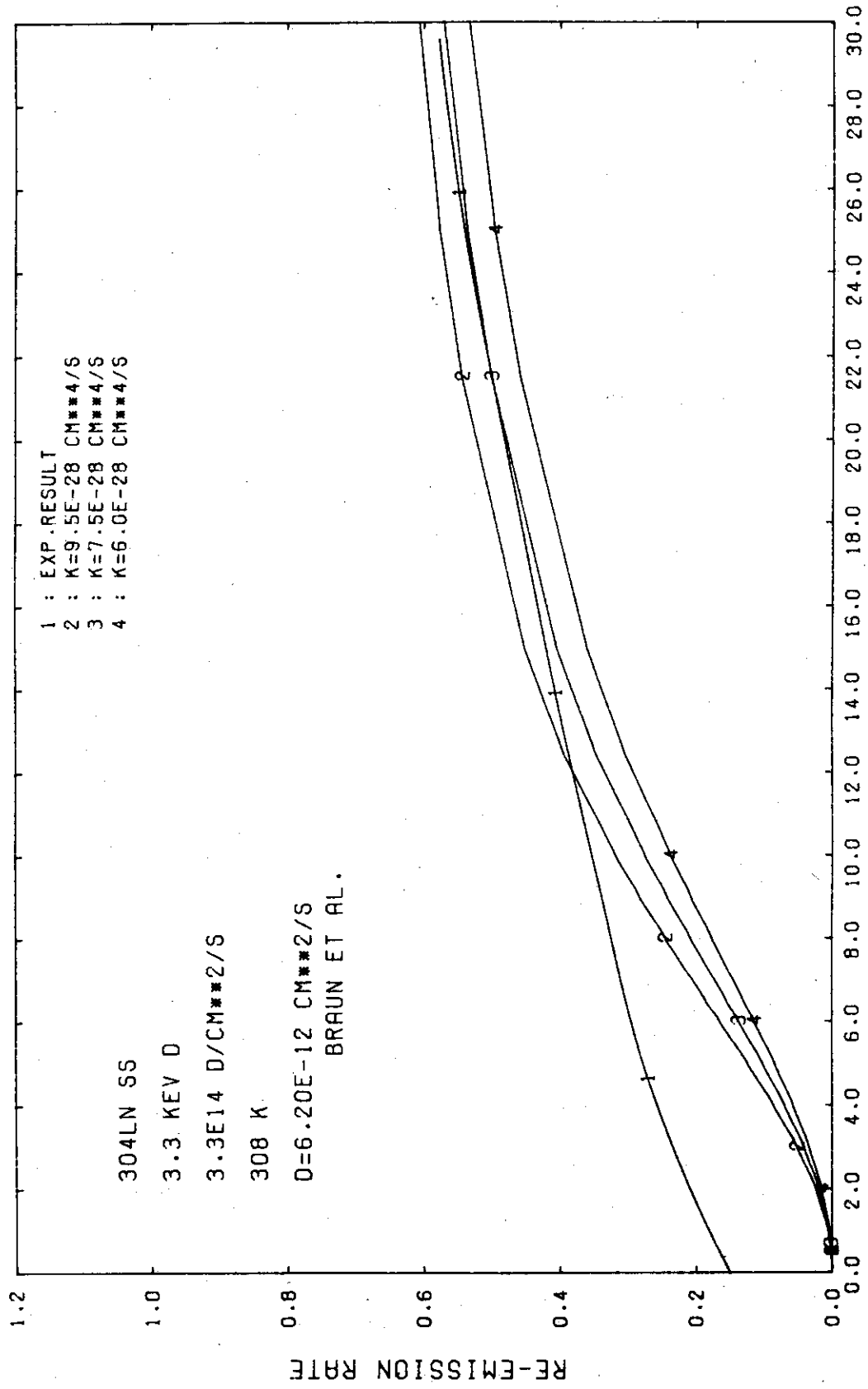

FIG.62 RE-EMISSION RATE FOR VARIOUS RECOMBINATION CONSTANTS WITH EXPERIMENTALLY OBTAINED DIFFUSION CONSTANT (RE07)

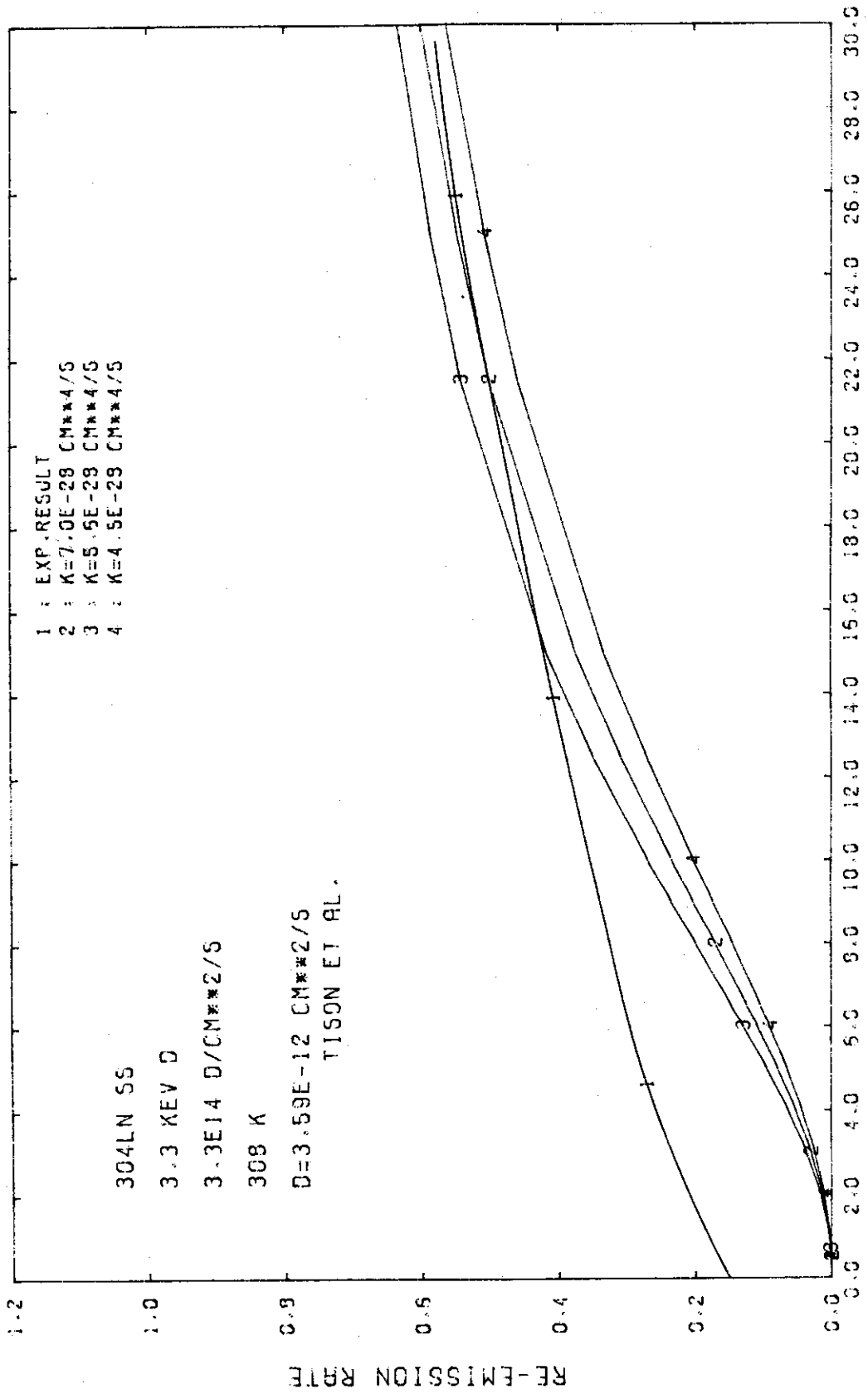

FIG.63 RE-EMISSION RATE FOR VARIOUS RECOMBINATION CONSTANTS WITH EXPERIMENTALLY OBTAINED DIFFUSION CONSTANT (REO7)

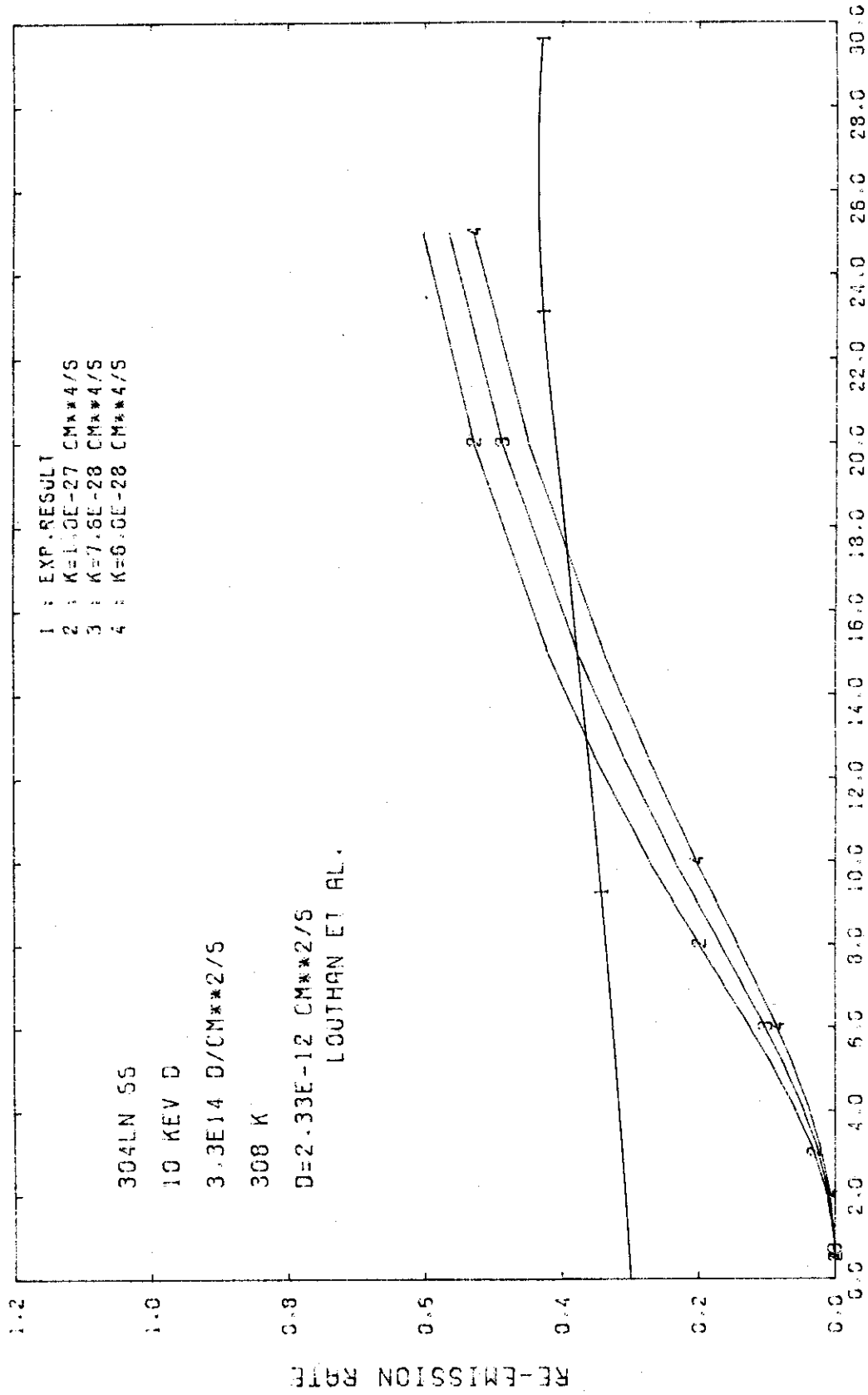

FIG.64 RE-EMISSION RATE FOR VARIOUS RECOMBINATION CONSTANTS WITH EXPERIMENTALLY OBTAINED DIFFUSION CONSTANT (REF7)

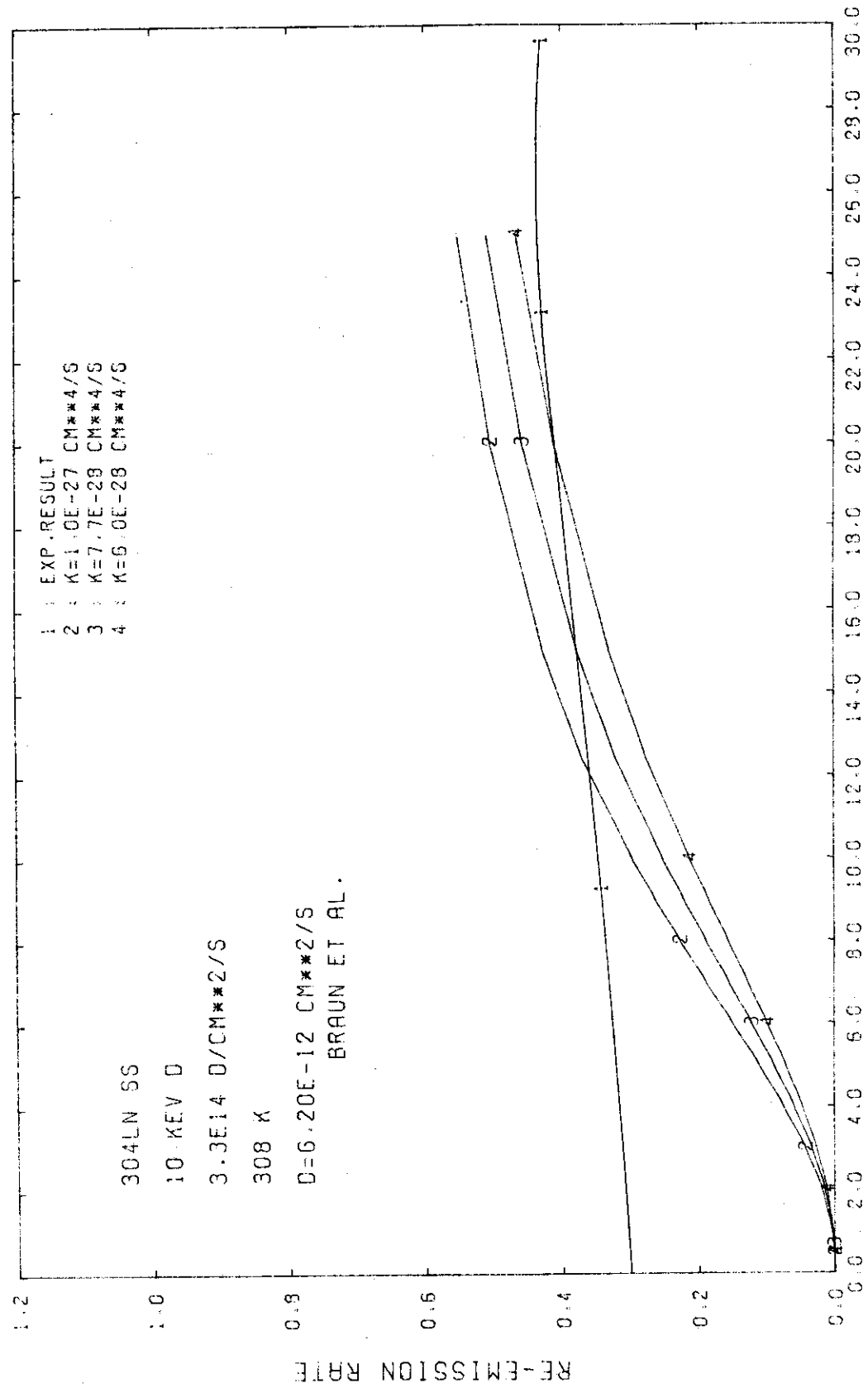

FIG.65 RE-EMISSION RATE FOR VARIOUS RECOMBINATION CONSTANTS WITH EXPERIMENTALLY OBTAINED DIFFUSION CONSTANT (REF7)

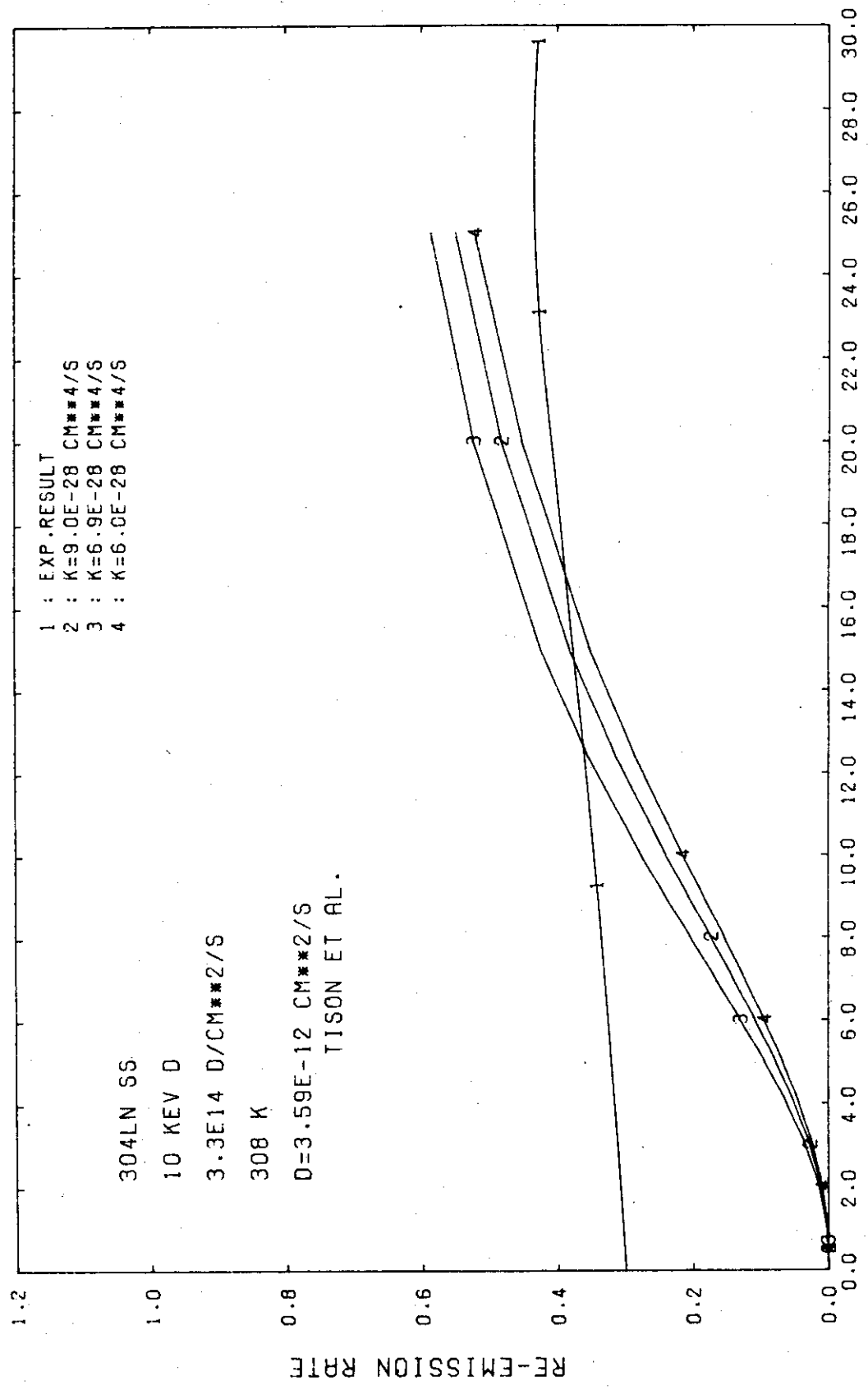

FIG.66 RE-EMISSION RATE FOR VARIOUS RECOMBINATION CONSTANTS WITH EXPERIMENTALLY OBTAINED DIFFUSION CONSTANT (RE07)

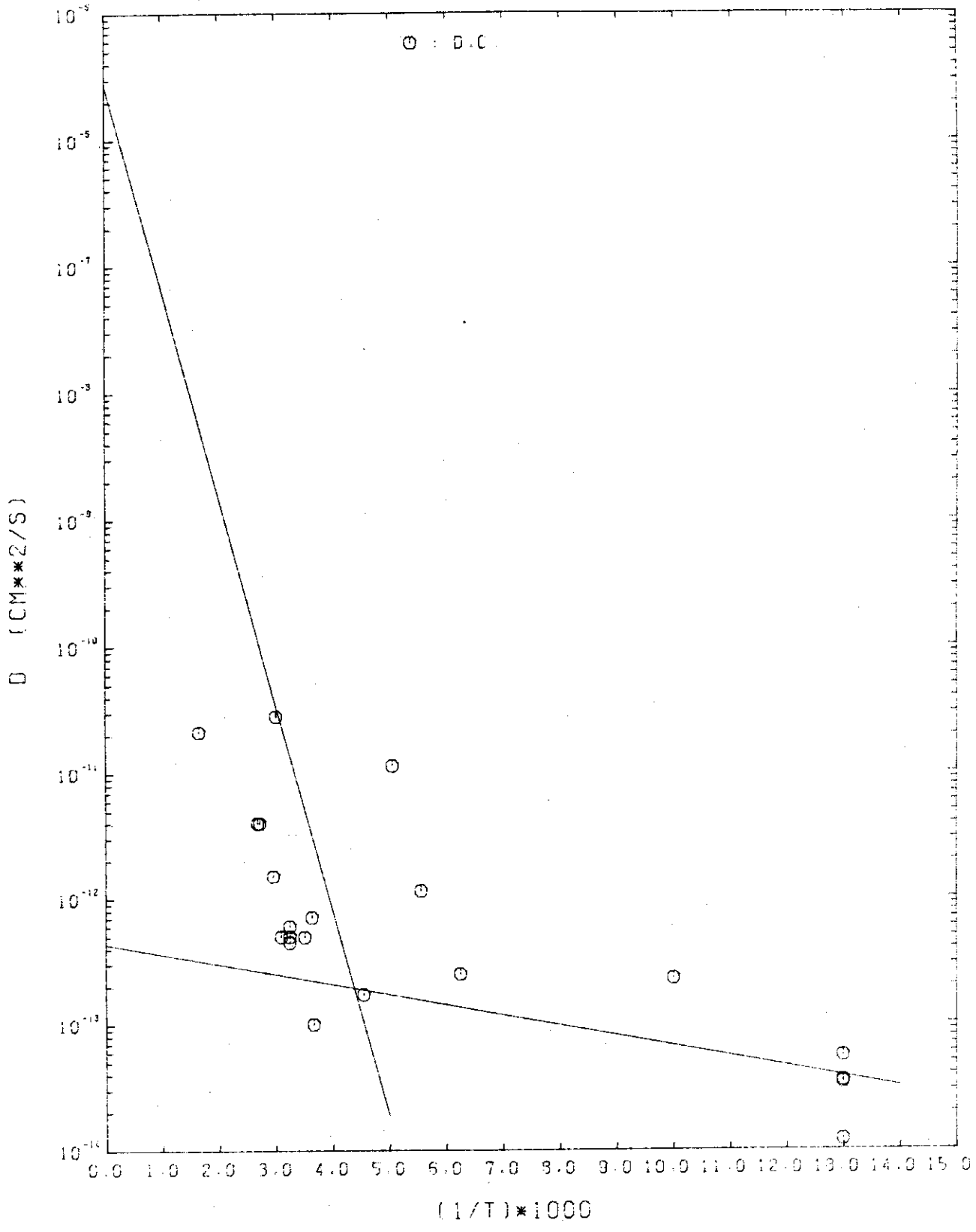

FIG.67 DIFFUSION CONSTANT OBTAINED FROM EXPERIMENTAL DATA ANALYSIS

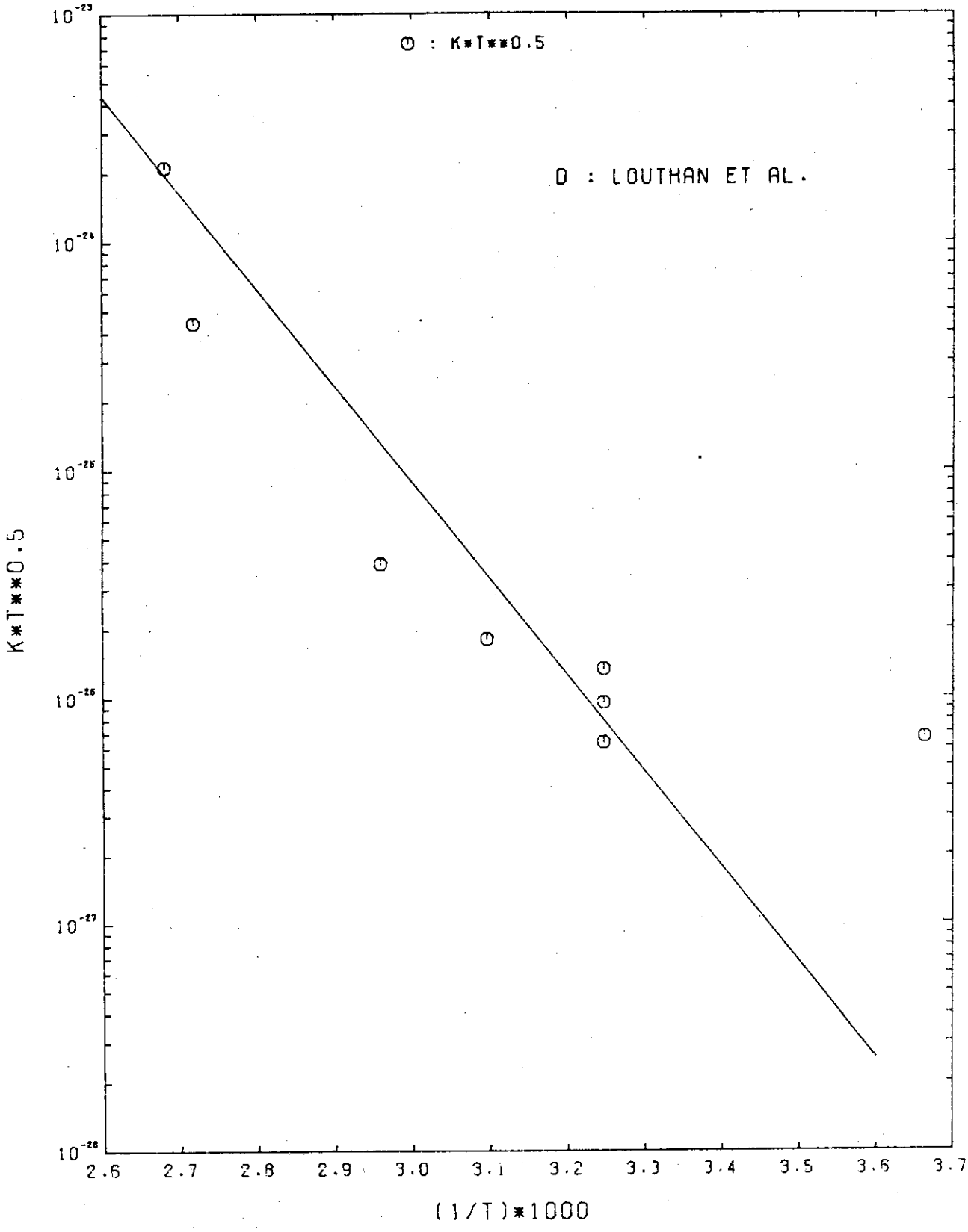

FIG.68 RECOMBINATION CONSTANT OBTAINED FROM EXPERIMENTAL DATA ANALYSIS

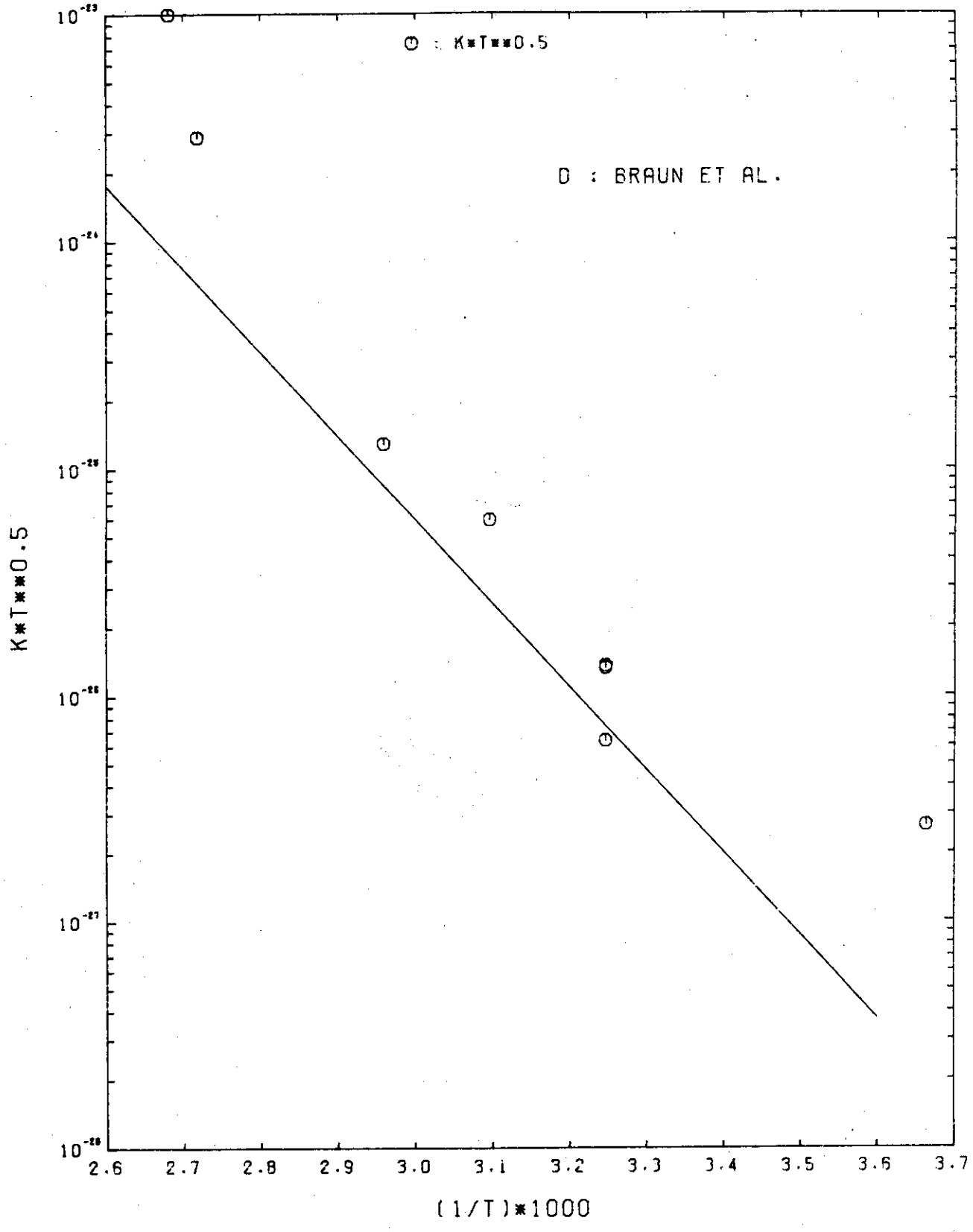

FIG.69 RECOMBINATION CONSTANT OBTAINED FROM EXPERIMENTAL DATA ANALYSIS

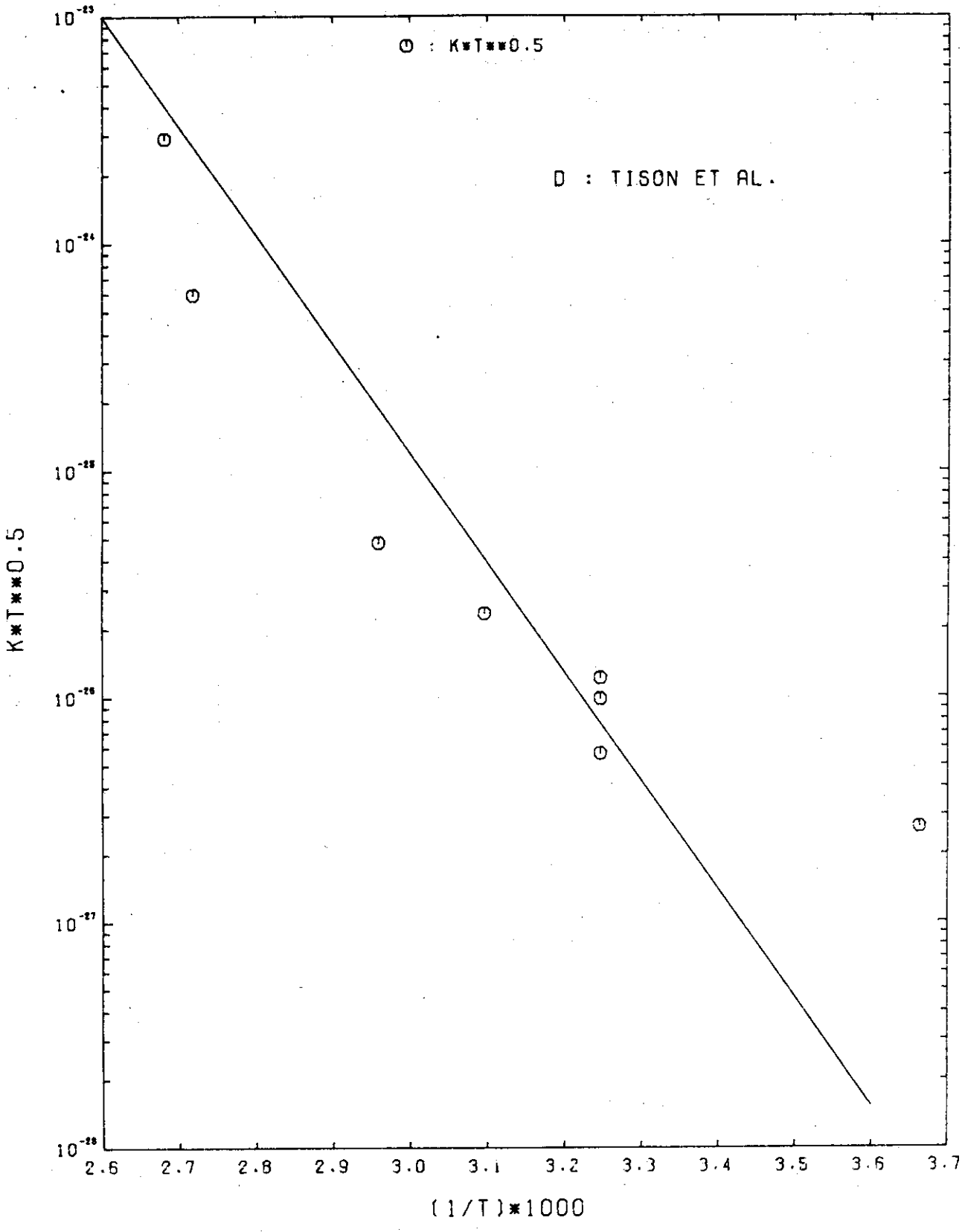

FIG.70 RECOMBINATION CONSTANT OBTAINED FROM EXPERIMENTAL DATA ANALYSIS

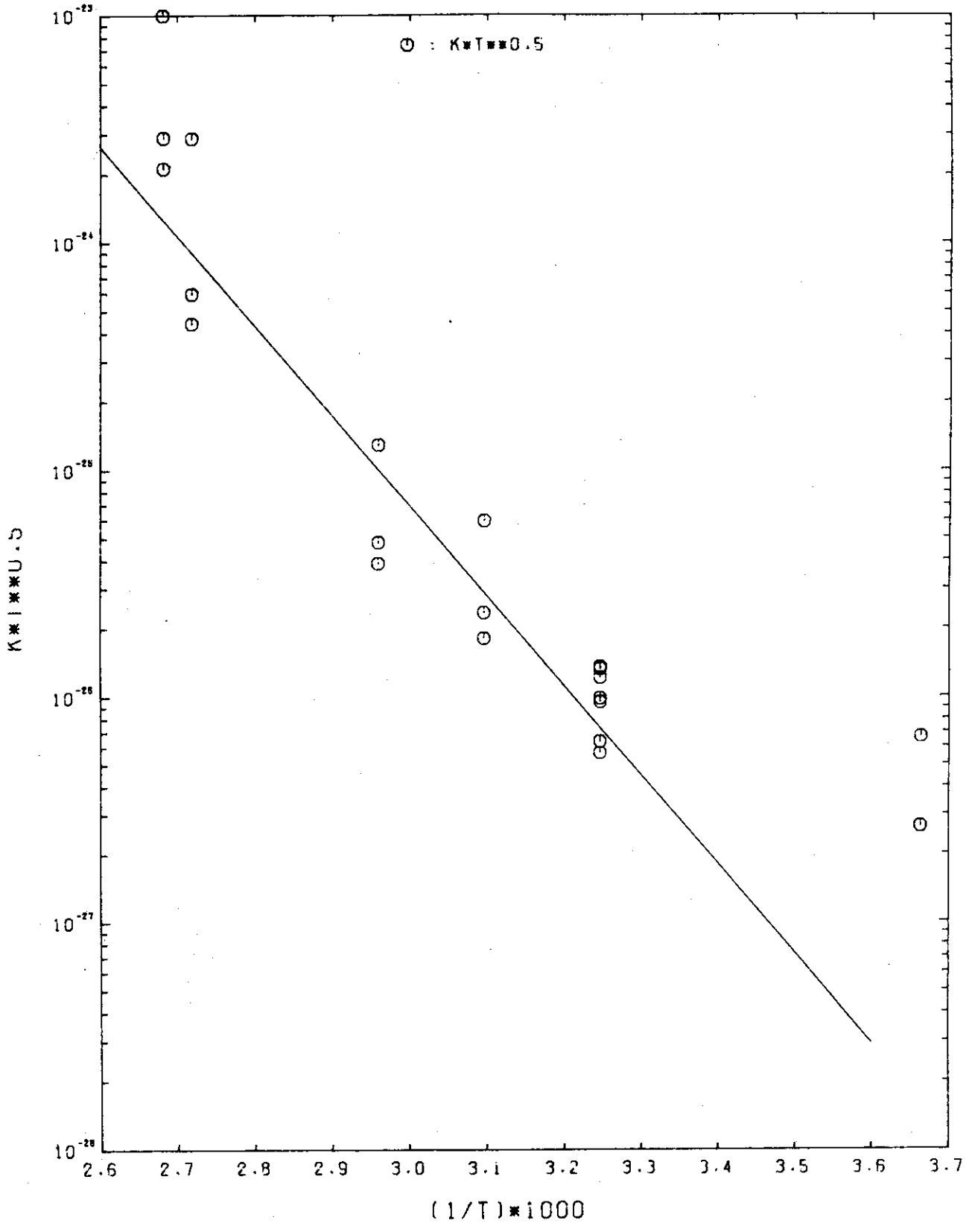

FIG.71 RECOMBINATION CONSTANT OBTAINED FROM EXPERIMENTAL DATA ANALYSIS

4. Concluding Remarks

In the present analysis, the effective diffusion constant and the recombination constant have been computed from the experimentally obtained re-emission data of hydrogen isotopes in stainless steel. The temperature dependence of the obtained parameters has been investigated. The effective diffusion constant has the smaller activation energy is low temperature compared to that in high temperature. It suggests that hydrogen isotopes in stainless steel diffuse through the tunneling effect in low temperature. In high temperature, the computed re-emission constant was obtained using the experimentally obtained diffusion constant.

In this analysis, the trapping effect was neglected to reduce the number of parameters. The trapping effect would be necessary to be considered for more precise analysis.

Appendix

In this appendix, the Crank-Nicloson's method[5] used to solve the diffusion equation is described. The diffusion equation is denoted in the form

$$\frac{\partial c}{\partial t} = F(c,m),$$

$$\frac{\partial m}{\partial t} = G(c,m). \qquad (A.1)$$

Here, c is the concentration of hydrogen isotope and m is that of trapped hydrogen isotopes. By the replacement of the differential operator in x coordinate in terms of the finite-difference, the following ordinary differential equation is obtained

$$\frac{dc_i}{dt} = f_i(\bar{c},\bar{m}),$$

$$\frac{dm_i}{dt} = g_i(\bar{c},\bar{m}), \qquad (A.2)$$

where c_i and m_i are the quantities at i-th node and index i runs over the integers from 1 to N. The vectors $\bar{c}$ and $\bar{m}$ mean $\bar{c}=(c_1, c_2, ---, c_N)$ and $\bar{m}=(m_1, m_2, ---, m_N)$, respectively.

In the Crank-Nicolson's computational sheme, the following time difference is used

$$\frac{dc_i}{dt} \longrightarrow \frac{c_i^{n+1} - c_i^n}{\Delta t},$$

$$\frac{dm_i}{dt} \longrightarrow \frac{m_i^{n+1} - m_i^n}{\Delta t},$$

$$f_i \longrightarrow \frac{1}{2}\left[f_i(\bar{c}^n, \bar{m}^n) + f_i(\bar{c}^{n+1}, \bar{m}^{n+1})\right],$$

$$g_i \longrightarrow \frac{1}{2}\left[g_i(\bar{c}^n, \bar{m}^n) + g_i(\bar{c}^{n+1}, \bar{m}^{n+1})\right]. \qquad (A.3)$$

Then, the following difference equations are obtained

$$\frac{c_i^{n+1} - c_i^n}{\Delta t} = \frac{1}{2}\left[f_i(\bar{c}^n, \bar{m}^n) + f_i(\bar{c}^{n+1}, \bar{m}^{n+1})\right],$$

$$\frac{m_i^{n+1} - m_i^n}{\Delta t} = \frac{1}{2}\left[g_i(\bar{c}^n, \bar{m}^n) + g_i(\bar{c}^{n+1}, \bar{m}^{n+1})\right]. \qquad (A.4)$$

The above non-linear algebraic equation is solved by the Newton-Raphson's method.

The transient c and m increase with the various time constants. The variable time increments are taken according to the variation of c and m.

References

[1] K. Ozawa, K. Fukushima and K. Ebisawa, "Data Compilation for Radiation Effects on Hydrogen Recycling in Fusion Reactor Materials", JAERI-M Report 84-089 (1984).

[2] K. Fukushima, N. Mitsutsuka and Y. Goshi, Toshiba R & D Center Research Report RR-2578 (1977, unpublished).

[3] B. L. Doyle : A Simple Theory for Maximum H Inventory and Release. A New Transport Parameter, J. Nucl. Mater. 111 & 112 (1982) 628.

[4] J. P. Biersack and L. G. Haggmark, "A Monte Carlo Computer Program for the Transport of Energetic Ions in Metals", Nucl. Instrum. Meth. 174 (1980) 257.

[5] G. E. Forsythe and W. R. Wasow, "Finite-Difference Methods for Partial Differential Equations", (John Wiley & Sons, 1960) Chap. 2.

[6] W. Bauer and G. J. Thomas : Helium and Hydrogen Re-emission during Implantation of Molybdenum, Vanadium, and Stainless Steel, J. Nucl. Mater. 53 (1974) 127.

[7] C. M. Braganza, S. K. Erentz, E. S. Hotston and G. M. McCraken : Ion-Induced Release of Deuterium Trapping in Stainless Steel, J. Nucl. Mater. 76 & 77 (1978) 298.

[8] K. L. Wilson : Hydrogen Recycling in Properties in Stainless Steel, J. Nucl. Mater. 103 & 104 (1981) 453.

[9] K. L. Wilson and M. I. Baskes : Deuterium Re-Emission from 304LN Stainless Steel, J. Nucl. Mater. 111 & 112 (1982) 622.

[10] K. L. Wilson, G. J. Thomas and W. Bauer : Low Energy Proton Implantation of Stainless Steel, Nucl. Tech. 29 (1976) 322.

[11] M. R. Lauthan, Jr. and R. G. Derrick : Hydrogen Transport in Austenitic Stainless Steel, Corr. Sci. 15 (1975) 565.

[12] M. Braun, B. Emmoth, F. Waelbroek and P. Wienhold : Determination of Deuterium Surface Recombination Rates on Stainless Steel, J. Nucl. Mater. 93 & 94 (1980) 861.

[13] See Ref. 9 .